ELECTRONIC FILE AVAILABLE

37; 40

UCRL-ID-135193

Geochemical Characterization of Seaplane Lagoon Sediments, Alameda Naval Air Station

Susan Carroll, Brad Esser, and Simon Randall
Earth and Environmental Sciences Directorate
Chemistry and Material Sciences Directorate
Lawrence Livermore National Laboratory

Peggy O'Day
Department of Geology
Arizona State University

Andrew Bono and George W. Luther III
College of Marine Studies
University of Delaware

CIRCULATION COPY
SUBJECT TO RECALL
IN TWO WEEKS

July 20, 1999

Lawrence Livermore National Laboratory

This is an informal report intended primarily for internal or limited external distribution. The opinions and conclusions stated are those of the author and may or may not be those of the Laboratory.
Work performed under the auspices of the Department of Energy by the Lawrence Livermore National Laboratory under Contract W-7405-Eng-48.

DISCLAIMER

This document was prepared as an account of work sponsored by an agency of the United States Government. Neither the United States Government nor the University of California nor any of their employees, makes any warranty, express or implied, or assumes any legal liability or responsibility for the accuracy, completeness, or usefulness of any information, apparatus, product, or process disclosed, or represents that its use would not infringe privately owned rights. Reference herein to any specific commercial product, process, or service by trade name, trademark, manufacturer, or otherwise, does not necessarily constitute or imply its endorsement, recommendation, or favoring by the United States Government or the University of California. The views and opinions of authors expressed herein do not necessarily state or reflect those of the United States Government or the University of California, and shall not be used for advertising or product endorsement purposes.

This report has been reproduced
directly from the best available copy.

Available to DOE and DOE contractors from the
Office of Scientific and Technical Information
P.O. Box 62, Oak Ridge, TN 37831
Prices available from (615) 576-8401, FTS 626-8401

Available to the public from the
National Technical Information Service
U.S. Department of Commerce
5285 Port Royal Rd.,
Springfield, VA 22161

UCRL-ID-135193

Geochemical Characterization of Seaplane Lagoon Sediments, Alameda Naval Air Station

Susan Carroll, Brad Esser, and Simon Randall

Earth and Environmental Sciences Directorate
Chemistry and Material Sciences Directorate
Lawrence Livermore National Laboratory
Livermore, CA 94550

Peggy O'Day

Department of Geology
Arizona State University
Tempe, AZ 85287

Andrew Bono and George W. Luther III

College of Marine Studies
University of Delaware
Lewes, DE 10058

Manuscript date: July 20, 1999

Geochemical Characterization of Seaplane Lagoon Sediments, Alameda Naval Air Station

1. Background

Our objective in the characterization of sediments from Seaplane Lagoon at the Alameda Naval Air Station (NAS) (Fig. 1) was to determine the geochemical interactions that control the partitioning of cadmium, chromium, cobalt, copper, lead, mercury, nickel, and zinc between the sediments and the porewaters. Our approach was to collect several cores at the east outfall location of the Seaplane Lagoon. We determined the porewater chemistry by (1) making in situ microelectrode measurements, (2) extracting porewaters, and (3) modeling geochemical reactions. We determined the sediment chemistry by measuring (1) elemental abundance, (2) mineralogy, and (3) trace-element speciation. This information should help the U.S. Navy determine the long-term hazard of the sediments if they are left in place and the short-term hazard if they are dredged.

We did not fully examine the geochemistry of sediments from the West Beach Landfill Wetlands site, because these sediments were distinct from the Seaplane Lagoon sediments. Our initial motivation for studying the Landfill Wetlands site was to determine the trace-element geochemistry in Seaplane Lagoon sediments that had been dredged and then disposed in the Landfill Wetlands. Unfortunately, the location of these dredged sediments is unknown. The cores we sampled were not from the Seaplane Lagoon.

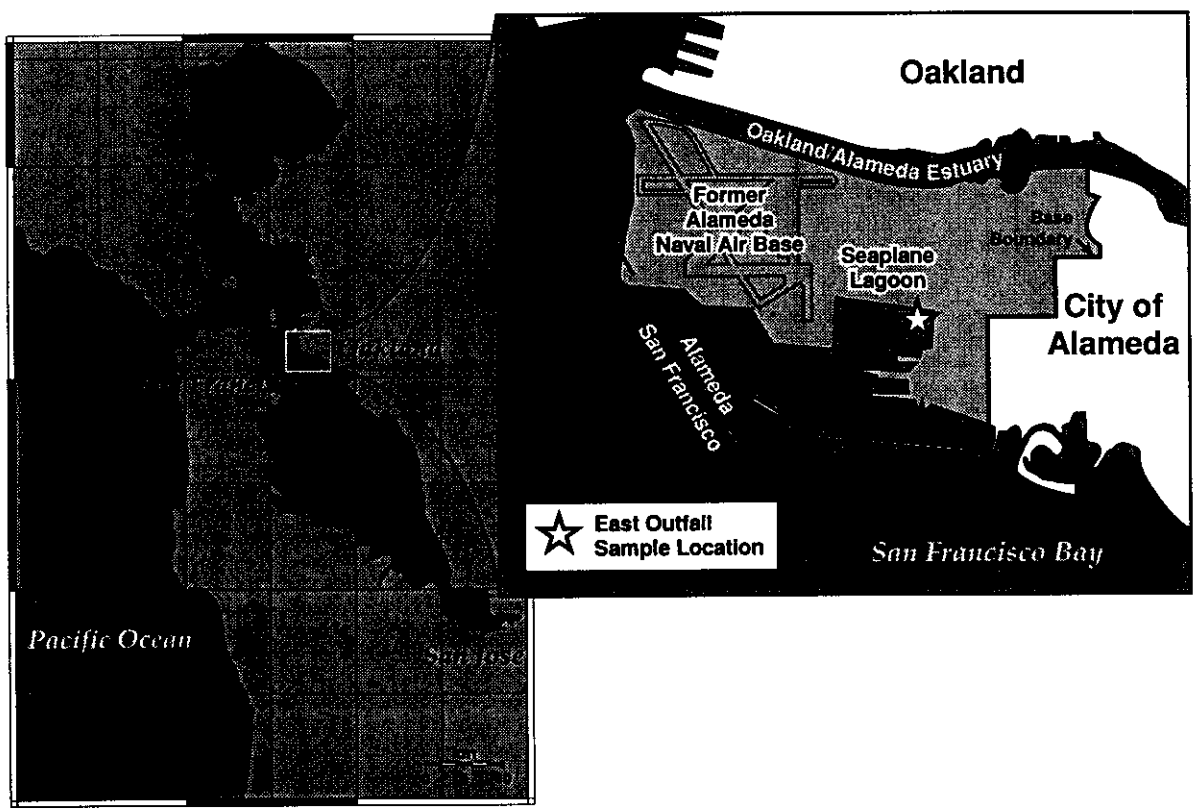

Figure 1. Study site: Seaplane Lagoon at the former Alameda Naval Air Station.

2. Sample Storage and Preparation

In this section, we discuss the cores collected at the Seaplane Lagoon and Landfill Wetlands sites, the storage of these samples, and the preparation techniques used for the geochemical analyses (Table 1; p. 5). Additional details of sample preparation can be found in Section 3. We sampled twelve cores at the east outfall location in the Seaplane Lagoon and two cores in the northern pond in the Landfill Wetlands. Table 2 (p. 6) lists temperature, pH, salinity, conductivity, dissolved oxygen, and turbidity in the Seaplane Lagoon at the time of core collection. These measurements were not made for the cores from the Landfill Wetlands.

2.1 Site 17: Seaplane Lagoon, Gravity Cores

At the Seaplane Lagoon, three 1- to 2-m cores (GH-CC-C1, -C2, and -C3) were collected in acrylic sleeves using gravity coring methods. These cores were wrapped with insulation material, stored upright in a 50-gallon drum that contained dry ice, and transported from the Alameda NAS to Lawrence Livermore National Laboratory (LLNL) between 18:00 and 19:00 on July, 8, 1997. In the LLNL geochemistry laboratory, these cores continued to be stored upright at 22°C for 10 to 20 days until they could be sectioned for sediment analysis. No attempt was made to keep the overlying waters oxygenated. Geochemical characterization of these cores was limited to bulk mineralogy and total metal concentrations of the sediments with depth, and speciation of trace metals in a few sediment samples. Porewaters were not analyzed because gravity coring disturbed the porewater chemistry. All three cores contained large (2–8 mm) pockets of trapped gas and/or water and disturbed "bubble tracks" up the length of the cores. Over time, significant settling of the sediments occurred (e.g., 3 cm of settling over a 1.2-m depth of sediment during 2 to 3 days).

2.1.1 Core GH-CC-C1

Core GH-CC-C1 was extruded directly from its core sleeve into photochemical trays, and a Teflon spatula was used to section the core into segments 3 to 20 cm long. The coherent lowermost sediment sections were extruded first; consequently, the samples were numbered from the bottom up. The uppermost 5 cm of sediment was lost during the extrusion. Sediment subsamples were taken from the top of these sections, and loaded into airtight bags for use in making x-ray absorption spectroscopy (XAS) samples (~1 g) and freeze drying (~10 g). The remainder of the material was discarded. The sediment remained in the bags at lab temperature (~22°C) for 2 hr before processing. During this time, light gray-brown streaks formed in the sediment suggesting that some oxidation occurred.

2.1.2 Cores GH-CC-C2 and GH-CC-C3

To avoid the processing problems that resulted in significant sediment loss during extrusion of the GH-CC-C1 core, we chose to process gravity cores GH-CC-C2 and -C3 using a technique similar to that described for the push cores in Section 2.2. We scored the core sleeves with a rotary saw so that 3-cm sections could be sequentially removed. The overlying water was siphoned off. A steel hacksaw blade was used to cut through the wall of the core sleeve. A Teflon plate was inserted to isolate the section from the remainder of the core. The newly exposed sediment at the top of the core sleeve was then capped with Parafilm and a clean core cap. From the center of each section, we removed ~1 g of sediment for trace metal speciation and also removed and froze ~10 g of sediment at –20°C in freeze-dry flasks for use in x-ray diffraction and bulk chemical analyses. Sediment nearest to the sleeve walls was discarded.

2.2 Site 17: Seaplane Lagoon, Push Cores

We chose a push core method to collect sediments and porewaters for detailed geochemical characterization because this coring method does not disturb the sediments. Nine 0.5-m sediment cores were collected in Plexiglas sleeves (10 cm OD, 9.5 cm ID) fit to a 4- to 5-m plastic pipe, which was pushed into the sediment by hand from a boat. A ball valve between the core sleeve and the extension pipe created a suction that held the sediment in the sleeve as it was raised to the surface of the water. The bottom of the core sleeve was capped underwater and then loaded into the boat, labeled, stored upright in an ice-cooled and

insulated sample box, and transported to the geochemistry laboratory at LLNL. The cores were stored upright at 22°C and particulate-free (HEPA-filtered) laboratory air was bubbled into the water overlying each core to mimic conditions at Seaplane Lagoon.

2.2.1 Cores GH-CC-SC1 and GH-CC-SC3

Core GH-CC-SC1 was discarded because it had a large water-filled void at its base, and the overlying sediment had progressively cracked as the sample stood on the benchtop after arrival at LLNL. Only solid samples were collected from core GH-CC-SC3, because it was used to develop porewater extraction protocols.

2.2.2 Cores GH-CC-SC2 and GH-CC-SC4

The processing of GH-CC-SC2 was optimized to provide information about the porewater redox chemistry. A gold-amalgam electrode was used to determine the in situ porewater concentrations of O_2, S(–II), Fe, and Mn in successive 3-cm sections down the length of the core. All sample processing (with the exception of the top 5 cm of microelectrode measurements, core sleeve scoring, and porewater squeezing during which the sediment was enclosed inside the core squeezers) was done under nitrogen in a glove box.

The processing of GH-CC-SC4 was optimized to provide information about the trace-metal content of the sediments. All sample processing (with the exception of the scoring and cutting of the core sleeve) was done in a laminar flow hood that contained positive-pressure, HEPA-filtered laboratory air to provide a clean work space.

For both cores, the sleeves were deeply scored at 3-cm intervals down the length of the core. The overlying water was then removed with a syringe. Sectioning of the core was done in a nitrogen-purged glove box for core GH-CC-SC2 and at ambient laboratory conditions for core GH-CC-SC4. A steel hacksaw blade was used to cut through the wall of the sleeve. Care was taken to ensure that the blade only contacted the sediment within 5–10 mm of the core sleeve wall. A 10-cm-wide Teflon plate was inserted to isolate the section from the remainder of the core. The core cap was then removed, and a subcore was made by inserting a 3-cm-deep by 7.6-cm-wide Teflon cup into the sediment. The Teflon-enclosed sediment was immediately transferred to the laminar flow hood for trace-element sampling (core GH-CC-SC4), or was loaded into the core squeezer in a nitrogen glove box (core GH-CC-SC2). The newly exposed sediment at the top of the core sleeve was then capped with Parafilm and a clean core cap. Samples for trace-metal speciation were made under a stream of nitrogen or argon gas in the laminar flow hood, sealed with Mylar tape, and placed directly into a –20°C freezer. The remainder of the sediment that had been enclosed by the Teflon cup (~50 mL) was placed in a freeze-dry flask and was frozen at –20°C. Excess sediments outside of the Teflon cup from core GH-CC-SC4 were used for pH measurements with an Orion SureFlow semi-microelectrode. All plasticware that contacted the sediment was rinsed in distilled and deionized water, washed in a phosphate-free detergent, and then thoroughly rinsed again in distilled and deionized water before drying on KayDry paper towels.

2.2.3 Cores GH-CC-SC5 to GH-CC-SC9

Cores GH-CC-SC5 to -SC9 and core GH-CC-SC2 were used to investigate the spatial and temporal variation of chemistry within the oxic-to-suboxic-to-anoxic sediments at Seaplane Lagoon. Samples for trace-metal speciation were also taken from subcores to investigate the impact of freezing our samples prior to analysis.

2.3 Site 2, West Beach Landfill Wetlands, Push Cores

At the Landfill Wetlands site, two push cores were collected in Plexiglas sleeves (10 cm OD, 9.5 cm ID) by pushing the sleeve directly into the sediment. The sediment had a high clay content, which limited the sampling to only the first 21 cm. The bottom of the core sleeve was capped underwater, labeled, stored upright in an ice-cooled and insulated sample box, and transported to LLNL. The cores were stored upright at 22°C and particulate-free (HEPA-filtered) laboratory air was bubbled into the water overlying each core to mimic conditions at Seaplane Lagoon. Microelectrode measurements of the top 5 cm were made prior to sectioning the core.

2.3.1 Cores W1-CC-SC1 and W1-CC-SC2

Using a technique identical to that used for the Seaplane Lagoon push cores, we scored the core sleeves with a rotary saw so that 3-cm sections could be sequentially removed. The core sleeves were then uncapped, and the overlying water was siphoned off. A steel hacksaw blade was used to make the final cut through the wall of the core sleeve at the uppermost score. Care was taken to minimize the blade's contact with the sediment. A 10-cm-wide Teflon spatula was inserted to isolate the uppermost 3-cm section from the remainder of the core. The newly exposed sediment at the top of the core sleeve was then capped with Parafilm and a clean core cap. About 1 g of sediment was removed with a plastic spatula from the center of each 3-cm-thick-sediment section to make samples for trace-metal speciation, and ~10 g of sediment were removed from the center of each section and frozen at –20°C in freeze-dry flasks to further process sediments. Sediment nearest to the sleeve walls was discarded.

Table 1. Summary of cores and geochemical measurements at Alameda Naval Air Station, California: Site 17—Seaplane Lagoon; Site 2—West Beach Landfill Wetlands.

Core	Latitude/ longitude	Date cored	Time	Analysis	Notes
Site 17, Seaplane Lagoon, East Outfall					
GH-CC-C1	37°46.22′/ 122°17.92′	7/8/97	10:00	–X-ray diffraction –Bulk sediment chemistry –Trace-metal speciation	Samples prepared: 7/18/98
GH-CC-C2	37°46.56′/ 122°17.94′	7/8/97	14:02	–X-ray diffraction –Bulk sediment chemistry –Trace-metal speciation	Samples prepared: 7/22/98
GH-CC-C3	37°46.75′/ 122°17.93′	7/8/97	15:15	–X-ray diffraction –Bulk sediment chemistry –Trace-metal speciation	Samples prepared: 7/28/98
GH-CC-SC1	37°46.779′/ 122°17.958′	7/10/97	11:15		Discarded
GH-CC-SC2	37°46.774′/ 122°17.965′	7/10/97	11:30	–Porewater redox chemistry –X-ray diffraction –Bulk sediment chemistry –Trace-metal speciation	Core processing optimized for porewater redox chemistry: 7/13–14/98
GH-CC-SC3	37°46.803′/ 122°17.968′	7/10/97	11:45	–X-ray diffraction –Bulk sediment chemistry –Trace-metal speciation	Porewater protocol development: 7/11/98
GH-CC-SC4	37°46.783′/ 122°17.949′	7/10/97	12:00	–Major- and trace-porewater concentrations –X-ray diffraction –Bulk sediment chemistry –Trace-metal speciation	Core processing optimized for porewater trace-element concentrations: 7/12/98
GH-CC-SC5	a	11/10/97	~12:00	–Porewater redox chemistry	Measurements made: 11/18/98
GH-CC-SC6	a	11/10/97	~12:00	–Porewater redox chemistry	Measurements made: 11/19/98
GH-CC-SC7	a	11/10/97	~12:00	–Porewater redox chemistry	Measurements made: 11/19/98
GH-CC-SC8	37°46.750′/ 122°17.920′	4/8/98	~12:00	–Porewater redox chemistry	Measurements made: 4/10/98
GH-CC-SC9	37°46.735′/ 122°17.945′	4/8/98	~12:00	–Porewater redox chemistry	Measurements made: 4/10/98
Site 2, West Beach Landfill Wetlands					
W1-CC-SC1	37°47.138′/ 122°19.823′	4/8/98	~14:00		Measurements made: 4/9/98
W1-CC-SC2	37°47.088′/ 122°19.753′	4/8/98	~14:00		Measurements made: 4/9/98

[a]Global positioning system (GPS) instrument could not acquire the three satellites necessary for location determination. Cores GH-CC-SC5 to -SC7 were collected approximately 2 m apart, and from the same general location as the previous short cores taken from the SE corner of the Seaplane Lagoon.

Table 2. Temperature, pH, salinity, conductivity, dissolved oxygen, and turbidity in the Seaplane Lagoon at the time of core collection.

Core	Temperature (°C)	pH	Salinity (parts per thousand)	Conductivity (mS/cm)	Dissolved oxygen (mg/L)	Turbidity
GH-CC-C1[a]	25.1	8.0	27.3	42.3	4.7	59
GH-CC-C2[a]	23.6	8.3	27.3	42.4	4.5	78
GH-CC-C3[a]	25.3	8.0	27.3	42.4	5.1	105
GH-CC-SC2[a] (represents -SC1 to -SC4)	21.0	8.3	28.3	43.7	9.0	43
GH-CC-SC5 to GH-CC-SC7[b]	16.9	7.9	25.5	40.0	8.4	7
GH-CC-SC5 to GH-CC-SC7[c]	16.6	8.0	29.3	44.8	8.3	7
GH-CC-SC8 to GH-CC-SC9[c]	14.2	8.3	15.5	25.6	12.2	10

[a]Measurement made immediately above sediment-water interface.

[b]Measurement made in surface waters.

[c]Measurement made in overlying waters at 1-m depth.

3. Experimental Methods and Materials

3.1 Porewater Chemistry

Geochemical characterization of porewaters as a function of sediment depth is limited by the amount of water that can be extracted from the sediments. We employed three different methods to obtain dissolved major- and trace-element and oxidation-reduction species needed to understand the partitioning of the trace metals from the sediments to the porewaters. In situ concentrations of dissolved O_2, S(–II), Mn(II), and Fe(II) were measured with a gold-amalgam microelectrode down the length of GH-CC-SC2 and within the top 5 cm of cores GH-CC-SC5 to -SC9, and W1-CC-SC1 and -SC2. Porewater collection from core GH-CC-SC2 was optimized for Fe(II), SO_4^{2-}, and HS^- concentrations; porewater from core GH-CC-SC4 was optimized for trace-element concentrations (Cd, Cr, Cu, Ni, Pb, and Zn).

3.1.1 Microelectrode Measurements

Gold-amalgam electrodes were used to determine the in situ porewater concentrations of O_2, S(–II), Fe(II), and Mn(II) down the length of core GH-CC-SC2 and within the top 5 cm of cores GH-CC-SC5 to -SC9 from the Seaplane Lagoon and cores W1-CC-SC1 and -SC2 from the Landfill Wetlands. The electrode was a fine-tipped (45 mm × 500 µm) glass-based Au/Hg amalgam (100-µm) electrode with AgCl-reference and Pt-counter electrodes. Calibrations of the electrode using square-wave voltammetry were conducted with a $MnCl_2$-4 H_2O standard in seawater purged with nitrogen. Sensitivity ratios of Fe(II) and S(–II) were calculated from relative Mn(II) ratios [Brendal and Luther, 1995]. Oxygen sensitivity (linear-sweep voltammetry) was checked against the fully aerated water (overlying water from the core) and Mn(II):O_2 sensitivity ratios. The Fe(III)- and FeS-colloid signals correspond only to those particles that can react at the electrochemical double layer. Therefore, colloid distributions are reported in current, but their absolute concentrations are unknown. All experiments with the cores were conducted at room temperature (19.5–22°C).

3.1.2 Analyses of Porewaters Extracted by Core Squeezer

Processing of core GH-CC-SC2 was optimized for porewater oxidation-reduction chemistry. Immediately after we made the microelectrode measurements, we used Reeburgh-type pneumatic core squeezers to extract the porewaters from successive 3-cm sections. Core sections were loaded in a nitrogen-purged glove box and then removed to a laminar flow hood for water extraction. Individual vials were filled under a stream of argon to minimize oxidation. Immediately after collection, Fe(II) was measured, total sulfur and carbon samples were stored at 4°C, and sulfur speciation, nitrogen and phosphorous samples were stored at –20°C. Nitrogen and phosphorous measurements were not made. Procedural blanks were made by filtering distilled and deionized water from trace-metal, clean, high-density polyethylene (HDPE) bottles through the core squeezers in the laminar flow hood.

3.1.3 Analyses of Porewaters Extracted by Centrifugation

Processing of core GH-CC-SC4 was optimized for porewater trace- and major-element concentrations. All sectioning of this core was done at ambient laboratory conditions, but great care was taken to minimize oxidation of sediments by loading and sealing argon-filled centrifuge tubes with the sediments under an argon stream. The sediment samples were centrifuged at 5000 rpm for 60 minutes to separate particles greater than 1-µm diam. No attempt was made to control the temperature of the samples in the centrifuge. These waters were then filtered with 0.22-µm polycarbonate filters and previously cleaned syringes (ultrapure nitric acid, and distilled and deionized water). Immediately after collection, trace- and major-element samples were acidified to pH < 2 with ultrapure nitric acid and were stored at 4°C; total chloride samples were stored at 4°C; and sulfur speciation samples were stored at –20°C. Samples were taken for nitrogen and phosphorous analyses, but these measurements

were not made. Several procedural blanks were processed through the same protocols as the porewater samples. Bottle blanks were also run by leaching acid-cleaned bottles with pH 2 nitric acid over the sample storage time.

3.1.4 Water Analyses

3.1.4.1 Trace Elements

Aluminum, cadmium , chromium, copper, iron, lead, manganese, nickel, and zinc were measured in Seaplane Lagoon porewaters using a Hewlett-Packard HP4500 inductively coupled plasma-mass spectrometer (ICP-MS). For aluminum, manganese, and iron analyses, very small (<1-mL) aliquots of porewater were diluted to a salinity of 1 psu with ultrapure 2% nitric acid. Diluted samples were spiked with an internal standard (10 ng/mL Sc and Y) and run under normal plasma conditions. Calibration was against matrix-matched standards prepared by adding known amounts of Al, Mn, and Fe to a seawater reference standard (NASS-4) diluted to 1 psu. The calibration range was 0.05 to 50 ng/mL . The ^{27}Al, ^{55}Mn, and ^{57}Fe count rates were normalized against ^{45}Sc and ^{89}Y internal standards to account for changes in instrumental response over time. Detection limits were determined from the reproducibility (3 s.d.) of procedural blanks, and are 1, 0.1, and 100 ng/mL for Al, Mn and Fe, respectively. Stated errors (2 s.d.) are generally less than 5–10%, and include propagated errors from count rate, calibration, and blank.

For cadmium, chromium, copper, lead, nickel, and zinc, small (10-mL) aliquots of porewater were weighed into 30-mL acid-cleaned Teflon vials, and were equilibrated with a mixed enriched isotope spike by heating for 48 hours. The enriched isotope spike solution contained:

- ^{111}Cd (95.3 at.%),
- ^{52}Cr (98.2 at.%),
- ^{65}Cu (99.6 at.%),
- ^{206}Pb (99.7 at.%),
- ^{61}Ni (88.8 at.%),
- ^{67}Zn (94.6 at.%).

Trace metals were extracted from the equilibrated porewater solutions by precipitating $Mg(OH)_2$ from seawater at pH 10, which scavenges a number of trace metals. Careful washing of the precipitate with pH 10 ultrapure ammonium hydroxide solution removes sea salts (Na, Cl, etc.), and produces a trace-metal concentrate suitable for isotope dilution ICP-MS analysis [Boyle and Wu, 1997]. After preconcentration, samples were analyzed for isotopic composition, and concentration was determined by applying the isotope dilution equation to measured:

- ^{110}Cd/^{111}Cd and ^{112}Cd/^{111}Cd,
- ^{53}Cr/^{52}Cr,
- ^{63}Cu/^{65}Cu,
- ^{207}Pb/^{206}Pb and ^{208}Pb/^{206}Pb,
- ^{60}Ni/^{61}Ni and ^{62}Ni/^{61}Ni,
- ^{68}Zn/^{66}Zn.

When two ratios were used, both ratios gave the same concentration after application of the isotope dilution equation. Chromium and copper were determined from aliquots of the preconcentrated solutions run under cool plasma conditions to reduce ArC and ArMg interferences. The ^{65}Cu was corrected for interference from ^{40}Ar^{25}Mg, the largest source of uncertainty, using measured mass 66/68 count ratio. Lead and zinc were determined from aliquots of the preconcentrated solutions run under hot plasma conditions to enhance sensitivity at high masses. Yields for Cd and Ni by $Mg(OH)_2$ precipitation are low, and most of the Cd and Ni in the original porewater solution ends up in the supernatant or in the washes. To recover this majority fraction, the supernatant and washes were combined, and residual trace metals were extracted using an automated preconcentration/matrix elimination system, the Cetac Corporation DSX-100. Processed solutions were analyzed under hot plasma conditions.

For all isotope dilution determinations, the error in the measured ratios was less than 10% (2 s.d.) and generally in the range of 1–4%. Error was not propagated though the isotope dilution equation, but samples were spiked close to the geometric mean of the natural and spike ratios to reduce the magnification of the concentration error. A conservative estimate of 2-standard-deviation precision in the concentration measurements is 10–15% for Cr, Ni, Cd, and Pb; and 15–20% for Cu and Zn. Detection limits were determined from the 3-standard-deviation reproducibility in procedural blanks.

Filtered leachate samples were collected in acid-cleaned 60- and 120-mL HDPE bottles, and were adjusted to pH < 2 with ultrapure nitric acid. The DSX-100 was used to preconcentrate the solutions 5 to 10 times. The preconcentrated solutions were spiked with an internal standard (10 ng/g Sc, Y, In, Tb, and Bi), and were run under hot plasma conditions. Quantitation was by external calibration against a series of standards in 2% nitric acid, and by internal standardization to correct for matrix effects and instrument drift. Reported errors include both measurement and calibration uncertainties. Yields were determined by processing reference seawater standards to which measured amounts of analyte metals had been added and equilibrated. Yields for Mn, Ni, Cu, Cd, Pb, and U were 60–65%; the yield for Zn was 80%, and the yield for Cr was 40%. Yields varied by 10–15%, which limited the reproducibility of this trace-metal analyses. Detection limits were determined by processing ion-exchange resin beads through the DSX-100 chemistry under the same conditions as the leachate samples. No significant differences were seen in different batches of resin. Accuracy was assessed by determining metal concentrations in two seawater reference standards, NASS-4 and CASS-3. Metals were also determined in water from Long's Marine Laboratory in Santa Cruz, California, collected at a different time than the water used in the leachate study.

3.1.4.2 Major Elements

All aqueous samples were diluted ten times with distilled and deionized water, and were analyzed by a Fisons Instruments (Model 3560) inductively coupled plasma-atomic emission spectrometer for total dissolved Al, Ca, Fe, K, Mg, Mn, S, and Si. The reproducibility of this technique was better than 2%. Calibration curves were made with 5 standards in distilled and deionized water. Calibration was checked after 10 sample analyses.

3.1.4.3 Sulfur

Sulfur speciation was determined by ion chromatography using a Beckman 421A controller, a LDC Milton Roy Conducto Monitor III conductivity detector, and a Waters 4.6 × 150 mm IC-Pak Anion HC column. The mobile phase was 0.45-µm filtered (helium-purged) 5-mM sodium phosphate dibasic. The flow rate was 2 mL per minute. The injection volume was 100 µL.

Sulfide, sulfate, sulfite, and thiosulfate were examined. Samples were diluted for the sulfide analysis, and undiluted for the sulfate, sulfite, and thiosulfate analyses. Multi-point calibration curves of $Na_2S{\cdot}9H_2O$ for sulfide, Na_2SO_4 for sulfate, Na_2SO_3 for sulfite, and $Na_2S_2O_3$ for thiosulfate were performed prior to analysis. Calibration checks were performed before, in the middle and after sample analysis. Matrix spikes of the samples were performed and were within 10% of the true value. The limit of detection for this analytical method was 5 mg/L for each of the analytes of interest. Precision and accuracy were ±10%.

3.1.4.4 Chloride

Chloride concentration of the samples were determined using an ion-specific probe. A multi-point NaCl calibration curve in distilled and deionized water was made prior to analysis. Calibration checks were performed before, in the middle, and after sample analysis. Matrix spikes of the samples were performed and were within 10% of the true value. The limit of detection for this analytical method was 0.010 mg/L. Precision and accuracy were >10%.

3.1.4.5 Total Carbon

Analysis for total inorganic carbon (TIC), total organic carbon (TOC), and total carbon (TC) were made with a O. I. Analytical TOC 700 carbon analyzer. To measure total inorganic carbon, the water samples were acidified to pH < 4 and were heated to 100°C; the evolved CO_2 was trapped in a cooled in-line molecular sieve; after 2 minutes, the trap was heated, and CO_2 was detected with an infrared cell. Total organic carbon was then measured by oxidizing dissolved organic carbon with sodium persulfate at 100°C to CO_2, which was trapped and detected. Total carbon was measured directly by combining the TIC and TOC methods into a single step; CO_2 was trapped and detected.

3.2 Sediment Chemistry

3.2.1 Mineralogy

Sediment mineralogy was determined by x-ray diffraction (XRD) on freeze dried and ground sediment samples from cores GH-CC-C1 to -C3 and GH-CC-SC2 to -SC4 and four clay-size (<2-µm) fractions from cores GH-CC-SC2 and

GH-CC-SC4. Data were collected from random orientation powder samples with a Scintag PAD V instrument using a Cu K-α source at 45 kV and 35 mA from 2 to 92 deg 2θ in 0.02-deg steps. X-ray entrance slits were 1 × 2 mm and exit slits were 0.3 × 0.2 mm. Raw data were calibrated against known standards (a Si, W, Ag composite, and a mica). Calibration was verified every 5 to 6 scans. The mineralogy of each sample was determined by comparison of sediment patterns with known standards for pure minerals phases. XRD cannot detect amorphous solids or minerals that are present at <2 to 5 wt%.

The clay-size fractions (<2 μm) from two samples were separated from the top sediment (sections of cores GH-CC-SC2-1 and -SC4-1) and two samples from deeper sediment (sections GH-CC-SC2-7 and -SC4-7) by dispersion in 85 mL of distilled and deionized water and centrifugation at 500 rpm for nine minutes to settle out >2-μm particles. The suspension was decanted, and the process was repeated six times. To concentrate the clay minerals, $MgCl_2$ was added to 1N, and the solution was centrifuged and then decanted. The $MgCl_2$ was removed from clay minerals by rinsing in distilled and deionized water, spinning down the suspension, decanting the solution, and repeating the process. XRD spectra were collected on air-dried and ethylene-glycol-saturated samples to separate some of the diagnostic clay peaks (e.g., smectite from chlorite). The air-dried samples were made by drying a smear of the clay slurry in a 100% humidified environment for 48 hours and then in air. The sample was then saturated with ethylene glycol for 12 to 24 hours. Diffraction patterns were collected from 2 to 62-deg 2θ for the air-dried samples and 2 to 42-deg 2θ for the ethylene-glycol-saturated samples.

3.2.2 Bulk Chemistry

The sediments were digested with UA2 acid mixtures (Unisolv, Inc.) in a microwave and neutralized and stabilized with UNSA2 solutions (Unisolv, Inc.). These solutions were analyzed for Ag, Al, As, B, Ba, Ca, Cd, Ce, Co, Cr, Cu, Fe, K, Li, Mg, Mn, Mo, Na, Ni, Pb, S, Sb, Se, Si, Sn, Sr, Ta, Th, Ti, Tl, U, V, W, and Zn. Analysis protocol adheres to EPA SW-846 Method 6010A augmented to include all elements listed above. A scandium spike was added to all samples to correct for viscosity effects resulting from the high silica content of these sediments. The quartz content prevented recovery of silica concentrations because silica did not stay in solution. The external standard was the National Institute of Standards and Technology Buffalo River sediment.

3.2.3 Trace-Element Speciation

Trace-element speciation in the reacted and leached Seaplane Lagoon sediments were determined from XAS for Cd, Cr, Pb, and Zn. We were not able to determine Cu, Hg, or Ni speciation in the sediments because the concentrations were too low to yield interpretable spectra. Absorption spectra of defrosted wet sediments (cores GH-CC-C1, -C3, and -SC4) and fresh sediments (core GH-CC-SC9) were collected at Stanford Synchrotron Radiation Laboratory on beamlines 4-1 and 4-3 at room temperature under dedicated conditions (3 GeV, 40–90 mA) for Cd, Cr, Pb and Zn using Si (220) and Si (111) monochromator crystals and an unfocused beam. The sediment samples were undiluted and fluorescence spectra were collected with a four-element Ge array detector provided by P. Allan and colleagues at Lawrence Berkeley National Laboratory, or a 13-element Ge array detector provided by the Stanford Synchrotron Radiation Laboratory. Reference solids (minerals and fresh precipitates) were collected in transmission-mode using Ar- or Kr-filled ion chambers. Energy calibration was obtained by simultaneous collection of an Ag (for Cd), Cr, Pb, and Zn foil spectrum. Harmonic rejection was achieved by detuning the incoming beam by 50% of maximum intensity. Typically 10 to 35 scans were collected and averaged for each sample. Data reduction and analysis and reference phase-shift and amplitude functions were generated using FEFF6 [Rehr, 1993; Rehr et al., 1992] based on atomic clusters from known crystal structures and were fit to experimental XAS spectra for model compounds to estimate values for σ^2 and S_0^2.

3.3 Leaching Experiments

Three samples of Seaplane Lagoon sediment GH-CC-SC4-11 were leached with filtered seawater from the Pacific Ocean (Long's Marine Laboratory, University of California, Santa Cruz) to determine the rate at which trace elements are released into waters when exposed to oxygen-rich waters. The experiments were performed in flow-through reactors at room temperature [Knauss and Wolery, 1986]. An identical control experiment

with seawater was also run to provide procedural blanks for the trace-metal analyses. Reaction vessels and water bottles were cleaned in a Class 100 clean room. In these experiments, the rate of trace element leached is proportional to the change in concentration between the input and output solutions. Input and output solutions were collected 20 times over a three month period. Sample pH was measured immediately after the sample was collected. Samples for trace-element analysis were acidified with trace-element-grade acid to prevent precipitation; sample bottles were double bagged and stored in a laminar flow hood or a class 100 clean room until they were analyzed by ICP-MS (see Section **3.1.4.1**). At the end of these experiments, the sediments were loaded into x-ray absorption holders and stored at -20°C until metal speciation analysis at the Stanford Synchrotron Radiation Laboratory (see Section **3.2.3**).

3.4 Geochemical Modeling of Porewaters

The aqueous data were analyzed with the Geochemist's Workbench geochemical code [Bethke, 1994] and SUPCRT92 database [Johnson et al., 1992] modified to include zinc-, cadmium-, and lead-carbonate, and zinc- and cadmium-hydroxide phases (Table 3, p. 12). For these calculations, we used porewater trace- and major-element concentrations, HS^- and SO_4^{2-} concentrations to calculate Eh, sediment pH from core GH-CC-SC4, field temperature, and alkalinity from total inorganic carbon analyses from core GH-CC-SC2. Manganese concentrations used were an average of the ICP-AES and ICP-MS measurements; aluminum, cadmium, chromium, copper, iron, lead, nickel, and zinc were measured by ICP-MS; calcium, magnesium, potassium, silica, sodium were measured by ICP-AES. Alkalinity is taken as HCO_3^- concentration, and is calculated as a function of depth for core GH-CC-SC4 from a linear regression of the inorganic-carbon concentration measured in core GH-CC-SC2 data. For the surface sediments at 1.5 cm, alkalinity is calculated from measured pH and atmospheric CO_2, because the linear extrapolation yielded negative values. The solution was charge balanced by adjusting the chloride concentration.

Table 3. Thermodynamic equilibria and constants *K* used in the geochemical modeling of the porewater chemistry in the Seaplane Lagoon sediments.

	log *K* (25°C)	Reference
$Al(OH)_3$(gibbsite) + $2H^+ = Al^{3+} + 3H_2O$	7.76	Pokrovskii and Helgeson, 1995
AlOOH(boehmite) + $3H^+ = 2Al^{3+} + 2H_2O$	7.56	Pokrovskii and Helgeson, 1995
$CaCO_3$(calcite) = $Ca^{2+} + CO_3^{2-}$	–8.48	Helgeson et al., 1978
$CaMg(CO_3)_2$(dolomite) = $Ca^{2+} + Mg^{2+}\ 2CO_3^{2-}$	–18.14	Helgeson et al., 1978
$CaSO_4$*$2H_2O$(gypsum) = $Ca^{2+} + SO_4^{2-} + 2H_2O$	–4.48	Robbie et al., 1979
$Cd^{2+} + H_2O = CdOH^+ + H^+$	–10.08	Baes and Mesmer, 1976
$Cd^{2+} + 2H_2O = Cd(OH)_2^0 + 2H^+$	–20.34	Baes and Mesmer, 1976
$Cd^{2+} + 3H_2O = Cd(OH)_3^- + 3H^+$	–33.29	Baes and Mesmer, 1976
$Cd^{2+} + 4H_2O = Cd(OH)_4^{2-} + 4H^+$	–47.33	Baes and Mesmer, 1976
$Cd^{2+} + CO_3^{2-} = CdCO_3^0$	3.00	Stipp et al., 1993
$Cd^{2+} + 2CO_3^{2-} = Cd(CO_3)_2^{2-}$	6.40	Stipp et al., 1993
$Cd^{2+} + CO_3^{2-} + H^+ = CdHCO_3^+$	11.83	Stipp et al., 1993
$Cd^{2+} + SO_4^{2-} = CdSO_4^0$	–0.003	Wagman et al., 1982
$Cd(OH)_2$(beta) + $2H^+ = Cd^{2+} + 2H_2O$	13.64	Baes and Mesmer, 1976
$CdS = S^{2-} + Cd^{2+}$	–28.84	Wagman et al., 1982
$CdSO_4$(angelsite) = $Cd^{2+} + SO_4^{2-}$	–0.11	Wagman et al., 1982
$CdCO_3$(otavite) = $Cd^{2+} + CO_3^{2-}$	–12.1	Stipp et al., 1993
CdO(monteponite) + $2H^+ = Cd^{2+} + H_2O$	15.1	Cox et al., 1989
$CrS + H^+ + 0.25O_2(aq) = 0.5H_2O + Cr^{3+} + S^{2-}$	16.46	Dellien et al., 1976
Cr_2O_3(eskolaite) + $6H^+ = 3H_2O + 2Cr^{3+}$	7.64	Wagman et al., 1982
CuS(covellite) = $S^{2-} + Cu^{2+}$	–35.77	Helgeson et al., 1978
$CuFeS_2$(chalcopyrite) = $Fe^{2+} + Cu^{2+} + 2S^{2-}$	–58.43	Helgeson et al., 1978
$Cu_2CO_3(OH)_2$(malachite) + $2H^+$ = $H_2O + CO_3^{2-} + 2Cu^{2+}$	–4.40	Helgeson et al., 1978
CuO(tenorite) + $2H^+ = Cu^{2+} + H_2O$	7.66	Helgeson et al., 1978
FeS_2(pyrite) + H_2O = $Fe^{2+} + 2S^{2-} + 0.5O_2(aq) + 2H^+$	–85.10	Helgeson et al., 1978
FeS(pyrrhotite) = $Fe^{2+} + S^{2-}$	–16.65	Helgeson et al., 1978
$FeCO_3$(siderite) = $Fe^{2+} + CO_3^{2-}$	–10.52	Helgeson et al., 1978
FeOOH(goethite) + $2H^+$ = $Fe^{2+} + 1.5H_2O + 0.25O_2(aq)$	–7.96	Robbie et al., 1979
$Na_{.33}Fe_2Al_{.33}Si_{3.67}O_{10}(OH)_2$(Na-nontronite) + $5.32H^+$ = $2Fe^{2+} + O.5O_2(aq) + 0.33Na^+ + 3.67SiO_2 + 3.66H_2O$	–28.51	Wolery, 1978
$Mg_5Al_2Si_3O_{10}(OH)_8$ (7-Å chlorite) + $16H^+$ = $2Al^{3+} + 12H_2O + 3SiO_2(aq) + 5Mg^{2+}$	70.61	Helgeson et al., 1978

Table 3 (Continued). Thermodynamic equilibria and constants *K* used in the geochemical modeling of the porewater chemistry in the Seaplane Lagoon sediments.

	log *K* (25°C)	Reference
$MnS(alabandite) = Mn^{2+} + S^{2-}$	–13.33	Helgeson et al., 1978
$MnCO_3(rhodochrosite) = Mn^{2+} + CO_3^{2-}$	–10.52	Helgeson et al., 1978
$NiS_2(vaesite) + H_2O = Ni^{2+} + 2S^{2-} + 0.5O_2(aq) + 2H^+$	–87.21	Helgeson et al., 1978
$NiS(millerite) = Ni^{2+} + S^{2-}$	–20.97	Vaughan and Craig, 1978
$NiCO_3 = CO_3^{2-} + Ni^{2+}$	–6.82	Wagman et al., 1982
$Ni(OH)_2 + 2H^+ = Ni^{2+} + 2H_2O$	7.64	Wagman et al., 1982
$PbS(galena) = Pb^{2+} + S^{2-}$	–27.28	Wagman et al., 1982
$Pb^{2+} + H_2O = PbOH^+ + H^+$	–7.7	Smith and Martell, 1989
$Pb^{2+} + 2H_2O = Pb(OH)_2^- + 2H^+$	–17.09	Smith and Martell, 1989
$Pb^{2+} + 3H_2O = Pb(OH)_3^- + 3H^+$	–28.09	Smith and Martell, 1989
$Pb^{2+} + CO_3^{2-} = PbCO_3$	6.58	Bilinski and Schindler,1982[a]
$Pb^{2+} + 2CO_3^{2-} = Pb(CO_3)^{2-}$	9.40	Bilinski and Schindler,1982[a]
$PbCO_3(cerrusite) = Pb^{2+} + CO_3^{2-}$	–13.54	Johnson et al., 1992
$Pb_3(CO_3)_2(OH)_2(hydrocerussite) + 2H^+ = 2CO_3^{2-} + 3Pb^{2+} + 2H_2O$	–18.81	Smith and Martell, 1989
$PbSO_4(anglesite) = Pb^{2+} + SO_4^{2-}$	–7.85	Helgeson et al., 1978
$SiO_2(quartz) = SiO_2(aq)$	–4.0	Helgeson et al., 1978
$SiO_2(\alpha\text{-cristobalite}) = SiO_2(aq)$	–3.45	Helgeson et al., 1978
$SiO_2(am.\ si.) = SiO_2(aq)$	–2.71	Helgeson et al., 1978
$ZnS(sphalerite) = Zn^{2+} + S^{2-}$	–24.38	Helgeson et al., 1978
$Zn^{2+} + H_2O = ZnOH^+ + H^+$	–8.96	Bourcier and Barnes, 1987
$Zn^{2+} + 2H_2O = Zn(OH)_2^0 + 2H^+$	–28.04	Wagman et al., 1982
$Zn^{2+} + 3H_2O = Zn(OH)_3^- + 3H^+$	–28.83	Wagman et al., 1982
$Zn^{2+} + 4H_2O = Zn(OH)_4^- + 4H^+$	–41.61	Wagman et al., 1982
$Zn^{2+} + CO_3^{2-} + H^+ = ZnHCO_3^+$	8.91	Bourcier and Barnes, 1987
$Zn^{2+} + CO_3^{2-} = ZnCO_3^0$	3.9	Zachara et al., 1989
$Zn^{2+} + SO_4^{2-} = ZnSO_4^0$	–0.026	Wagman et al., 1982
$Zn(OH)_2(\beta) + 2H^+ = Zn^{2+} + 2H_2O$	11.93	Wagman et al., 1982
$Zn(OH)_2(\varepsilon) + 2H^+ = Zn^{2+} + 2H_2O$	11.66	Wagman et al., 1982
$Zn(OH)_2(\gamma) + 2H^+ = Zn^{2+} + 2H_2O$	11.88	Wagman et al., 1982
$ZnSO_4(solid) = Zn^{2+} + SO_4^{2-}$	3.55	Wagman et al., 1982
$ZnCO_3(smithsonite) = Zn^{2+} + CO_3^{2-}$	–9.87	Johnson et al., 1992
$Zn_5(OH)_6(CO_3)_2$ (hydrozincite) $+ 6H^+ = 5Zn^{2+} + 2CO_3^{2-} + 6H_2O$	9.65	Schindler et al., 1969

[a] Bilinski and Schindler, 1982 experimental values extrapolated to $I = 0$.

4. Results

4.1 Porewater Chemistry

4.1.1 Porewater Chemistry Across Oxic, Suboxic, and Anoxic Boundaries

Cycling of trace metals among the water column, surface sediments, and deeper sediments in estuary sediments is linked to oxygen, manganese, iron, and sulfur chemistry. For this reason, we measured dissolved O_2, Mn(II), Fe(II), and total S(–II) concentrations and relative concentrations of Fe(III)- and FeS- and elemental S-colloids in the top 5 cm of push cores collected from the east outfall location of Seaplane Lagoon on July 10, 1997, November 10, 1997, and April 8, 1998. Two cores were also collected at the Landfill Wetlands site on April 8, 1998.

The greatest opportunity for the mobility of Mn, Fe, S, and associated trace metals is within the suboxic sediment zone. We define the suboxic zone at sediment depths below the dissolved-oxygen minimum and above the dominance of dissolved sulfide. The results of our study show that depth or size of the suboxic zone in the Seaplane Lagoon sediments may exceed 5 cm, and varies spatially over a short distance and over the course of the year (Table 4, pp. 41–51; Figs. 2–4, pp. 20–22).

Although the size of the suboxic zone varies, the porewater profiles are consistent with general oxidation-reduction reactions (Fig. 5, p. 23). As an example, we use the porewater profile from Seaplane Lagoon core GH-CC-SC2 (Fig. 2, p. 20). Anaerobic respiration occurs within the first 3 mm and is shown by the depletion of dissolved oxygen from the overlying waters into the surface sediments. Denitification most probably occurs between measurable oxygen and Mn(II) (the electrode does not detect nitrogen species). Manganese reduction is shown by the accumulation of dissolved Mn(II) at 14 mm. Precipitation of manganese as Mn(IV)-oxides at depths less than 14 mm and as $MnCO_3$ or MnS at depths greater than 18 mm is indicated by lack of dissolved Mn(II) in the porewaters. Iron reduction begins at 18 mm as dissolved Fe(II) and Fe(III)-colloid increase with depth. Precipitation of FeS or FeS_2 is shown by an increase in dissolved S(–II) and a decrease in dissolved Fe(II) and Fe(III)-colloids at 40 mm. Note that dissolved Fe(II) concentrations include the Fe(III)-colloids because Fe(III)-colloids are reduced to dissolved Fe(II), which is further reduced at the electrode surface [Brendal and Luther, 1995]. At the present time, it is not possible to quantify the Fe(III) colloid component. Sulfate reduction occurs at depths greater than 40 mm and is shown by the increase of dissolved S(–II) with depth. The reproducibility of the dissolved oxygen and sulfide data shows that aerating the overlying waters in the core maintains the chemistry profile in the core.

Figure 3 (p. 21) shows porewater profiles of cores GH-CC-SC5, -SC6, and -SC7 collected within seven meters of one another on November 10, 1997. Comparison of these three cores shows that local disturbances, such as bioturbation, increase the diffusion of oxygen into the sediments and extend the size of the suboxic zone. Moving from east to west, core GH-CC-SC5 is the most reduced with trace concentrations of Mn(II) and Fe(II) from 15 to 40 mM and increasing dissolved S(–II) concentrations at depths greater than 31 mM. The trace-iron and -manganese concentrations in core GH-CC-SC5 compared to other cores indicates that sulfide minerals precipitate at these depths. Core GH-CC-SC6 is the most oxidized sample with dissolved oxygen to 10 mM, increasing concentrations of dissolved Fe(II) and Fe(III)-colloids from 15 to 50 mM, with no detectable dissolved S(–II). The oxidation-reduction state of core GH-CC-SC7 is between that of the other two cores with higher concentrations of dissolved Fe(II) and Fe(III)-colloids than those in core GH-CC-SC5.

Figure 4 (p. 22) shows porewater profiles of cores GH-CC-SC8 and -SC9 collected within a few meters of one another on April 8, 1998. These cores show similar local heterogeneity observed in the November 1997 cores, with core GH-CC-SC8 being more oxidized than core GH-CC-SC9 as is indicated by the absence of dissolved sulfides in core GH-CC-SC8.

Figure 6 (p. 24) shows the porewater profiles of Landfill Wetlands cores W1-CC-SC1 and -SC2 taken on April 8, 1998. The porewater profiles are distinct from one another showing local heterogeneity within the wetlands pond. The most notable difference between the two cores is the

absence of dissolved Fe(II) and Fe(III)-colloids in core W1-CC-SC2. There are several distinctions between the Seaplane Lagoon cores and the Landfill Wetland cores. The Landfill Wetland cores have a smaller oxic zone with dissolved O_2 depletion within 1 mm below the sediment-water interface, and with dissolved S(–II) increases at more shallow depths (1 to 9 mm). Additionally, the Wetlands cores have small amounts of dissolved Mn(II) in waters directly above the sediment–water interface, and in one core, elemental sulfur was detected.

4.1.2 Porewater Chemistry to 50-cm Depth

The porewater chemistry of the Seaplane Lagoon sediments is shown as trace- and major-element chloride, HS^-, SO_4^{2-}, SO_3^-, and pH for core GH-CC-SC4; and as HS^-, SO_4^{2-}, SO_3^-, total carbon, total inorganic carbon, and total organic carbon for core GH-CC-SC2 (Tables 5 and 6, pp. 52–53; Fig. 7, pp. 25–27). In core GH-CC-SC4, there are distinct trends in the porewater composition with depth. Calcium, magnesium, potassium, sodium, and chloride and sulfide concentrations increase with depth to 25.5 cm and at greater depths are constant. The manganese depth profile is more complicated. Manganese decreases to a minimum at 4.5 cm, increases to a maximum at 16.5 cm, and decreases at greater depths. Aluminum concentrations are quite low and constant (with the exception of one outlying data point). Silica concentrations increase by about two times between 1.5 and 4.5 cm and are constant at greater depths. Iron concentrations could only be detected above 4.5 cm. Cadmium, chromium, and lead concentrations increase with depth following similar trends observed for their sediment concentrations. Zinc concentrations increase to maximum at 22.5 cm, decrease to 28.5 cm, and increase at greater depths. Copper concentrations are constant to 22.5 cm, and increase at greater depths. Nickel concentrations show a slight decrease with depth. In core GH-CC-SC2, the dissolved total-inorganic and the sulfide concentrations increase with depth.

4.1.3 Geochemical Modeling

We summarize the porewater geochemistry of Seaplane Lagoon sediments in Table 7 (pp. 54–55) as sulfide, carbonate, oxide/hydroxide, and silicate saturation versus depth. The thermodynamic saturation index *SI* for a solid phase is equal to the ratio of its ion activity product *IAP* and its equilibrium solubility constant K_{sp}:

$$SI = \frac{IAP}{K_{sp}} . \qquad (1)$$

A solution is supersaturated, undersaturated or at equilibrium, if log *SI* is greater than, less than, or equal to zero, respectively. The uncertainty of the log *SI* values is ±0.5.

Dissolved trace-element concentrations are not limited by sulfide phases, despite the fact that the Seaplane Lagoon porewaters are dominated by dissolved sulfides. With the exception of chromium and manganese, the porewaters are supersaturated with respect to all sulfide phases by several orders of magnitude. The porewaters are close to MnS saturation, and are 10 orders of magnitude below CrS saturation (we do not have thermodynamic data for Cr_2S_3). Nor are the dissolved trace-element concentrations limited by the solubility of pure secondary carbonates or oxides/hydroxides. Cadmium, copper, lead, nickel, and zinc are all undersaturated with respect to $CdCO_3$ (otavite) and $Cd(OH)_2$, $Cu_2CO_3(OH)_2$ (malachite), CuO (tenorite), $PbCO_3$ (cerussite), $NiCO_3$ and $Ni(OH)_2$, and $ZnCO_3$ (smithsonite), and β-$Zn(OH)_2$. Dissolved chromium concentrations are 10 to 13 orders higher than Cr_2O_3 (eskolaite) saturation. Dissolved manganese concentrations are close to $MnCO_3$ saturation.

Dissolved silica concentrations are close to saturation with respect to β-cristobalite, a quartz polymorph, but supersaturated with respect to quartz. This result agrees with many groundwater studies. The dissolved aluminum concentrations are close to saturation with respect to $Al(OH)_3$, gibbsite and not 7-Å chlorite, which was identified in the XRD analysis of the sediments. The dissolved calcium concentrations are undersaturated with respect to $CaCO_3$ (calcite) in the surface sediments (1.5 cm), but supersaturated at greater depths. In the top 5 cm, dissolved iron concentrations are closest to FeOOH (goethite) saturation. At depths greater than 5 cm, iron solubility decreases to levels below the detection limit.

4.1.4 Leaching Experiments

The results from the flow-through leaching experiments of Seaplane Lagoon sediment at 31.5 cm depth (GH-CC-SC4-11) are shown in Figs. 8 and 9

(pp. 28–29) and Table 8 (pp. 56–57). Cadmium and zinc are the most reactive, and chromium is the least reactive trace elements in these sediments. The net release of the trace elements to seawater relative to the initial trace-element concentration in the sediment is plotted versus time in Fig. 8 (p. 28) (a ratio of 1000:1 means all of the trace element has leached from the sediment). These curves are simple integrations of the trace-element release rates normalized to the sediment's trace-element concentrations. After 90 days of reaction, 20–40% of the cadmium, 6–12% of the zinc, 1–4 % of the copper, manganese, nickel, and lead, and less than 0.2% of the chromium have been leached into the seawater.

Figure 9 (p. 29) is a plot of the trace-element concentrations measured in the output and input solutions versus time. The difference between the these concentrations is proportional to the leaching rate at that point in time. Cadmium and zinc leaching rates increase during the first 20 days, and then begin to decrease, approaching the blank concentrations at the end of the experiment. Copper leaching behavior is similar to cadmium and zinc, but the absolute concentrations are much lower. Manganese leaching rates decrease from the onset of the experiment to near blank concentrations at the end of the experiment. Lead- and nickel-leaching rates are constant and low. Chromium leaching rates are minimal or nonexistent.

4.2 Sediment Chemistry

Seaplane Lagoon sediment chemistry was determined at the east outfall location from three push cores (GH-CC-SC2, -SC3, and -SC4) and three gravity cores (GH-CC-C1, -C2, and -C3) at 3-cm intervals from the surface sediments to about 40 cm from the push cores and to about 100 cm from the gravity cores. Major- and trace-element chemistry is reported in Table 9 (pp. 58–63) (B, K, Na, Si, and Sn are not tabulated because B and Sn are present in the digestion solutions, because of poor recoveries of K and Na, and because Si was incompletely dissolved in the digestion procedure).

We discuss the depth profiles of cadmium, chromium, cobalt, copper, lead, mercury, and zinc plus the depth profiles of iron, manganese, and sulfur (Figs. 10 and 11, pp. 30–33), because iron, manganese, and sulfur have important roles in the overall oxidation-reduction state of the sediments. Cadmium, chromium, copper, lead, mercury, and zinc trace-element concentrations increase from low values in the surface sediments to higher values at depths greater than 20 to 30 cm below the sediment–water surface. The concentrations range from 10 to 400 ppm (1200 ppm in sample GH-CC-C1-2) for cadmium, from 230 to 1150 ppm (1730 ppm in sample GH-CC-C1-2) for chromium, from 100 to 240 ppm for copper, from 180 to 1400 ppm for lead, from 0.6 to 2 ppm for mercury, and from 240 to 630 ppm for zinc. Trace-element concentrations are low in the deepest samples of the gravity cores. Cobalt and nickel concentrations do not increase with depth. Cobalt concentrations are low and vary between 14 and 30 ppm, and peak concentrations at depths of 20 to 40 cm are as high as 160 ppm. Nickel concentrations vary from 110 to 180 ppm. Iron concentrations increase from about 4.5 wt% in the surface sediments to about 5.5 wt% at a depth of 16.5 cm, and decrease at depths greater than 35 cm. Sulfur concentrations increase from 1 wt% in the surface sediments to about 1.5 wt% at depths of 30 to 40 cm, and are constant at greater depths. Core GH-CC-C1 is an exception, with half as much sulfur as the other cores. Manganese concentrations are constant with depth and are about 450 ppm (950 ppm in sample GH-CC-C1).

4.3 Sediment Mineralogy

The sediments are primarily quartz with about 10–15 wt% in the clay size fraction (<2 μm). There is no difference in the bulk mineralogy as a function of depth. Minerals identified in XRD patterns are 80–90% quartz, ~2 wt% hornblende, ~2 wt% mica, ~2 wt% chlorite, ~2 wt% smectite, ~2 wt% illite, and ~2 wt% pyrite. Reported mineral abundances are estimated by assigning minimum XRD detection limits to the trace-mineral components (~2 wt%).

4.4 Trace-Metal Speciation

Table 10 (pp. 64–65) and Figs. 12–18 (pp. 34–40) show XAS results of cadmium, chromium, lead, and zinc speciation in representative sediments at the Seaplane Lagoon. Concentrations of cobalt, copper, mercury, and nickel are too low to yield interpretable x-ray-absorption spectra. We present our results with both the absorption edge spectra and x-ray absorption fine structure (XAFS) spectra. We examine speciation differences in the surface sediments (samples

GH-CC-SC4-1 at 1.5 cm and GH-CC-SC9-1 at 0 cm) and the deeper sediments (samples GH-CC-SC4-12 at 34.5 cm and GH-CC-SC9-12 at 30 cm); speciation differences between sediments leached with oxygen-rich seawater for three months (GH-CC-SC4-11 at 31.5 cm) and the above samples; and speciation differences resulting from freezing samples to preserve them (core GH-CC-SC4) and fresh (core GH-CC-SC9) samples. We also show results from samples GH-CC-C1-2 at 55 cm for cadmium and GH-CC-C3 at 55 cm for zinc.

4.4.1 Cadmium

Cadmium is present as a disordered CdS solid in the deeper Seaplane Lagoon sediments [Table 10 (pp. 64–65); Figs. 12 and 13 (pp. 34–35)]. Cadmium XAFS spectra are identical (despite the poor data quality for GH-CC-SC9-12) and indicate cadmium coordination by only first-neighbor sulfur atoms, which is characteristic of crystalline CdS(s) compounds (greenockite and hawleyite). However there is no evidence for Cd or Fe atoms beyond the first-neighbors, which is expected from well-crystallized CdS or CdS-FeS mixtures. We compare the sediment spectra with freshly precipitated CdS-FeS spectra to distinguish between sorbed or precipitated cadmium. For all precipitated samples, regardless of the initial solution ratio of cadmium-to-iron, the spectra are identical and show only first-neighbor sulfur atoms, and no evidence for second-neighbor cadmium or iron neighbors. Quantitative results from least-squares fits are the same for the sediment samples and these laboratory precipitates. These results suggest a high degree of local disorder in precipitated CdS(s) and no evidence for solid solution with iron. Cadmium concentrations in the surface sediments are below the detection limit of the analytical technique.

Cadmium speciation changes when the sediments are exposed to oxygen-rich seawater. In the leached sample, cadmium is associated with an oxide or carbonate solid as well as with a sulfide as is shown by the first-neighbor oxygen and sulfur distances. However, the absence of second-neighbor atom(s) in the spectrum precludes direct identification of this new "oxygen" component. We estimate that 66% of the Cd is present as the oxide or carbonate solid, and 33% is present as the sulfide phases from the ratio of fitted peak heights for sulfur and oxygen.

4.4.2 Chromium

Chromium is present as Cr(III) sorbed to clay or iron hydroxide surfaces in the surface and deeper Seaplane Lagoon sediments [Table 10 (pp. 64–65); Figs. 14 and 15 (pp. 36–37)]. The absorption edge of chromium is rich in spectral features and reflects the Cr(III) or Cr(VI) oxidation states. From qualitative comparison with reference solid compounds, it is readily apparent that the sediment spectra lack the prominent pre-edge feature indicative of Cr(VI); the sediments contain only Cr(III). The absorption edge features are very similar among the surface and deeper sediments and among the fresh and frozen sediments. Further comparison of the sediment edge spectra with reference spectra indicates chromium is not bonded by sulfur. This is corroborated by least-squares fits of XAFS spectra, which show Cr-O bonding. In the fresh sediments, we fit only the first-neighbor Cr-O distances typical of Cr(III) in octahedral coordination. Sample GH-CC-SC4-12 has better signal-to-noise than the other two samples and, consequently, more distant atomic neighbors were fit. In addition to a first-neighbor Cr-O distances, two second-neighbor iron atoms can be fit, although it should be noted that other third-row transition metals near to iron will also produce an adequate fit. The nearest second-neighbor peak is at 3.43 Å, which is a characteristic distance for bidentate corner-sharing among transition metal octahedra, that can be explained by chromium sorption to a clay or hydroxide surface. The absence of second-neighbor atoms at ≈3.0 Å suggests that Cr is not nucleating a CrOOH-like phase and forming edge-shared clusters with iron or manganese as found in laboratory studies of chromium sorption and co-precipitation. We have not yet analyzed chromium in the leached sample.

4.4.3 Lead

Lead is associated with an oxide or carbonate phase in the deeper Seaplane Lagoon Sediments [Table 10 (pp. 64–65); Fig. 16 (p. 38)]. Comparison of the energy position of lead absorption edges of model spectra and sediments shows that lead in the sediments is bonded by oxygen and not by sulfur. Two distinct Pb-O distances (2.39 Å and 2.63–2.65 Å) can be resolved in two of the sediment spectra (GH-CC-SC9-12 and GH-CC-SC4-12), although the relative peak amplitudes for the two

distances are very different between the two samples. The fitted Pb-O distances fall with the range of those found for a variety of lead oxide, hydroxide, and carbonate minerals. However, the spectra do not support the possibility of lead associated with residual paint that may have been used at Alameda NAS, primarily in the form of lead chromate ($PbCr_2O_4$) and lead oxides (PbO, PbO_2). The shorter Pb-O distance of 2.39 Å in the sediment spectra does not match the shortest Pb-O distance in lead chromate (2.52 Å), and there is no evidence for chromium atoms at 3.32 to 4.14 Å, which should be apparent in a crystalline mineral. Likewise, both forms of crystalline lead oxide (PbO-tetrahedral and PbO-orthorhombic) and lead dioxide (PbO_2) have first-neighbor oxygen atoms at distances shorter than those found for lead in the sediments (2.15–2.32 Å) and second-neighbor lead atoms at distances less than 4 Å, which are not evident in the spectra of the sediment sample.

We observe no changes in lead speciation when the sediments are exposed to oxygen-rich seawater. The edge spectrum of the leached sample is identical to that of the other samples. On the basis of the similarity among the lead-edge spectra, we assume that lead is still associated with oxide, hydroxide, or carbonate mineral. We only collected lead-edge spectrum on the leached sample, because of limitations of the beamline setup at the time.

4.4.4 Zinc

Zinc is present as two solid components in the surface and the deeper Seaplane Lagoon sediments [Table 10 (pp. 64–65); Figs. 17 and 18 (pp. 39–40)]. Analyses of zinc XAFS spectra show first-neighbor sulfur and oxygen atoms, with sulfur atoms dominating the total signal (≈70–85% based on the ratios of fitted peak heights). Least-square fits show that the spectra can be deconvoluted into a sulfide component with interatomic distances matching the sphalerite (ZnS) structure, and an oxide component with distances consistent with the substitution of zinc into clay minerals or sorption onto edge sites of the octahedral layers. In the sphalerite structure, first-neighbor atoms are sulfur, and the nearest second-neighbor atoms are zinc at a distance of 3.82 Å. In the sediment spectra, there are clearly second-neighbor atoms at 3.13–3.16 Å that are not present in sphalerite and must be associated with the oxide component. The oxide component contains a first-neighbor oxygen (1.96–2.02 Å), and scattering from the second-neighbor atoms can be reasonably, although not uniquely, fit with iron. The fitted distances are similar to metal–metal distances found for edge-shared octahedra in phyllosilicates and layered hydroxides with brucite-like structures. Fits to the XAFS spectra can be improved by including second-neighbor Zn-Si at 3.47–3.48 Å, consistent with interatomic distances found for the substitution of zinc into the octahedral layer of phyllosilicates.

Zinc speciation changes when the sediments are exposed to oxygen-rich seawater. The zinc spectrum for the leached sediment sample shows a significant reduction in amplitude of the sulfide component (about 25%) and a corresponding increase in the oxide component (about 75%). Interatomic distances from the fitted spectrum are the same (within error) as the other samples for the sulfide component. The oxide component present after leaching is different from that found in the other samples. Second-neighbor atoms are best fit with either iron or zinc, or a mixture of the two at 3.13 and 3.32 Å, rather than with silica atoms. This result suggests that as the zinc sulfide dissolves, it reprecipitates in the sediment as a zinc–iron oxyhydroxide.

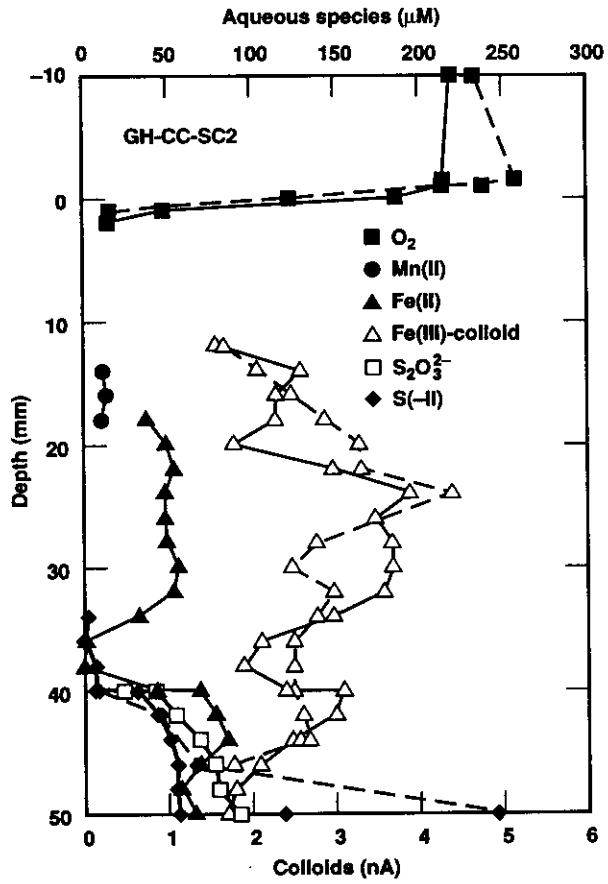

Figure 2. Microelectrode results of porewater chemistry from Seaplane Lagoon core GH-CC-SC2 measured on July 10, 1997 (dashed lines) and July 13, 1997 (solid lines).

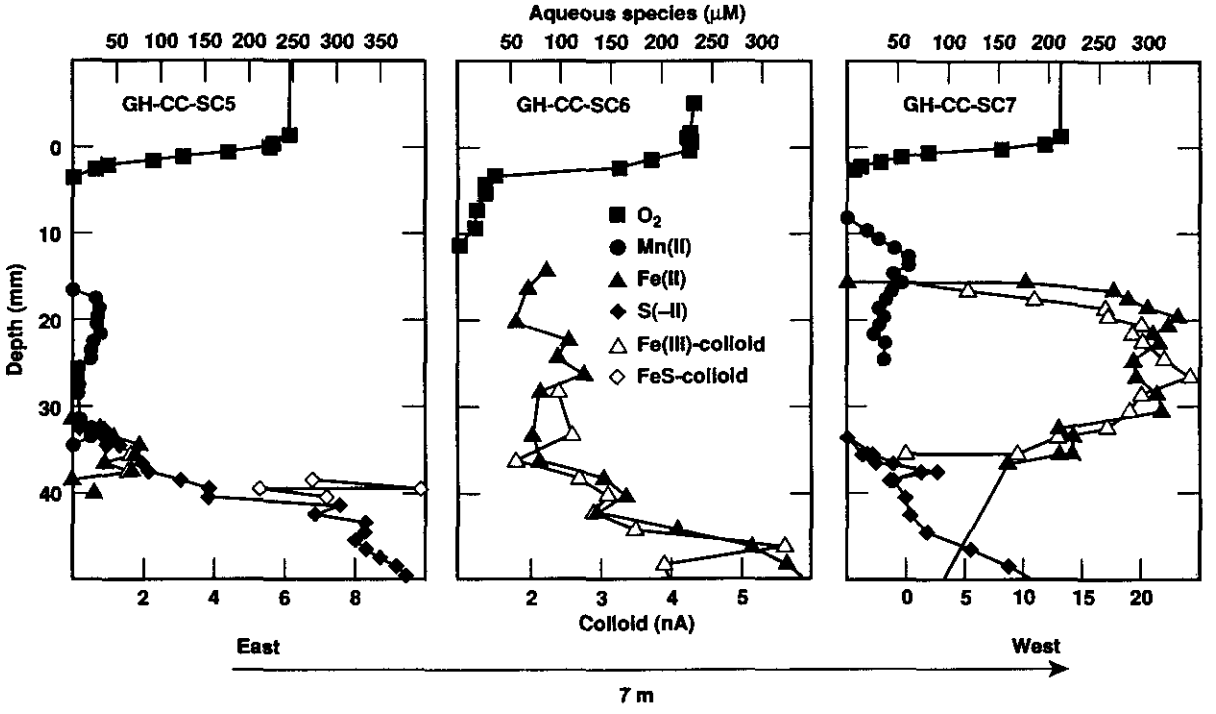

Figure 3. Microelectrode results of porewater chemistry from Seaplane Lagoon cores CC-GH-SC5, -SC6, -SC7 collected on Nov. 10, 1997 and measured on Nov. 18 and 19, 1997.

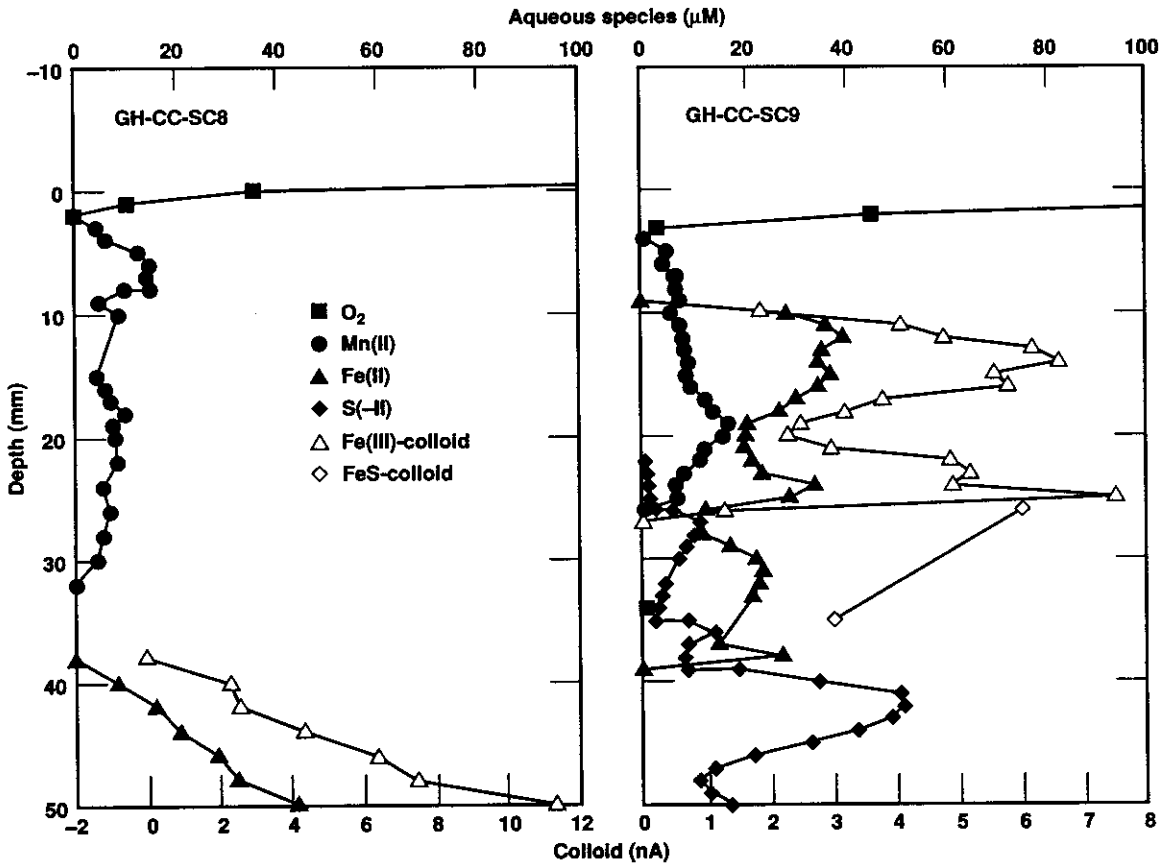

Figure 4. Microelectrode results of porewater chemistry from Seaplane Lagoon cores CC-GH-SC8 and GH-CC-SC9 collected on April 8, 1998 and measured on April 10, 1998.

Oxidation of organic carbon

Anerobic respiration:

$$CH_2O + O_2(g) = CO_2(g) + H_2O$$

Denitrification:

$$CH_2O + 4/5NO_3^- + H^+ = CO_2(g) + 2/5N_2(g) + 7/5H_2O$$

Manganese reduction:

$$CH_2O + 2MnO_2 + 4H^+ = CO_2(g) + 2Mn^{2+} + 3H_2O$$

Iron reduction:

$$CH_2O + 4Fe(OH)_3(am) + 8H^+ = CO_2(g) + 4Fe^{2+} + 11H_2O$$

Sulfate reduction:

$$CH_2O + 1/2SO_4^{2-} + 1/2H^+ = CO_2(g) + 1/2HS^- + H_2O$$

Secondary redox and precipitation reactions

Iron and manganese oxidation:

$$2Mn^{2+} + 4HCO_3^- + O_2(g) = 2MnO_2 + 4CO_2(g) + 2H_2O$$

$$4Fe^{2+} + 8HCO_3^- + O_2(g) + 2H_2O = 4Fe(OH)_3(am) + 8CO_2(g)$$

$$2Fe^{2+} + MnO_2 + 2HCO_3^- + 2H_2O = 2Fe(OH)_3(am) + Mn^{2+} + 2CO_2(g)$$

Carbonate and sulfide precipitation:

$$Fe^{2+} + 2HCO_3^- = FeCO_3 + CO_2(g) + H_2O$$
$$Mn^{2+} + 2HCO_3^- = MnCO_3 + CO_2(g) + H_2O$$

$$Fe^{2+} + 2HCO_3^- + H_2S = FeS + 2CO_2(g) + 2H_2O$$
$$Mn^{2+} + 2HCO_3^- + H_2S = MnS + 2CO_2(g) + 2H_2O$$

Figure 5. Generalized oxidation-reduction and precipitation reactions with depth in estuary sediments, where CH_2O is generic organic carbon.

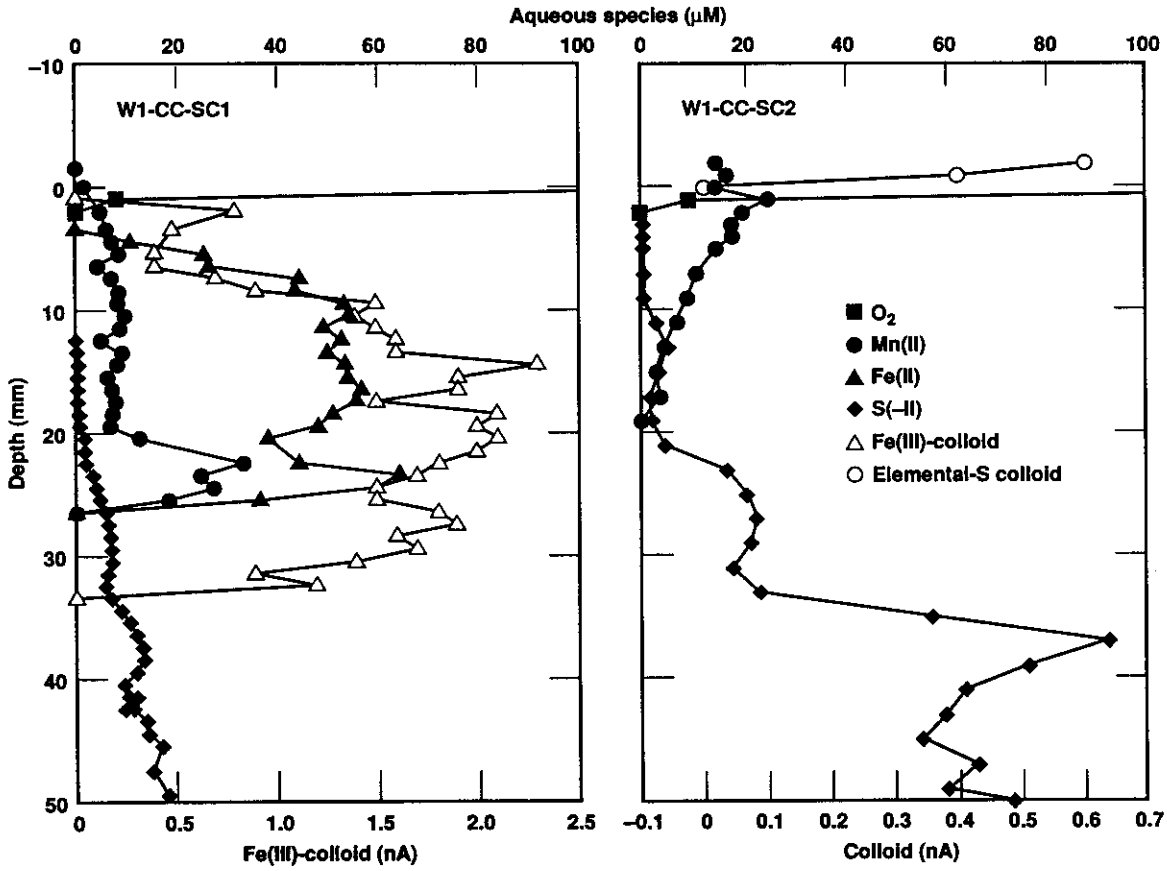

Figure 6. Microelectrode results of porewater chemistry from West Beach Landfill Wetlands cores W1-CC-SC1 and -SC2 collected on April 8, 1998 and measured on April 9, 1998.

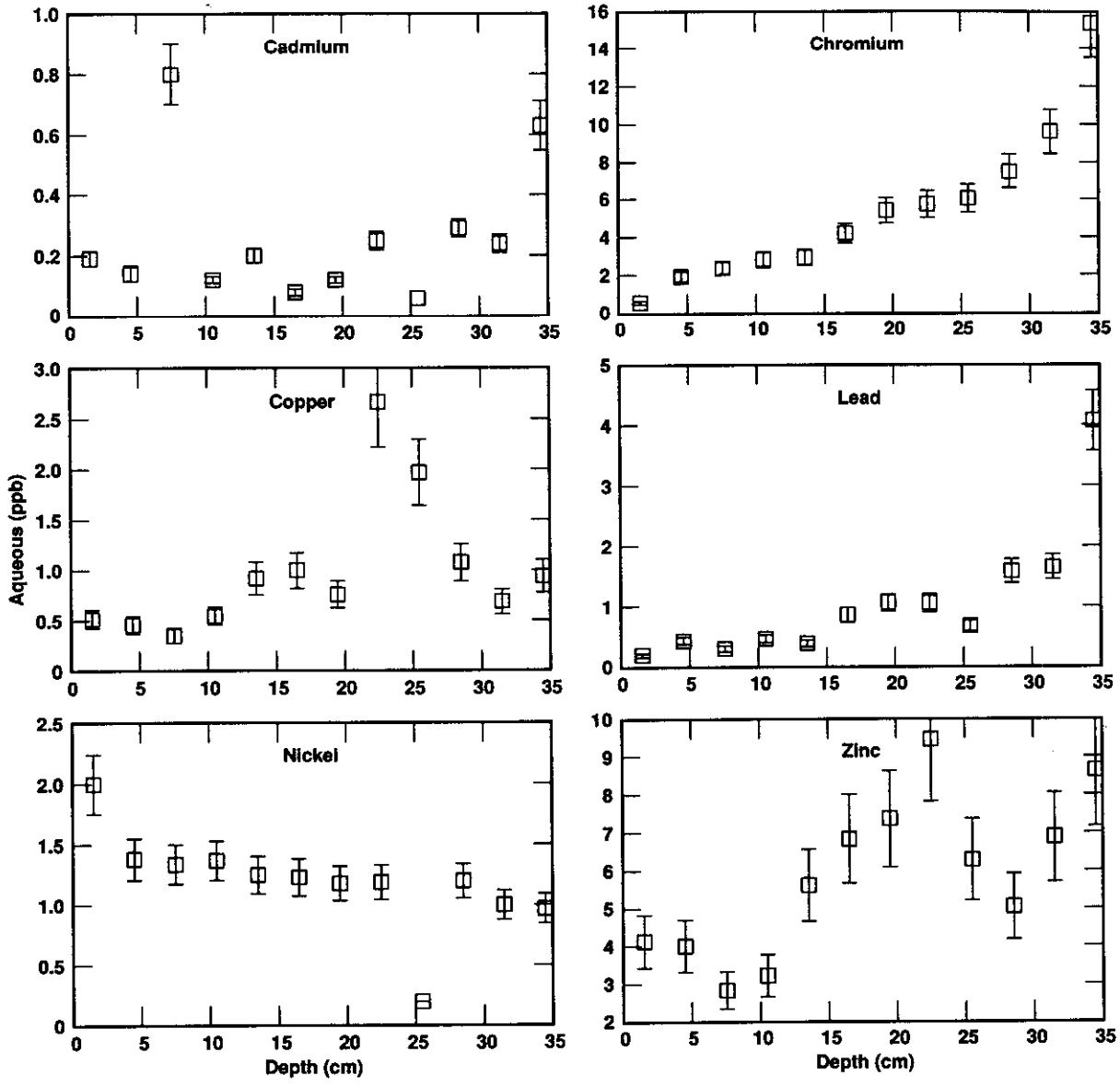

Figure 7. Chemical composition of porewaters extracted from core GH-CC-SC4. Dissolved carbon data is from core GH-CC-SC2. Both cores were collected on July 10, 1997.

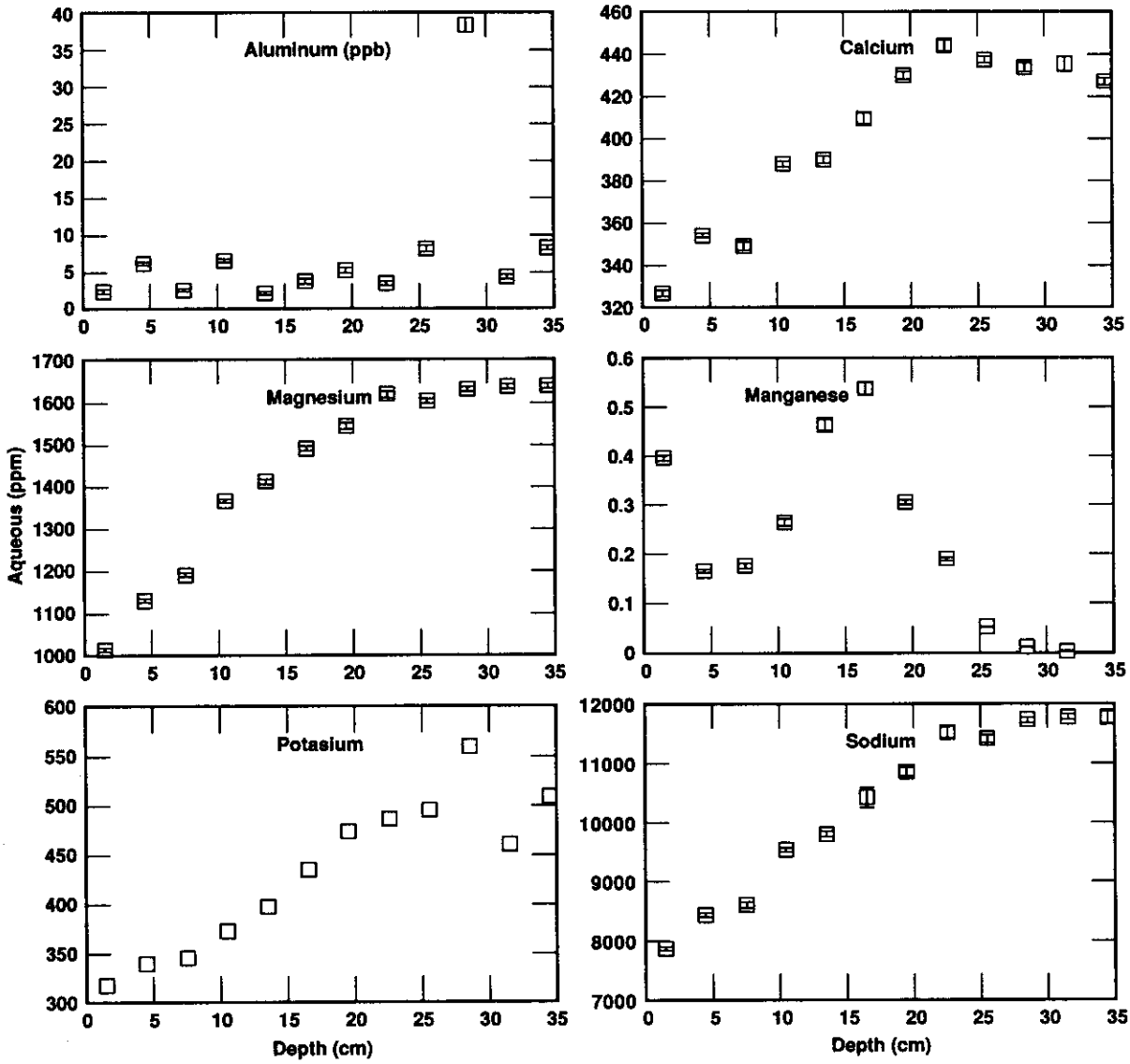

Figure 7. (Continued.)

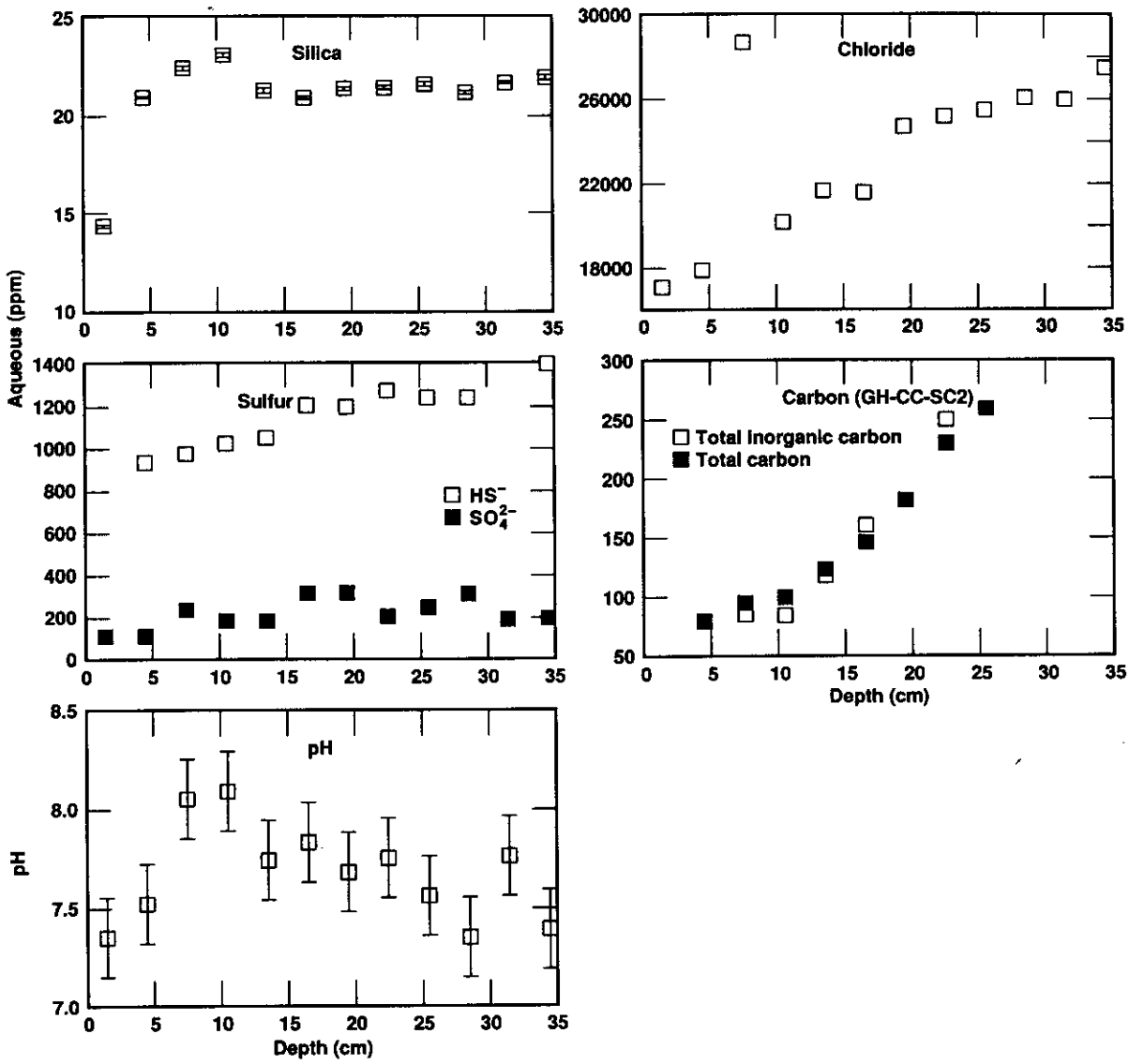

Figure 7. (Continued.)

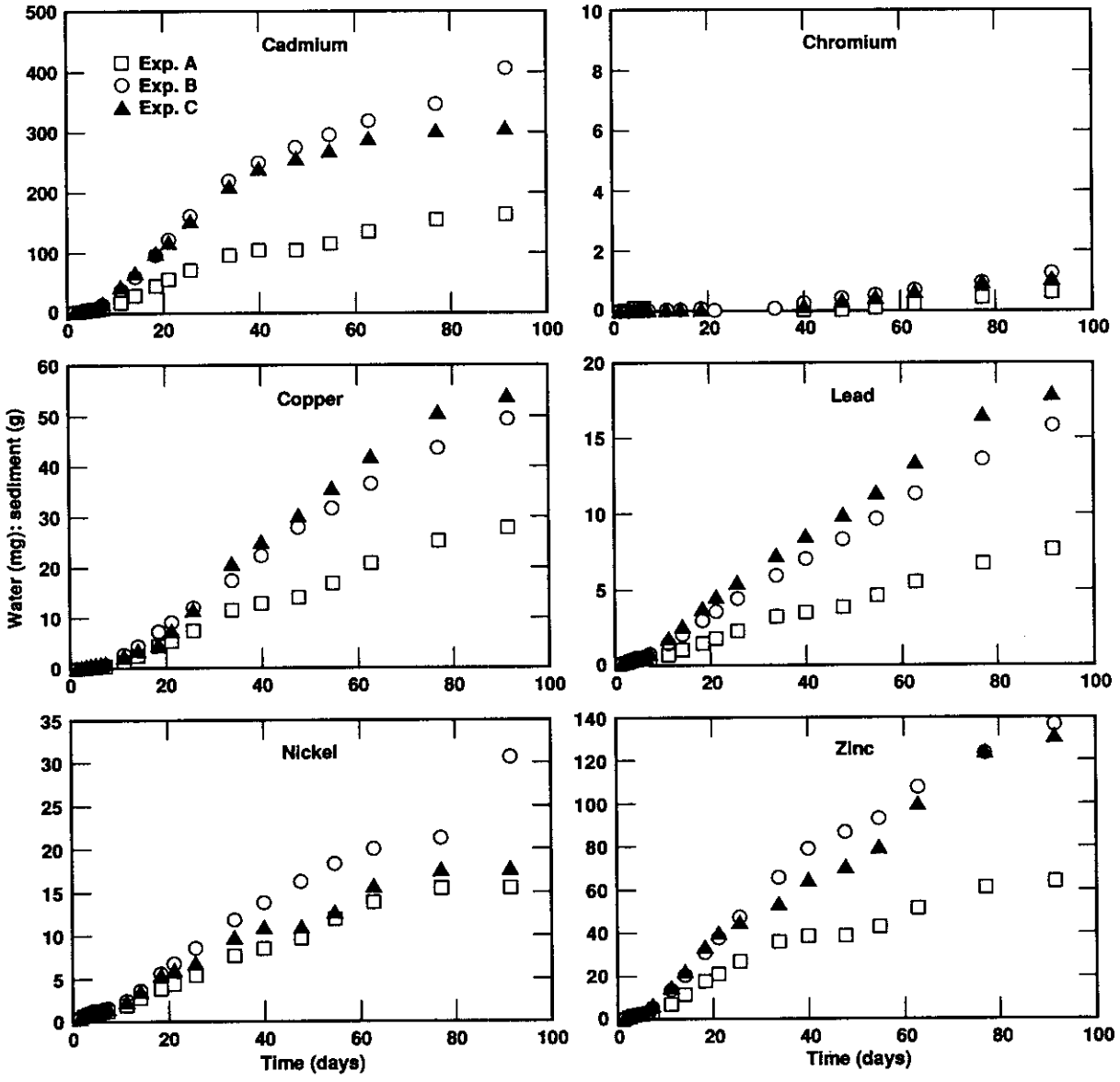

Figure 8. Total trace elements dissolved during the leaching experiments (GH-CC-SC4-11) relative to initial trace element concentration in the sediment.

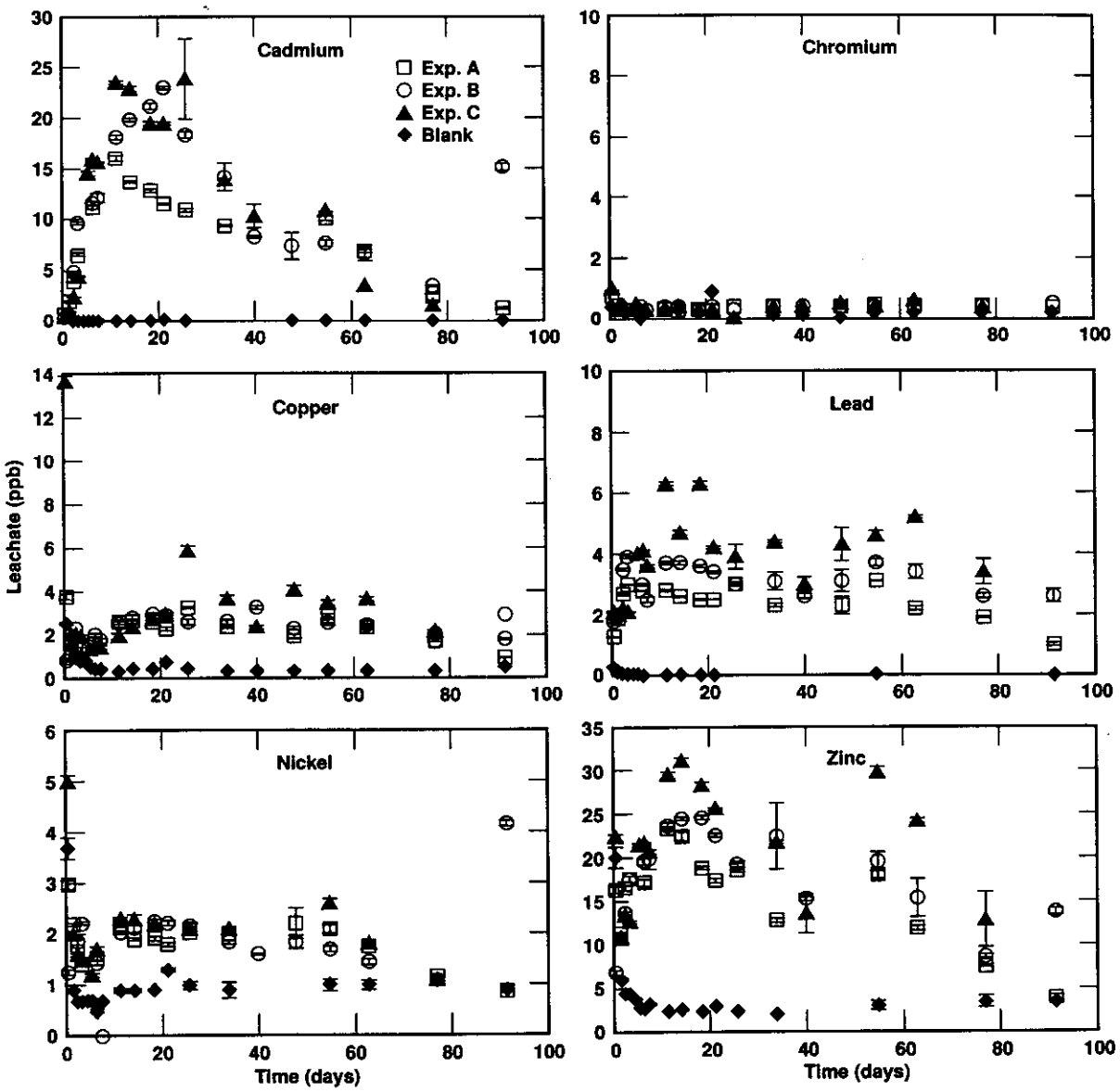

Figure 9. Dissolved trace element concentrations in the seawater (Blank) and leachate solutions from replicate leaching experiments (A, B, C) of sediment CH-CC-SC4-11 Seaplane Lagoon.

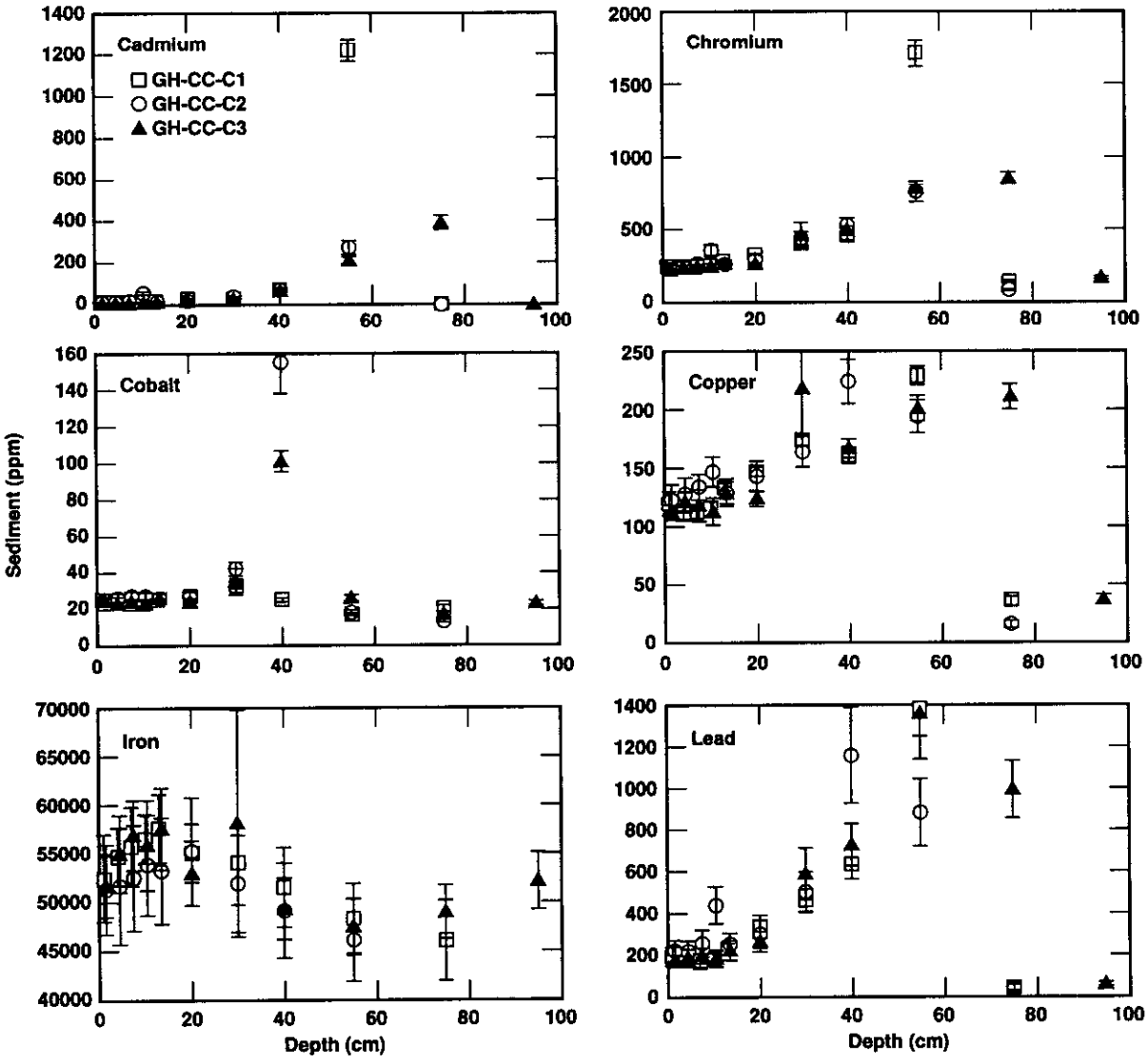

Figure 10. Chemical composition of Seaplane Lagoon sediments from cores GH-CC-C1, -C2, and -C3.

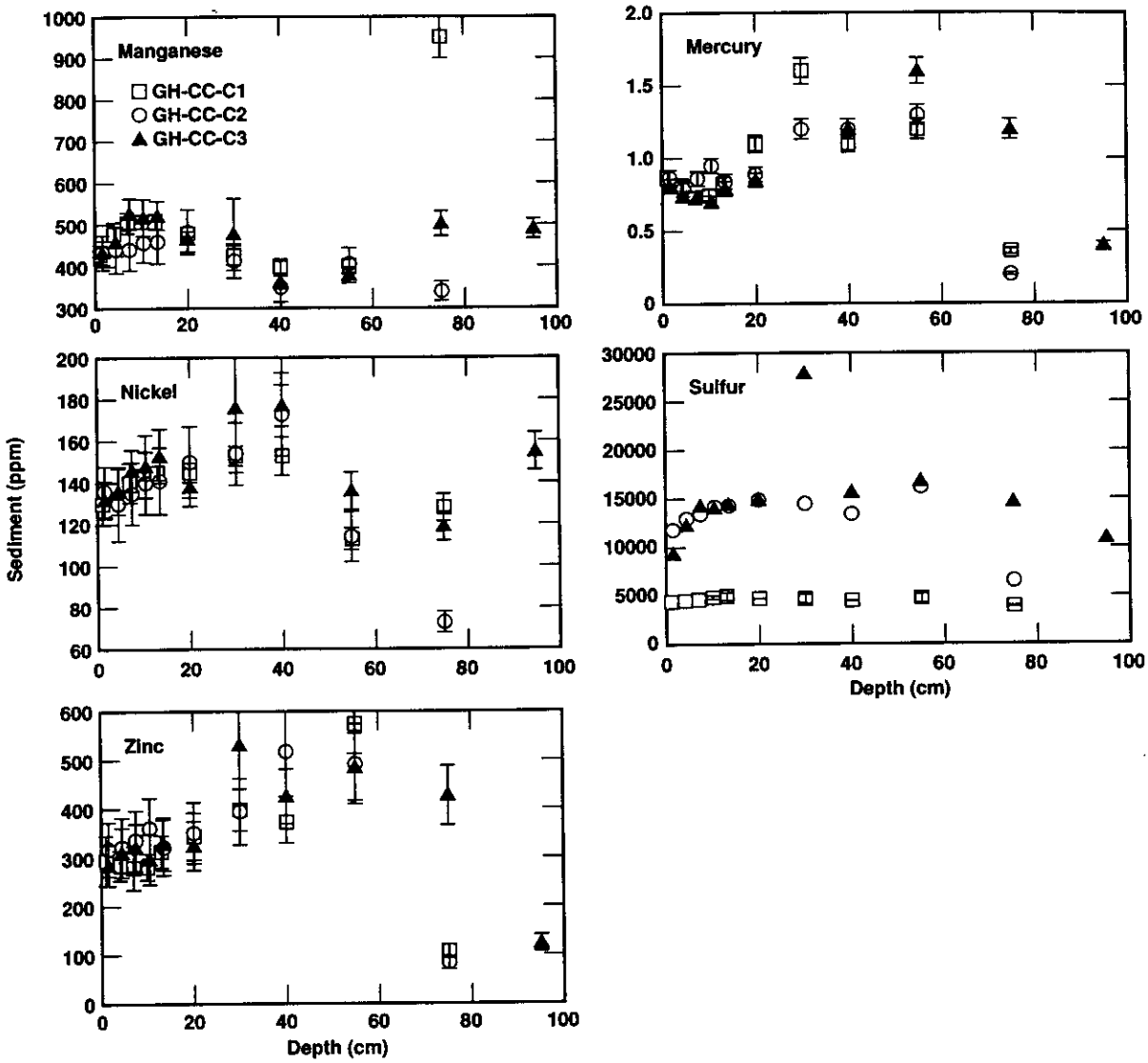

Figure 10. (Continued.)

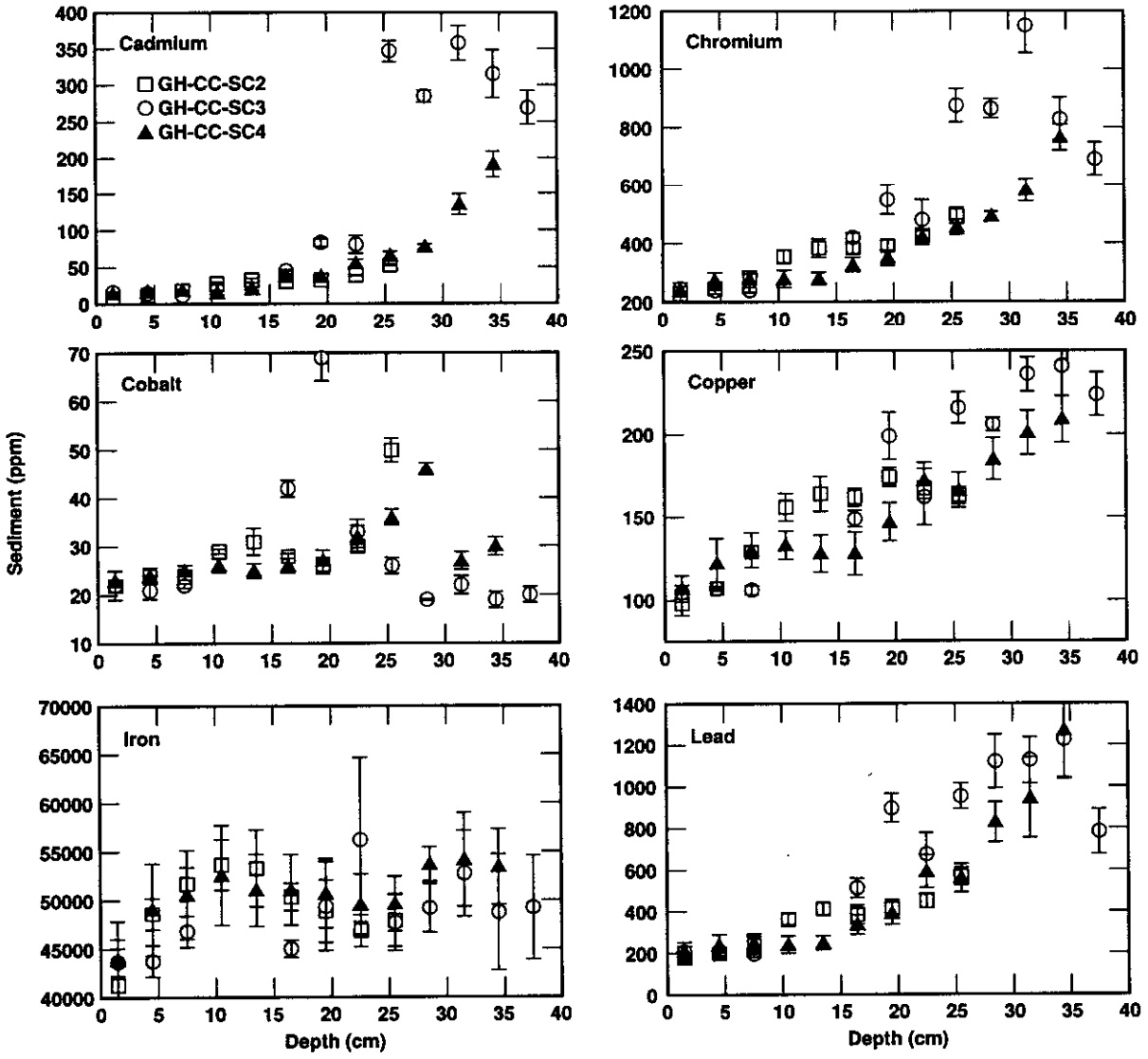

Figure 11. Chemical composition of Seaplane Lagoon sediments from cores GH-CC-SC2, -SC3, and -SC4.

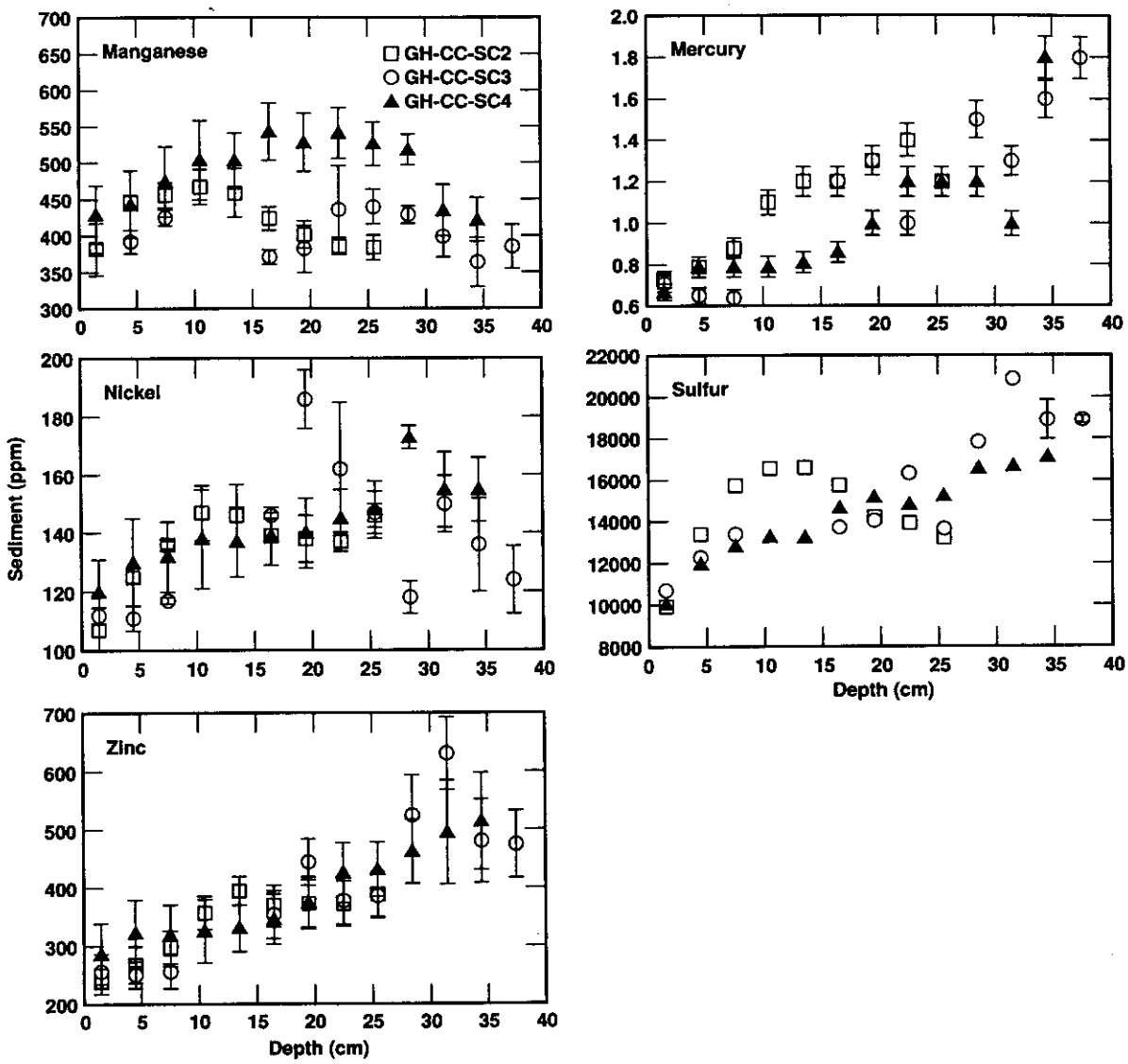

Figure 11. (Continued.)

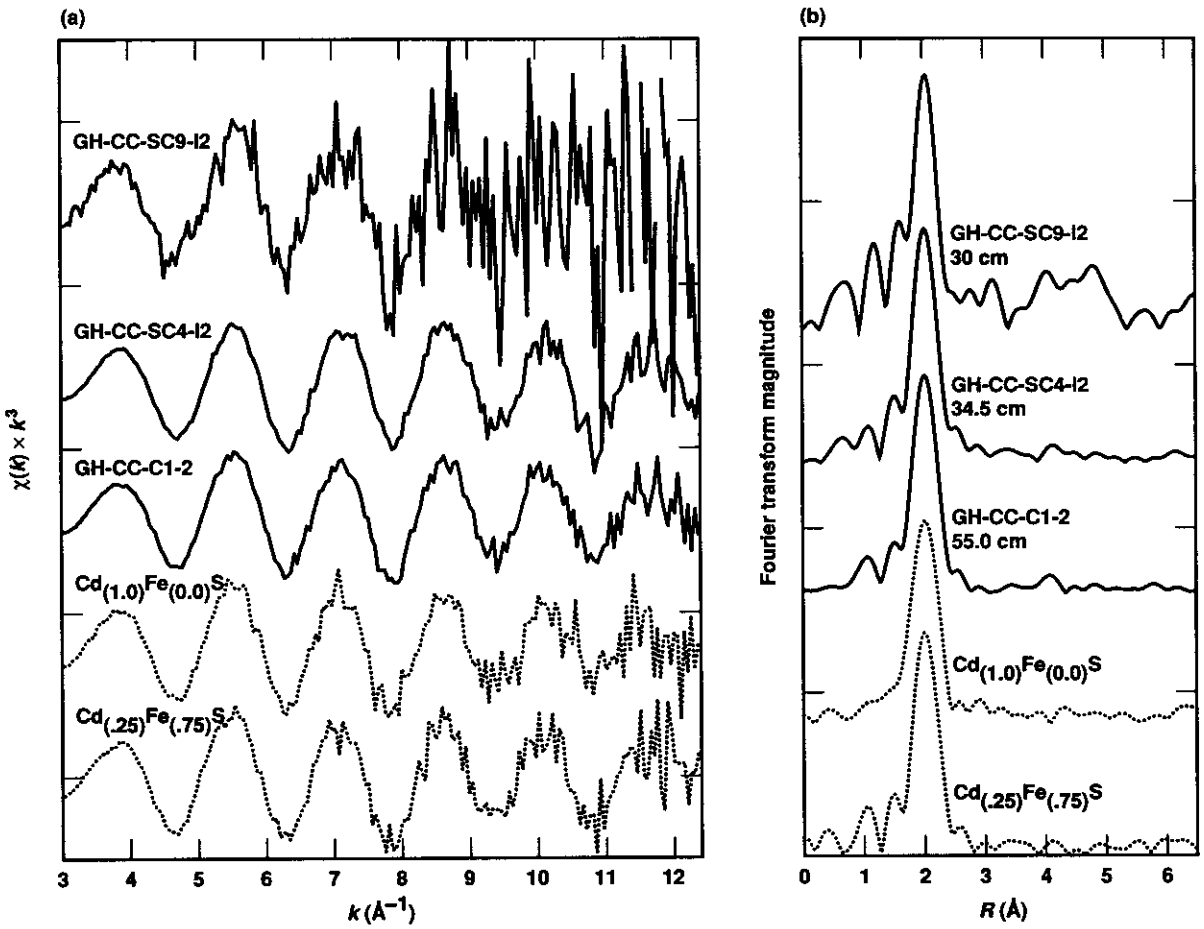

Figure 12. (a) Cadmium XAFS, and (b) radial distribution functions (not corrected for phase shift) for Seaplane Lagoon sediments CdS and $Cd_{0.25}Fe_{0.75}S$ precipitates.

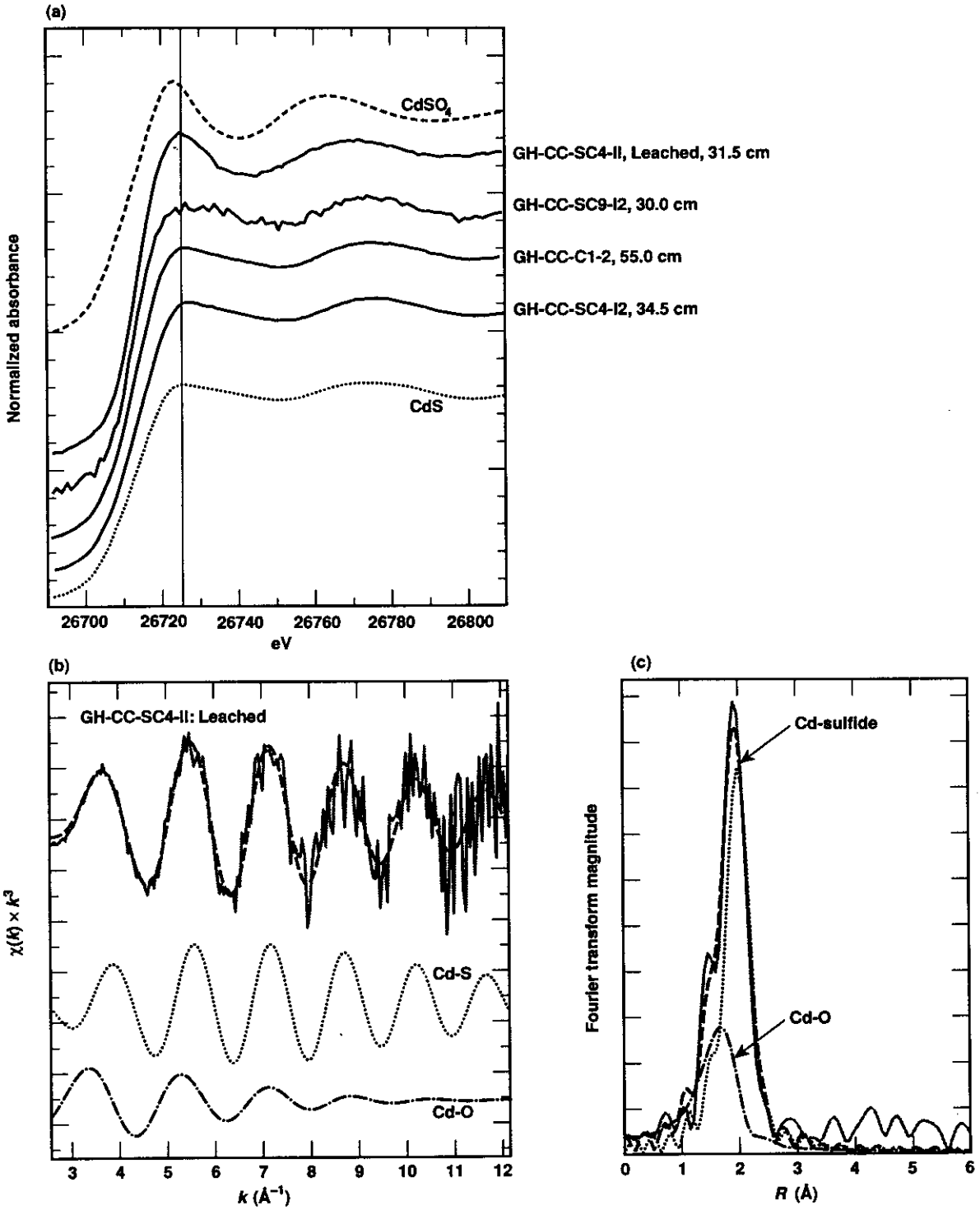

Figure 13. (a) Cadmium adsorption edge spectra comparing CdS and $CdSO_4$ references with unreacted and leached Seaplane Lagoon sediments; (b) cadmium XAFS; and (c) radial distribution functions (not corrected for phase shift) for the leached sediment showing Cd-S and Cd-O components.

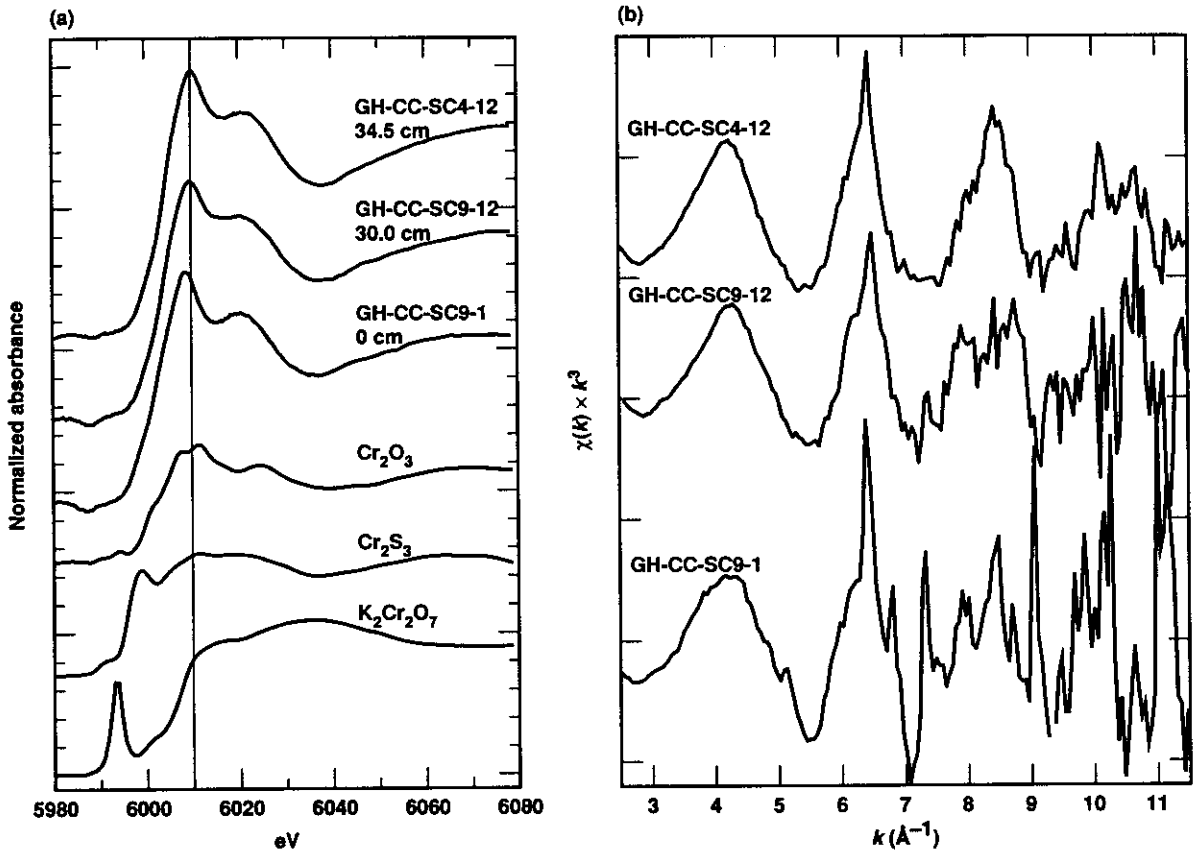

Figure 14. Chromium adsorption edge spectra, comparing Cr_2O_3, Cr_2S_3, and $K_2Cr_2O_7$ references with surface and deeper sediments from Seaplane Lagoon; (b) chromium XAFS of surface and deeper sediments from Seaplane Lagoon.

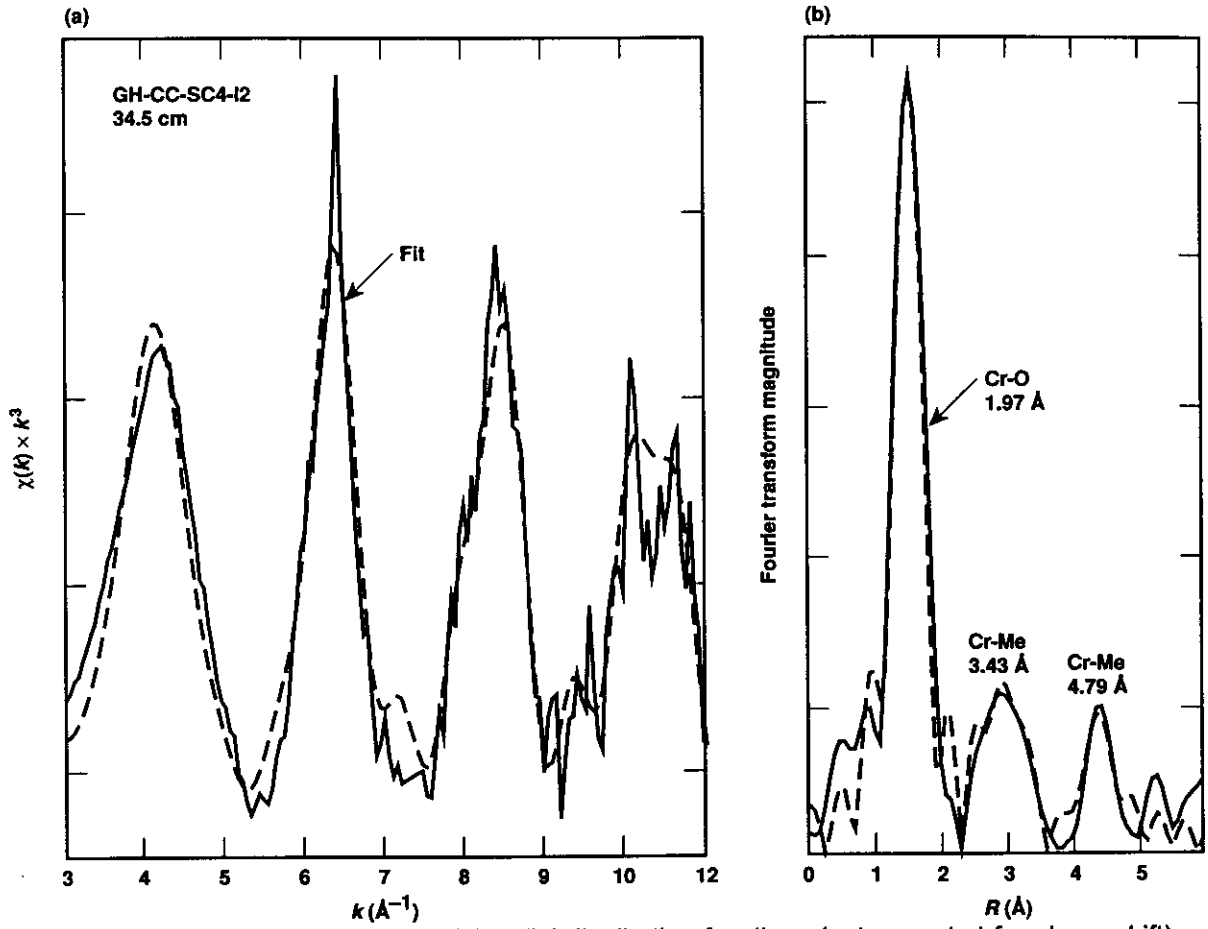

Figure 15. (a) Chromium XAFS and (b) radial distribution functions (not corrected for phase shift) for Seaplane Lagoon sediment from 34.5-cm depth (sample GH-CC-SC4-12). Dashed lines are fits to the data.

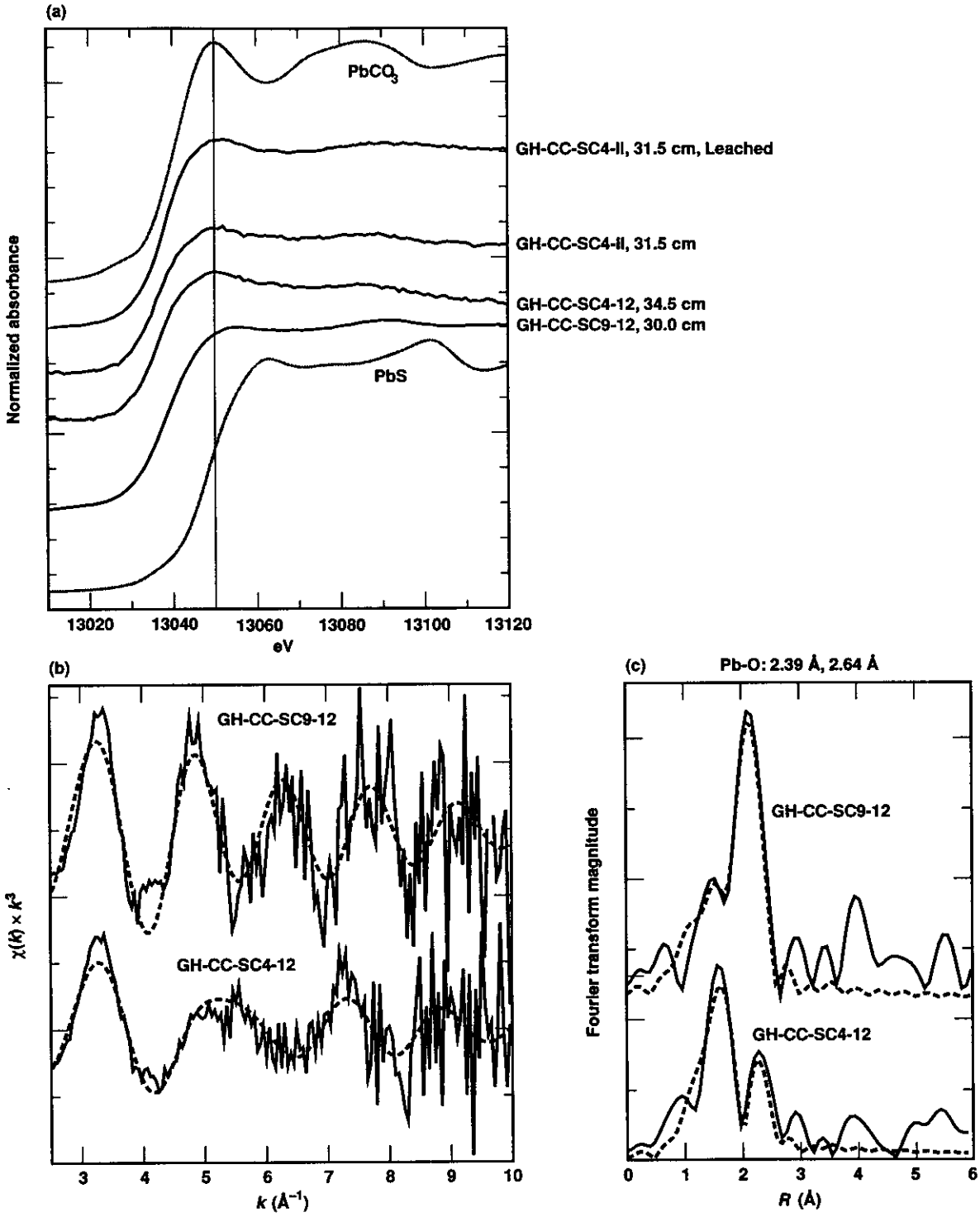

Figure 16. (a) Lead adsorption edge spectra comparing PbS and $PbCO_3$ references with unreacted and leached Seaplane Lagoon sediments, (b) lead XAFS, and (c) radial distribution functions (not corrected for phase shift) for unreacted sediments showing two Pb-O distances at 2.39 and 2.65 Å. Dashed lines are fits to the data.

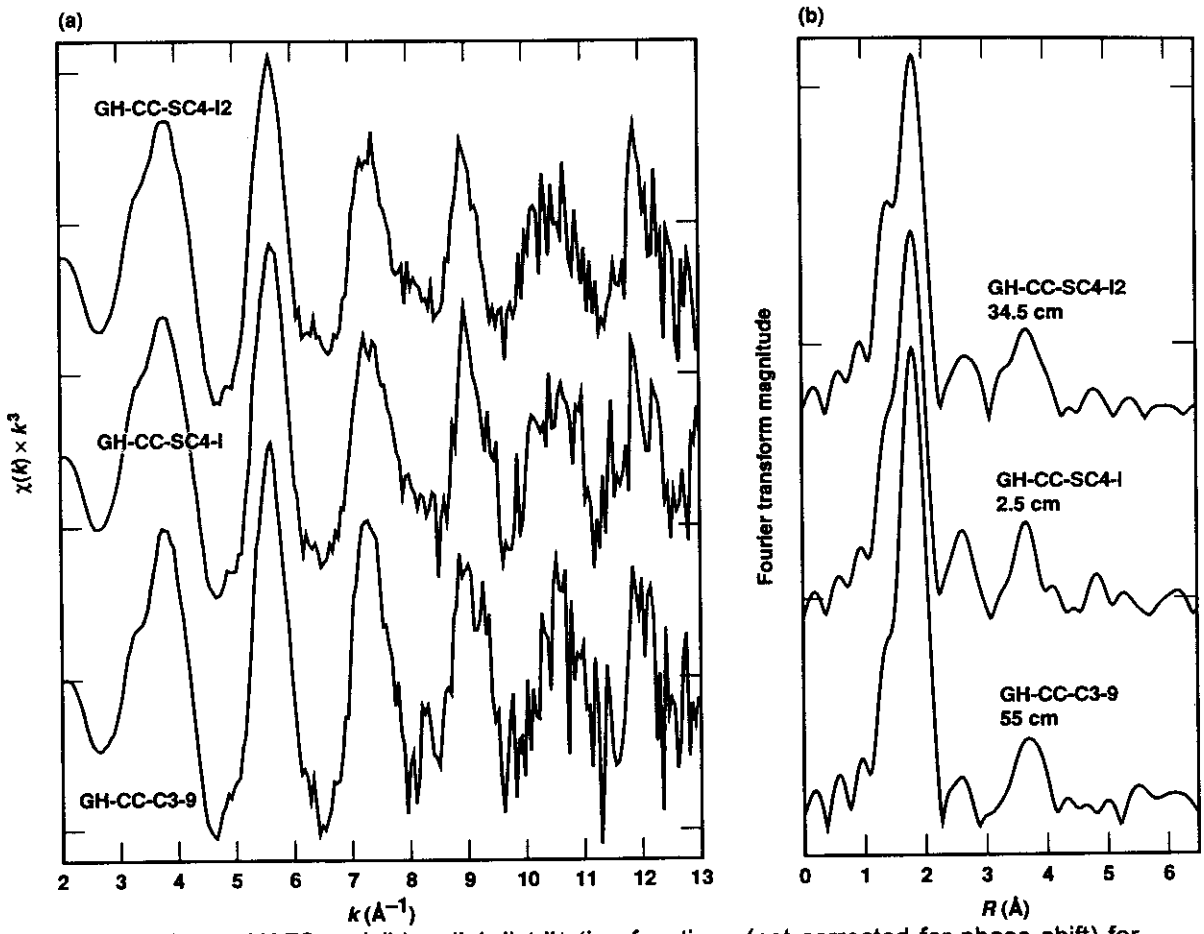

Figure 17. (a) Zinc XAFS and (b) radial distribution functions (not corrected for phase shift) for Seaplane Lagoon sediments at 2.5-, 34.5-, and 55-cm depth.

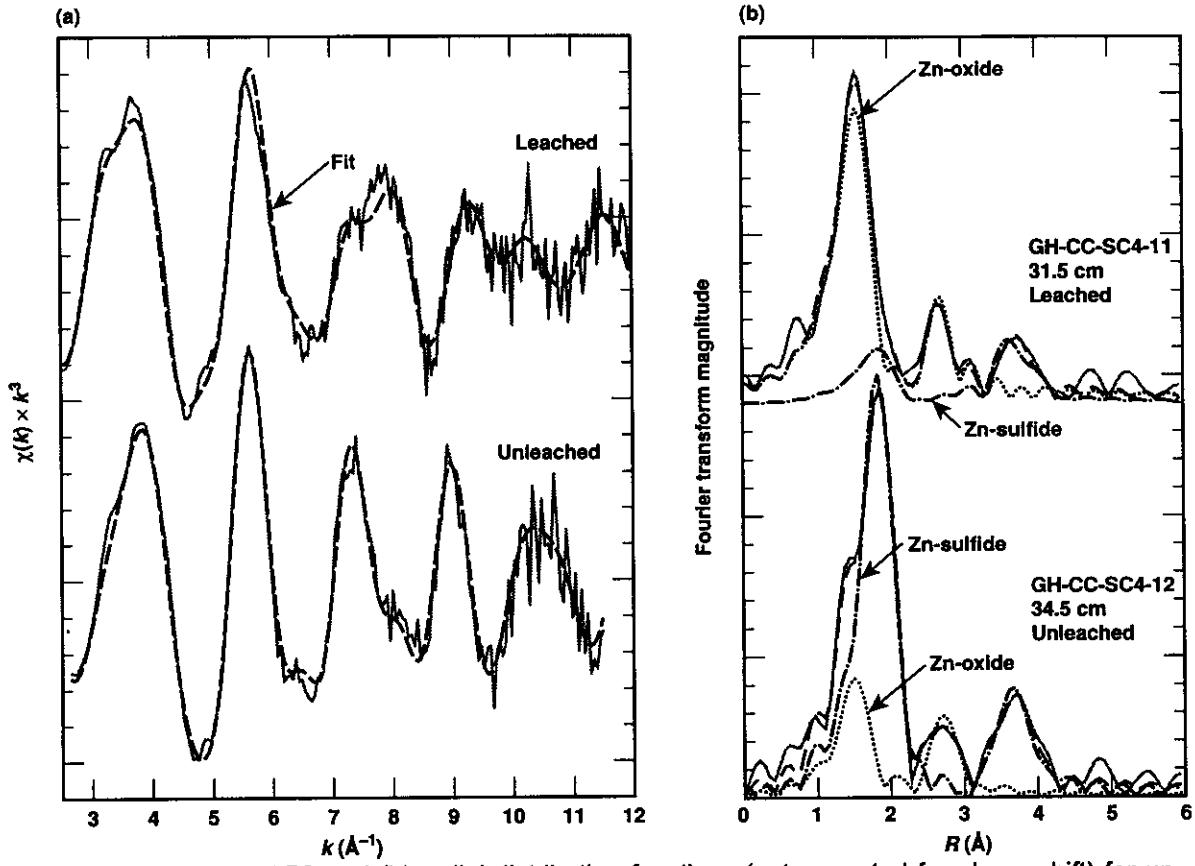

Figure 18. (a) Zinc XAFS and (b) radial distribution functions (not corrected for phase shift) for unreacted and leached Seaplane Lagoon sediments showing Zn-sulfide and Zn-oxide components. Dashed lines are fits to the data.

Table 4. Dissolved O_2, Mn(II), Fe(II), and total S(–II) concentrations and relative concentrations of Fe(III)- and FeS- and elemental S-colloids in the top 5 cm of the push cores collected from the east outfall location of Seaplane Lagoon on July 10, 1997, November 10, 1997, and April 8, 1998, and at the West Beach Landfill Wetlands on April 8, 1998.

Table 4-1. Seaplane Lagoon, Core GH-CC-SC2. Analyzed on July 10, 1997.

Depth (mm)	O_2 (µM)	±	S(–II) (µM)	±	Fe(III) (nA)	±
–10.0	232.7	9.7				
–1.5	257.3	13.7				
–1.0	238.2	6.7				
0.0	123.5	8.6				
1.0	15.8	9.6				
2.0						
10.0						
12.0					1.7	0.0
14.0					2.1	0.0
16.0					2.5	0.3
18.0					2.9	0.1
20.0					3.3	0.4
22.0					3.3	0.4
24.0					4.4	0.3
28.0					2.8	0.0
30.0					2.5	0.0
32.0					3.0	0.2
34.0					2.8	0.3
36.0					2.5	0.1
38.0					2.5	0.0
40.0			8.2	2.7	2.5	0.4
42.0			45.0	5.4	2.6	0.1
42.0			45.0	3.4		
44.0					2.7	0.0
44.0					2.6	0.2
46.0					1.8	0.0
46.0			66.2	4.9		
50.0			245.5	18.2		

Table 4-2. Seaplane Lagoon, Core GH-CC-SC2. Analyzed on July 13, 1997.

Depth (mm)	O_2 (µM)	±	Mn(II) (µM)	±	Fe(II) (µM)	±	$S_2O_3^*$ (µM)	±	S(–II) (µM)	±	Fe(III) (nA)	±
–10.0	219.1	11.9										
–1.5	214.5	6.3										
–1.0	214.0	7.6										
0.0	186.3	4.3										
1.0	47.9	1.2										
2.0	14.8	5.0										
12.0											1.6	0.3
14.0			11.6	3.0							2.6	0.1
16.0			13.7	0.0							2.3	0.4
18.0			10.5	0.0	38.6	4.2					2.3	0.3
20.0					49.0	2.1					1.8	0.2
22.0					53.5	0.1					3.0	0.1
24.0					48.5	12.0					3.9	1.1
26.0					48.5	1.7					3.5	0.6
28.0					49.0	2.1					3.7	0.1
30.0					56.5	5.9					3.7	0.2
32.0					53.5	5.1					3.6	0.2
34.0					32.7	4.2			2.0	0.2	3.0	0.3
36.0					0.0	0.0			0.0	0.0	2.1	0.3
38.0					0.0	0.0			6.7	0.8	1.9	0.3
40.0					44.6	16.8	23.2	0.4	6.6	1.0	2.4	0.2
40.0					69.4	27.0	42.3	15.4	31.3	8.2	3.1	0.2
42.0					79.3	9.1	54.2	4.7	43.7	5.3	3.0	0.1
44.0					86.2	29.4	68.4	9.0	51.0	7.2	2.5	0.0
46.0					69.4	12.0	77.3	3.1	55.0	6.9	2.1	0.1
48.0					57.5	27.0	79.3	1.8	54.3	7.7	1.8	0.0
50.0					66.4	4.5	92.1	3.5	56.1	7.4	1.7	0.1
50.0									118.9	8.8		

Table 4-3. Seaplane Lagoon, Core GH-CC-SC5. Analyzed on November 18, 1997.

Depth (mm)	O_2 (μM)	±	Mn(II) (μM)	±	Fe(II) (μM)	±	S(−II) (μM)	±	S(−II) (μM)	±	Fe(III) (nA)	±	FeS (nA)	±
−100.0	243.8	3.0												
−1.5	246.3	14.4												
−0.5	227.2	2.2												
0.0	222.9	1.1												
0.5	175.9	6.3												
1.0	124.9	4.1												
1.5	90.8	3.2												
2.0	39.0	6.6												
2.5	25.0	3.1												
3.5	0.0													
16.5			0.0											
17.5			25.9	4.3										
18.5			30.3	3.8										
19.5			27.9	2.1										
20.5			27.2	0.0										
21.5			30.5	3.5										
22.5			23.2	13.0										
23.5			19.7	5.6										
24.5			20.2	6.7										
25.5			7.1	2.9										
26.5			5.6	4.3										
27.5			7.1	2.9										
28.5			5.6	4.3										
31.5			8.1		0.0				3.6	2.5				
32.5			20.2		33.9		34.9	3.7	7.0	0.6				
32.5									29.6	0.4				
33.5			19.7	0.0	48.2	0.4	42.5	2.4	33.8	0.9				
34.5			0.0		77.2	7.9	52.9	1.9	38.1	0.5				
35.5					74.9	3.7	67.7	0.3			1.7	0.6		
36.5					36.7	0.0	78.6	1.2						
37.5					66.4	3.7	85.4	3.3			1.6	nr		
38.5					0.0		121.9	9.9					6.8	6.5
39.5							155.3	7.7					9.9	nr
39.5													5.3	2.1
40.5							154.0						7.2	0.0
41.5							302.8							
42.5							274.9	11.8						
43.5							331.9	19.1						
44.5							331.9	18.1						
45.5							321.2	4.3						
46.5							333.2	6.3						
47.5							349.0	4.9						
48.5							368.2	4.3						
49.5							379.3	3.5						

nr = not reported.

Table 4-4. Seaplane Lagoon, Core GH-CC-SC6. Analyzed on November 19, 1997.

Depth (mm)	O_2 (µM)	±	Fe(II) (µM)	±	Fe(III) (nA)
-5.0	233.7	2.6			
-1.5	228.8	7.3			
-1.0	226.4	3.8			
-0.5	230.0	3.5			
0.0	227.5	1.2			
0.5	227.9	5.0			
1.5	190.2	1.2			
2.5	158.3	5.1			
3.5	34.2	3.8			
4.5	24.8	1.0			
5.5	25.0	1.2			
7.5	16.9	2.5			
9.5	14.5	3.3			
11.5	0.0				
14.5			86.2	nr	
16.5			67.0	nr	
20.5			54.3	nr	
22.5			108.6	nr	
24.5			95.8	nr	
26.5			124.5	nr	
28.5			79.8	nr	2.4
33.5			73.4	nr	2.6
36.5			79.8	nr	1.8
38.5			143.7	nr	2.7
40.5			166.0	nr	3.1
42.5			137.3	nr	2.9
44.5			217.1	nr	3.5
46.5			290.5	nr	5.6
48.5			325.7	nr	3.9
50.5			344.8	nr	4.0

nr = not reported.

Table 4-5. Seaplane Lagoon, Core GH-CC-SC7. Analyzed on November 19, 1997.

Depth (mm)	O_2 (µM)	±	Mn(II) (µM)	±	Fe(II) (µM)	±	Anode S(–II) (µM)	±	Cathode S(–II) (µM)	±	Fe(III) (nA)	±
–330.0	243.4	2.4										
–1.5	212.0	5.3										
–0.5	197.2	4.1										
0.0	152.7	6.4										
0.5	80.7	5.7										
1.0	54.2	5.6										
1.5	32.8	5.6										
2.0	13.3	2.3										
2.5	7.3	1.9										
4.0	0.0											
8.0			0.0									
9.5			19.5	0.8								
10.5			30.9	0.8								
11.5			47.1	3.9								
12.5			61.1	8.4								
13.5			61.3	7.3								
14.5			45.8	9.3								
15.5			53.9	0.6	0.0							
15.5					178.5	40.7					0.0	
16.5			44.0	12.0	266.2	22.4					5.4	2.8
17.5			37.9	10.5	279.9	19.6					11.1	3.4
18.5			30.7	21.5	300.3	22.5					17.0	1.5
19.5			35.7	26.1	329.3	32.7					17.2	5.2
20.5			30.9	15.2	319.5	17.5					20.1	0.3
21.5			25.9	88.0	305.5	22.0					19.3	2.3
22.5			36.5	58.2	310.2	16.5					20.3	0.0
24.5			35.9		283.5	3.0					22.1	3.5
26.5					288.5	9.0					24.3	1.2
28.5					309.2	9.0					20.1	1.1
30.5					314.8	72.9					19.2	0.6
32.5			44.4		212.0	216.8					17.2	0.4
33.5					225.2	21.0	0.0		0.0		13.0	1.5
35.5			249.8	102.0	224.7	110.9	15.2	3.4			9.6	4.6
35.5			83.8	39.2	212.2	1.0	19.5	0.0	24.9	1.9	0.0	
36.5			54.7	30.7	160.5	122.9	27.6	2.3	44.8	8.7		
37.5							89.1	0.4	73.4	0.4		
38.5							42.6	23.8	45.7	5.6		
40.5									57.7	4.1		
42.5									62.1	1.1		
44.5									80.0	4.6		
46.5									122.7	1.5		
48.5									160.8	2.5		
50.5					93.3	20.0			191.0	11.7		

Table 4-6. Seaplane Lagoon, Core GH-CC-SC8. Analyzed on April 10, 1998.

Depth (mm)	O_2 (µM)	±	Mn(II) (µM)	±	Fe(II) (µM)	±	Fe(III) (nA)	±
–87.0	249.5	13.0						
–2.0	220.6	5.2						
–1.0	179.8	15.1						
0.0	35.8	4.2						
1.0	10.6	3.2						
2.0	0.0		0.0	0.0				
3.0			4.4					
4.0			6.3	3.1				
5.0			12.8	5.0				
6.0			15.1	6.3				
7.0			14.4	4.2				
8.0			15.3	3.3				
8.0			10.0	4.2				
9.0			4.8	0.9				
10.0			8.8					
15.0			4.4	4.2				
16.0			6.0	3.3				
17.0			7.3	5.5				
18.0			10.0	0.0				
19.0			7.5	0.0				
20.0			8.2	1.6				
22.0			8.4	3.9				
24.0			5.6	0.0				
26.0			6.9	3.1				
28.0			5.6	0.0				
30.0			4.4	0.0				
32.0			0.0	0.0				
38.0					0.0	0.0	0.0	0.0
40.0					8.8	5.9	2.3	0.5
42.0					16.6	8.1	2.6	0.4
44.0					21.2	8.1	4.4	0.0
46.0					28.5	5.9	6.4	0.3
48.0					32.6	0.0	7.5	1.6
50.0					44.5	8.1	11.4	0.4

Table 4-7. Seaplane Lagoon, Core GH-CC-SC9. Analyzed on April 10, 1998.

Depth (mm)	O_2 (µM)	±	Mn(II) (µM)	±	Fe(II) (µM)	±	S(−II) (µM)	±	Fe(III) (nA)	±	FeS (nA)	±
−88.0	279.3											
−2.0	282.8	15.5										
−1.0	218.2	8.1										
0.0	220.6	11.4										
1.0	144.2	22.9										
2.0	45.4	19.2										
3.0	2.8	1.2										
4.0	0.0	0.0	0.0	0.0								
5.0			4.4	4.4								
6.0			3.8	3.9								
7.0			6.5	6.0								
7.0			6.0	2.8								
8.0			6.3	11.1								
9.0			6.9	2.2	0.0	0.0			0.0	0.0		
10.0			5.2	3.9	28.5	2.2			1.9	2.1		
11.0			7.1	3.9	36.5	2.7			4.1	1.5		
12.0			7.5	0.0	39.9	2.2			4.8	2.1		
13.0			7.8	5.5	35.7	5.5			6.2	1.8		
14.0			8.5	1.1	35.0	2.7			6.6	0.5		
15.0			8.2	4.4	37.3	5.5			5.6	1.3		
16.0			9.1	1.1	35.0	2.7			5.8	0.2		
17.0			11.9	3.1	30.6	9.8			3.8	0.3		
18.0			13.5	1.1	26.9	9.8			3.2	1.0		
19.0			16.5	3.3	20.7	5.9			2.5	0.4		
20.0			15.4	1.1	20.7	8.1			2.3	0.0		
21.0			11.9	0.0	20.2	7.8			3.0	0.5		
22.0			11.0	3.3	21.8	5.5	0.0	0.0	4.9	0.3		
23.0			7.8	1.1	23.3	0.0	0.5	0.2	5.2	1.2		
24.0			6.0	1.1	34.2		0.7	0.1	4.9	2.3		
25.0			6.3		29.5	0.0	0.9	0.3	7.5	6.8		
26.0			0.0	0.0	12.4		2.3	0.5	1.3	1.0	6.0	6.2
26.0							5.5	0.1				
27.0							11.0	2.9	0.0	0.0		
28.0					11.7	2.7	9.6	4.7				
29.0					17.1	11.0	8.1	3.4				
30.0					22.5	8.2	6.6	2.9				
31.0					24.1	8.2						
32.0					23.3		3.9	1.5				
33.0					21.8	5.5	3.4	0.6				
34.0	0.0						2.6	0.0				
35.0							2.1	0.4			3.0	4.1
35.0							8.5	3.7				
36.0							13.7	10.2				

Table 4-7 (Continued). Seaplane Lagoon, Core GH-CC-SC9. Analyzed on April 10, 1998.

Depth (mm)	O_2 (µM)	±	Mn(II) (µM)	±	Fe(II) (µM)	±	S(–II) (µM)	±	Fe(III) (nA)	±	FeS (nA)	±
37.0					14.8	13.7	8.5	2.6				
38.0					27.5	5.9	7.7	1.1				
39.0					0.0	0.0	8.3	1.1				
39.0							18.4	4.8				
40.0							34.4	12.9				
41.0							50.7	5.0				
42.0							51.5	2.8				
43.0							49.0	9.3				
44.0							42.1	6.7				
45.0							32.8	9.2				
46.0							21.6	6.9				
47.0							13.7	4.6				
48.0							10.5	4.8				
49.0							12.8	4.5				
50.0							16.9					

Table 4-8. Landfill Wetlands, Core W1-CC-SC1. Analyzed on April 9, 1998.

Depth (mm)	O_2 (µM)	±	Mn(II) (µM)	±	Fe(II) (µM)	±	S(–II) (µM)	±	Fe(III) (nA)	±
–2.5	276.4	16.2								
–1.5	273.9	39.8	0.0	0.0						
0.0	160.1		1.5							
1.0	7.9	1.5							0.0	0.0
2.0	0.0	0.0	4.8	4.0					0.8	0.4
3.5			6.0		0.0	0.0			0.5	
4.5			7.0		11.2					
5.5			8.4	16.2	26.0	21.2			0.4	
6.5			4.2	4.7	26.7	22.5			0.4	
7.5			6.9	8.9	44.8	9.6			0.7	0.4
8.5			8.4	5.4	43.7	26.1			0.9	0.2
9.5			8.1	2.1	53.8	3.8			1.5	0.7
10.5			9.6	11.5	54.7	11.0			1.4	0.4
11.5			8.7	2.3	49.7	0.5			1.5	0.0
12.5			4.8	2.2	53.1	24.4	0.0	0.0	1.6	0.1
13.5			9.1	6.0	50.5	1.1	0.2	0.1	1.6	0.0
14.5			8.1	10.7	54.0	41.5	0.4	0.1	2.3	0.2
15.5			6.2	2.3	54.5	18.7	0.3	0.0	1.9	0.1
16.5			7.2		57.3	9.3	0.2	0.1	1.9	0.2
17.5			7.8	9.1	56.3	8.0	0.2	0.2	1.5	1.2
18.5			7.2		51.4	11.3	0.5	0.0	2.1	0.2
19.5			6.7	17.8	48.6	26.4	0.6	0.4	2.0	0.0
20.5			12.5	15.2	38.5	16.5	1.7	1.0	2.1	0.4
21.5							1.6	0.4	2.0	
22.5			33.1		44.8		1.8	0.4	1.8	1.4
23.5			24.7	19.1	64.5	4.9	3.3	0.4	1.7	0.6
24.5			27.2	4.7	60.3	35.7	3.8	0.6	1.5	0.5
25.5			18.3	15.2	37.1	26.1	4.6	0.1	1.5	0.0
26.5			0.0	0.0	0.0		5.9	0.6	1.8	0.2
27.5							6.4	0.4	1.9	0.4
28.5							6.7	0.1	1.6	0.0
29.5							6.9	0.4	1.7	0.5
30.5							7.1	0.3	1.4	0.4
31.5							6.2	0.4	0.9	0.7
32.5							5.7	0.1	1.2	
33.5							6.9	0.6	0.0	0.0
34.5							8.8	0.4		
35.5							10.5	1.0		
36.5							11.8	0.4		
37.5							13.1	0.8		
38.5							13.4	0.1		
39.5							11.9	0.3		

Table 4-8 (Continued). Landfill Wetlands, Core W1-CC-SC1. Analyzed on April 9, 1998.

Depth (mm)	O_2 (µM)	±	Mn(II) (µM)	±	Fe(II) (µM)	±	S(–II) (µM)	±	Fe(III) (nA)	±
40.5							9.4	1.8		
41.5							10.3	2.7		
41.5							11.9	0.6		
42.5							9.5	0.4		
42.5							11.3	0.4		
43.5							13.9	2.5		
44.5							14.2	0.1		
45.5							16.9	0.5		
47.5							15.1	2.0		
49.5							18.2	0.4		

Table 4-9. Landfill Wetlands, Core W1-CC-SC2. Analyzed on April 9, 1998.

Depth (mm)	O_2 (μM)	±	Mn(II) (μM)	±	S(0) (nA)	±	S(–II) (μM)	±
–2.0	278.8	24.6	14.9	3.4	0.6	0.1		
–1.0	263.4	29.5	16.9	0.0	0.4			
0.0	198.4	35.4	14.8	1.3	0.0	0.0		
1.0	9.6	1.5	25.1	0.0				
2.0	0.0	0.0	20.1	0.9			0.0	0.0
3.0			17.9	1.3			0.5	0.3
4.0			18.2	0.0			0.4	0.2
5.0			14.8	1.3			0.5	0.2
7.0			11.0	1.3			0.7	0.6
9.0			9.1	0.4			0.7	0.4
11.0			7.2	0.4			3.1	1.0
13.0			4.7	0.4			5.4	1.0
15.0			3.1	0.0			3.5	2.3
17.0			3.8	0.0			1.7	0.9
19.0			0.0				2.2	0.8
21.0							4.8	1.0
23.0							16.9	2.3
25.0							20.9	0.3
27.0							22.7	0.5
29.0							21.7	0.5
31.0							18.0	0.4
33.0							23.4	1.0
35.0							57.3	19.6
37.0							92.0	
39.0							76.0	31.9
41.0							64.0	14.7
43.0							59.9	12.8
45.0							55.4	9.2
47.0							66.4	3.5
49.0							60.4	11.1
50.0							73.2	23.0

Table 5. Porewater trace- and major-elements extracted from Seaplane Lagoon core GH-CC-SC4 on July 10, 1998. Calcium, iron, potassium, magnesium, manganese, sodium, and silica were measured by ICP-AES. Aluminum, cadmium, chromium, copper, iron, lead, manganese, nickel, and zinc were measured by ICP-MS. Uncertainty for potassium was not reported.

ICP-AES

Sample ID	Depth (cm)	Ca (ppm)	±	Fe (ppm)	±	K (ppm)	Mg (ppm)	±	Mn (ppm)	±	Na (ppm)	±	Si (ppm)	±
GH-CC-SC4-1ME	1.5	327.0	1.1	2.20	0.009	317.9	1016.8	1.8	0.366	0.002	7869.0	15.0	14.38	0.03
GH-CC-SC4-2ME	4.5	354.5	0.5	0.20	0.005	339.9	1132.9	2.0	0.195	0.003	8438.0	20.3	20.90	0.02
GH-CC-SC4-3ME	7.5	349.5	1.6	<0.2		345.9	1192.4	2.3	0.182	0.004	8601.8	33.5	22.39	0.07
GH-CC-SC4-4ME	10.5	388.3	1.0	<0.2		373.7	1367.9	3.4	0.275	0.002	9538.7	22.9	23.04	0.07
GH-CC-SC4-5ME	13.5	390.4	1.3	<0.2		397.9	1413.8	4.4	0.375	0.001	9802.7	37.3	21.25	0.08
GH-CC-SC4-6ME	16.5	409.8	2.3	<0.2		434.8	1492.6	3.4	0.431	0.001	10422.5	156.3	20.88	0.04
GH-CC-SC4-7ME	19.5	430.2	1.5	<0.2		473.6	1545.6	5.4	0.271	0.002	10855.5	58.6	21.33	0.06
GH-CC-SC4-8ME	22.5	444.4	2.4	0.69	0.001	486.8	1619.8	5.5	0.173	0.001	11520.6	78.3	21.40	0.06
GH-CC-SC4-9ME	25.5	437.8	1.1	<0.2		495.8	1604.4	3.7	<0.1		11421.2	65.1	21.57	0.07
GH-CC-SC4-10ME	28.5	434.1	1.7	<0.2		560.3	1632.6	3.9	<0.1		11724.8	29.3	21.15	0.06
GH-CC-SC4-11ME	31.5	435.6	3.0	<0.2		461.1	1638.8	2.9	<0.1		11777.1	29.4	21.65	0.03
GH-CC-SC4-12ME	34.5	427.4	1.5	<0.2		509.4	1639.8	4.6	<0.1		11766.6	94.1	21.89	0.09

ICP-MS

Sample ID	Depth (cm)	Al (ppb)	±	Cd (ppb)	±	Cr (ppb)	±	Cu (ppb)	±	Fe (ppb)	±	Mn (ppb)	±	Ni (ppb)	±
GH-CC-SC4-1TE	1.5	2.4	0.2	0.19	0.02	0.53	0.06	0.52	0.09	3000	60	395	4.0	2.00	0.24
GH-CC-SC4-2TE	4.5	6.2	0.1	0.14	0.02	1.89	0.23	0.46	0.08	1400	70	165	1.7	1.38	0.17
GH-CC-SC4-3TE	7.5	2.6	0.1	0.80	0.10	2.35	0.28	0.35	0.06	1000	70	175	3.5	1.34	0.16
GH-CC-SC4-4TE	10.5	6.6	0.1	0.12	0.01	2.80	0.34	0.55	0.09	500	25	263	5.3	1.37	0.16
GH-CC-SC4-5TE	13.5	2.2	0.1	0.20	0.02	2.91	0.35	0.92	0.16	<110		462	9.2	1.25	0.15
GH-CC-SC4-6TE	16.5	3.8	0.3	0.08	0.01	4.19	0.50	1.00	0.17	<110		536	10.7	1.23	0.15
GH-CC-SC4-7TE	19.5	5.3	0.2	0.12	0.01	5.40	0.65	0.76	0.13	<110		304	3.0	1.18	0.14
GH-CC-SC4-8TE	22.5	3.5	0.2	0.25	0.03	5.74	0.69	2.67	0.45	<110		188	1.9	1.19	0.14
GH-CC-SC4-9TE	25.5	8.2	0.3	<0.06		6.04	0.72	1.97	0.33	<110		52	0.5	<0.2	
GH-CC-SC4-10TE	28.5	38.4	0.8	0.29	0.03	7.51	0.90	1.08	0.18	<110		10	0.3	1.20	0.14
GH-CC-SC4-11TE	31.5	4.4	0.2	0.24	0.03	9.61	1.15	0.69	0.12	<110		2	0.1	1.00	0.12
GH-CC-SC4-12TE	34.5	8.3	0.2	0.63	0.08	15.38	1.85	0.94	0.16	<110		<1		0.97	0.12

ICP-MS (Continued)

Sample ID	Depth (cm)	Pb (ppb)	±	Zn (ppb)	±
GH-CC-SC4-1TE	1.5	0.19	0.02	4.12	0.70
GH-CC-SC4-2TE	4.5	0.43	0.05	4.00	0.68
GH-CC-SC4-3TE	7.5	0.30	0.04	2.82	0.48
GH-CC-SC4-4TE	10.5	0.46	0.06	3.21	0.55
GH-CC-SC4-5TE	13.5	0.38	0.05	5.61	0.95
GH-CC-SC4-6TE	16.5	0.86	0.10	6.83	1.16
GH-CC-SC4-7TE	19.5	1.06	0.13	7.36	1.25
GH-CC-SC4-8TE	22.5	1.05	0.13	9.45	1.61
GH-CC-SC4-9TE	25.5	0.67	0.08	6.28	1.07
GH-CC-SC4-10TE	28.5	1.58	0.19	5.04	0.86
GH-CC-SC4-11TE	31.5	1.65	0.20	6.88	1.17
GH-CC-SC4-12TE	34.5	4.07	0.49	8.64	1.47

Table 6. Porewater concentrations of HS^-, SO_4^{2-}, SO_3^-, total carbon (TC), total inorganic carbon (TIC), and total organic carbon (TOC) Cl- and pH from Seaplane Lagoon cores collected on July 10, 1998.

Core GH-CC-SC2

Sample ID	Depth (cm)	HS^- (ppm)	SO_4^{2-} (ppm)	SO_3^- (ppm)	Sample ID	Depth (cm)	TC (ppm)	TIC (ppm)	TOC (ppm)
GH-CC-SC2-0 S		848	118	294	GH-CC-SC2-0 C		NA	NA	NA
GH-CC-SC2-1 S	1.5	869	109	236	GH-CC-SC2-1 C	1.5	NA	NA	NA
GH-CC-SC2-2 S	4.5	977	163	322	GH-CC-SC2-2 C	4.5	80		<14
GH-CC-SC2-3 S	7.5	816	99	195	GH-CC-SC2-3 C	7.5	95	86	<14
GH-CC-SC2-4 S	10.5	907	110	209	GH-CC-SC2-4 C	10.5	100	84	18
GH-CC-SC2-5 S	13.5	786	101	216	GH-CC-SC2-5 C	13.5	123	119	17
GH-CC-SC2-6 S	16.5	866	90	202	GH-CC-SC2-6 C	16.5	147	161	<14
GH-CC-SC2-7 S	19.5	782	79	147	GH-CC-SC2-7 C	19.5	182	NA	NA
GH-CC-SC2-8 S	22.5	839	55	205	GH-CC-SC2-8 C	22.5	230	250	<14
GH-CC-SC2-9 S	25.5	836	106	241	GH-CC-SC2-9 C	25.5	259	NA	NA

Core GH-CC-SC4

Sample ID	Depth (cm)	HS^- (ppm)	SO_4^{2-} (ppm)	SO_3^- (ppm)	Sample ID	Cl^- (ppt)	pH
GH-CC-SC4-1 S	1.5	2593	119	204	GH-CC-SC4-CL1	17.1	7.35
GH-CC-SC4-2 S	4.5	935	115	211	GH-CC-SC4-CL2	17.9	7.52
GH-CC-SC4-3 S	7.5	973	240	564	GH-CC-SC4-CL3	28.7	8.05
GH-CC-SC4-4 S	10.5	1024	191	356	GH-CC-SC4-CL4	20.2	8.09
GH-CC-SC4-5 S	13.5	1053	185	204	GH-CC-SC4-CL5	21.7	7.74
GH-CC-SC4-6 S	16.5	1207	316	575	GH-CC-SC4-CL6	21.6	7.83
GH-CC-SC4-8 S	19.5	1196	316	734	GH-CC-SC4-CL7	24.7	7.68
GH-CC-SC4-7 S	22.5	1274	208	215	GH-CC-SC4-CL8	25.2	7.75
GH-CC-SC4-9 S	25.5	1242	248	163	GH-CC-SC4-CL9	25.5	7.56
GH-CC-SC4-10 S	28.5	1242	315	483	GH-CC-SC4-CL10	26.1	7.35
GH-CC-SC4-11 S	31.5	1438	191	108	GH-CC-SC4-CL11	26.0	7.76
GH-CC-SC4-12 S	34.5	1398	194	162	GH-CC-SC4-CL12	27.5	7.39

Table 7. Porewater water chemistry from Seaplane Lagoon, Alameda NAS compared with sulfide, carbonate, oxide, hydroxide, and silicate minerals reported as the saturation index at 25°C (log *SI*). Calculations used trace and major elements; sulfide and sulfate are from core GH-CC-SC4, and total inorganic carbon is from core GH-CC-SC2.

Sulfides

Sample ID	Depth (cm)	CdS	CrS	CuS Covellite	$CuFeS_2$ Chalcopyrite	FeS_2 Pyrite	FeS Pyrrhotite	MnS Alabandite	NiS Millerite	PbS Galena	ZnS Sphalerite
GH-CC-SC4-1	1.5	10.6	-10.8	9.0	19.7	14.4	4.6	0.5	5.9	10.4	9.5
GH-CC-SC4-2	4.5	10.1	-10.7	8.4	17.7	12.5	3.3	-0.1	5.5	10.4	9.2
GH-CC-SC4-3	7.5	12.5	-10.5	8.3				0.5	6.1	10.7	9.6
GH-CC-SC4-4	10.5	10.6	-10.4	8.3				0.7	6.2	10.7	9.7
GH-CC-SC4-5	13.5	10.5	-10.4	8.5				0.6	5.8	10.3	9.6
GH-CC-SC4-6	16.5	10.2	-10.2	8.6				0.8	5.9	10.7	9.8
GH-CC-SC4-7	19.5	10.2	-10.1	8.4				0.4	5.7	10.2	9.7
GH-CC-SC4-8	22.5	10.6	-10.0	8.9				0.2	5.8	10.6	9.8
GH-CC-SC4-9	25.5		-10.1	8.8				-0.5		10.2	9.5
GH-CC-SC4-10	28.5	10.1	-10.0	8.5				-1.5	5.3	10.5	9.1
GH-CC-SC4-11	31.5	10.6	-9.7	8.3				-1.7	5.8	10.7	9.7
GH-CC-SC4-12	34.5	10.6	-9.6	8.5					5.4	10.9	9.4

Carbonates

Sample ID	Depth (cm)	$CaCO_3$ Calcite	$CdCO_3$ Otavite	$Cu_2CO_3(OH)_2$ Malachite	$FeCO_3$ Siderite	$MnCO_3$ Rhodochrosite	$NiCO_3$	$PbCO_3$ Cerussite	$ZnCO_3$ Smithsonite
GH-CC-SC4-1	1.5	-1.1	-6.0	-27.3	-1.4	-2.2	-8.1	-3.7	-4.7
GH-CC-SC4-2	4.5	-0.7	-5.9	-27.4	-2.1	-2.2	-7.9	-3.1	-4.6
GH-CC-SC4-3	7.5	0.4	-3.1	-26.7		-1.1	-6.8	-2.4	-3.7
GH-CC-SC4-4	10.5	0.9	-4.5	-26.1		-0.5	-6.4	-2.0	-3.2
GH-CC-SC4-5	13.5	0.8	-4.4	-25.8		0.0	-6.5	-2.1	-3.0
GH-CC-SC4-6	16.5	1.0	-4.6	-25.6		-0.1	-6.3	-1.7	-2.7
GH-CC-SC4-7	19.5	1.0	-4.5	-25.9		-0.4	-6.4	-1.6	-2.8
GH-CC-SC4-8	22.5	1.1	-4.1	-24.9		-0.5	-6.2	-1.6	-2.6
GH-CC-SC4-9	25.5	1.0		-25.2		-1.1		-1.8	-2.8
GH-CC-SC4-10	28.5	0.9	-4.3	-25.8		-2.0	-6.5	-1.5	-3.1
GH-CC-SC4-11	31.5	1.5	-3.9	-26.0		-2.3	-6.1	-1.3	-2.5
GH-CC-SC4-12	34.5	1.0	-3.8	-25.9			-6.5	-1.0	-2.7

Table 7 (Continued). Porewater water chemistry from Seaplane Lagoon, Alameda NAS compared with sulfide, carbonate, oxide, hydroxide, and silicate minerals reported as the saturation index at 25°C (log *SI*). Calculations used trace and major elements; sulfide and sulfate are from core GH-CC-SC4, and total inorganic carbon is from core GH-CC-SC2.

Oxides/Hydroxides										
Sample ID	Depth (cm)	$Al(OH)_3$ Gibbsite	$Cd(OH)_2$	Cr_2O_3 Eskolaite	CuO Tenorite	$Fe(OH)_2$	FeOOH Goethite	$Ni(OH)_2$	$Mn(OH)_2$	β-$Zn(OH)_2$
GH-CC-SC4-1	1.5	0.5	-10.3	10.0	-12.7	-4.2	-0.9	-6.1	-6.4	-5.1
GH-CC-SC4-2	4.5	0.8	-10.2	11.5	-12.8	-5.0	-1.6	-5.9	-6.4	-4.8
GH-CC-SC4-3	7.5	-0.1	-7.4	12.5	-12.4			-4.9	-5.4	-4.0
GH-CC-SC4-4	10.5	0.2	-9.2	12.7	-12.4			-4.8	-5.2	-3.9
GH-CC-SC4-5	13.5	0.1	-9.7	12.2	-12.5			-5.6	-5.7	-4.3
GH-CC-SC4-6	16.5	0.2	-10.0	12.7	-12.4			-5.4	-5.5	-4.1
GH-CC-SC4-7	19.5	0.5	-10.1	12.7	-12.7			-5.7	-6.0	-4.4
GH-CC-SC4-8	22.5	0.3	-9.7	12.8	-12.2			-5.6	-6.0	-4.2
GH-CC-SC4-9	25.5	0.8		12.5	-12.5				-7.0	-4.7
GH-CC-SC4-10	28.5	1.7	-10.4	12.3	-12.9			-6.4	-8.1	-5.2
GH-CC-SC4-11	31.5	0.4	-9.7	13.3	-12.8			-5.6	-8.1	-4.3
GH-CC-SC4-12	34.5	1.0	-10.0	13.0	-13.0			-6.4		-4.9

Silicates				
Sample ID	Depth (cm)	SiO_2 Quartz	SiO_2 β-Cristobalite	$Mg_5Al_2Si_3O_{10}(OH)_8$ 7A-Chlorite
GH-CC-SC4-1	1.5	0.7	-0.3	0.0
GH-CC-SC4-2	4.5	0.9	-0.1	2.8
GH-CC-SC4-3	7.5	0.8	-0.2	6.4
GH-CC-SC4-4	10.5	0.9	-0.2	7.7
GH-CC-SC4-5	13.5	0.8	-0.2	4.0
GH-CC-SC4-6	16.5	0.8	-0.2	5.2
GH-CC-SC4-7	19.5	0.8	-0.1	9.4
GH-CC-SC4-8	22.5	0.8	-0.2	4.7
GH-CC-SC4-9	25.5	0.9	-0.1	3.9
GH-CC-SC4-10	28.5	0.9	-0.1	3.5
GH-CC-SC4-11	31.5	0.8	-0.1	4.9
GH-CC-SC4-12	34.5	0.9	-0.1	2.6

Table 8. Results of leaching experiments with sediment GH-CC-SC4-11 (runs A, B, C, and blank) as dissolved trace-metal concentrations.

Table 8-1. Core GH-CC-SC4-11-A.

Sample ID	Time (days)	Flow rate (g/day)	pH	Cd (ppb)	±	Cr (ppb)	±	Cu (ppb)	±	Ni (ppb)	±	Pb (ppb)	±	Zn (ppb)	±
SC4-11-A-1	0.47	a	8.01	0.78	0.02	0.75	0.51	3.82	0.11	2.98	0.08	1.26	0.01	16.45	0.37
SC4-11-A-2	1.42	41.92	7.78	2.12	0.03	0.44	0.24	1.29	0.10	2.20	0.03	1.92	0.02	11.39	0.10
SC4-11-A-3	2.35	42.65	7.81	3.95	0.05	0.24	0.13	1.34	0.04	1.79	0.03	2.67	0.03	16.59	0.29
SC4-11-A-4	3.34	42.97	7.82	6.50	0.09	0.31	0.11	1.47	0.05	1.42	0.04	2.98	0.01	17.55	0.23
SC4-11-A-5	4.41	43.47	7.87	na	na	na	na	na	na	na	na	na	na	na	na
SC4-11-A-6	5.42	43.58	7.87	na	na	na	na	na	na	na	na	na	na	na	na
SC4-11-A-7	6.39	43.91	7.83	11.20	0.14	0.22	0.11	1.85	0.13	1.55	0.03	2.84	0.01	17.16	0.37
SC4-11-A-8	7.37	43.75	7.81	na	na	na	na	na	na	na	na	na	na	na	na
SC4-11-A-9	11.36	44.64	7.93	16.14	0.25	0.32	0.05	2.66	0.10	2.18	0.04	2.82	0.03	23.43	0.16
SC4-11-A-10	14.19	45.04	7.82	13.74	0.11	0.28	0.04	2.68	0.12	1.90	0.02	2.65	0.01	22.48	0.43
SC4-11-A-11	18.43	45.31	7.82	12.77	0.16	0.31	0.06	2.64	0.07	1.92	0.04	2.51	0.03	18.88	0.14
SC4-11-A-12	21.23	45.53	7.86	11.54	0.04	0.26	0.10	2.34	0.07	1.80	0.03	2.50	0.01	17.41	0.24
SC4-11-A-13	25.72	46.56	7.77	10.92	0.13	0.39	0.28	3.31	0.04	2.03	0.02	3.01	0.01	18.63	0.24
SC4-11-A-14	33.86	46.91	7.82	9.45	0.11	0.41	0.05	2.43	0.08	2.00	0.04	2.32	0.05	12.82	0.20
SC4-11-A-15	39.91	47.81	7.87	na	na	na	na	na	na	na	na	na	na	na	na
SC4-11-A-16	47.75	41.16	8.05	na	na	0.38	0.09	1.99	0.08	2.21	0.30	2.30	0.28	na	na
SC4-11-A-17	54.75	44.60	7.81	10.11	0.23	0.44	0.11	2.90	0.09	2.10	0.07	3.13	0.01	18.08	0.41
SC4-11-A-18	62.91	44.80	7.85	6.93	0.14	0.41	0.15	2.39	0.06	1.76	0.01	2.21	0.06	11.91	0.22
SC4-11-A-19	76.90	48.08	7.87	2.81	0.04	0.41	0.13	1.77	0.04	1.16	0.03	1.88	0.02	7.58	0.08
SC4-11-A-20	91.41	47.53	7.94	1.34	0.10	0.36	0.21	1.00	0.01	0.88	0.02	1.02	0.05	3.91	0.36

Table 8-2. Core GH-CC-SC4-11-B.

Sample ID	Time (days)	Flow rate (g/day)	pH	Cd (ppb)	±	Cr (ppb)	±	Cu (ppb)	±	Ni (ppb)	±	Pb (ppb)	±	Zn (ppb)	±
SC4-11-B-1	0.47	a	7.98	0.42	0.02	nd	nd	0.91	0.04	1.26	0.04	1.83	0.05	6.88	0.25
SC4-11-B-2	1.42	41.52	7.85	na	na	na	na	na	na	na	na	na	na	na	na
SC4-11-B-3	2.35	42.12	7.82	4.89	0.05	nd	nd	1.06	0.06	1.86	0.05	3.51	0.03	13.66	0.16
SC4-11-B-4	3.34	42.59	7.86	9.71	0.11	0.32	0.113	1.41	0.09	2.21	0.04	3.87	0.04	17.59	0.26
SC4-11-B-5	4.41	43.10	7.86	na	na	na	na	na	na	na	na	na	na	na	na
SC4-11-B-6	5.42	a	7.86	na	na	na	na	na	na	na	na	na	na	na	na
SC4-11-B-7	6.39	43.73	7.86	11.59	0.13	0.37	0.114	2.07	0.06	1.45	0.05	3.03	0.02	19.62	0.33
SC4-11-B-8	7.37	43.84	7.84	12.12	0.42	0.28	0.074	1.85	0.12	nd	nd	2.54	0.08	19.94	1.06
SC4-11-B-9	11.36	44.77	7.93	18.20	0.18	0.36	0.053	2.57	0.12	2.04	0.03	3.69	0.04	23.71	0.28
SC4-11-B-10	14.19	45.36	7.79	19.87	0.15	0.37	0.045	2.85	0.12	2.12	0.07	3.72	0.05	24.53	0.16
SC4-11-B-11	18.43	46.43	7.80	21.20	0.24	0.33	0.057	3.01	0.07	2.25	0.04	3.61	0.04	24.59	0.17
SC4-11-B-12	21.23	46.81	7.80	23.01	0.09	0.45	0.096	2.96	0.11	2.22	0.04	3.38	0.04	22.65	0.18
SC4-11-B-13	25.72	47.68	7.80	18.43	0.29	0.33	0.276	2.66	0.11	2.17	0.06	2.99	0.06	19.27	0.32
SC4-11-B-14	33.86	48.92	7.81	14.20	1.41	0.38	0.050	2.66	0.10	1.85	0.04	3.09	0.29	22.52	3.77
SC4-11-B-15	39.91	50.83	7.86	8.27	0.09	0.37	0.045	3.31	0.07	1.61	0.01	2.62	0.07	15.25	0.25
SC4-11-B-16	47.75	41.34	7.86	7.42	1.28	0.42	0.087	2.35	0.06	1.84	0.13	3.11	0.35	na	na
SC4-11-B-17	54.75	44.49	7.79	7.74	0.28	0.40	0.112	2.61	0.11	1.70	0.05	3.68	0.10	19.64	1.02
SC4-11-B-18	62.91	44.76	7.80	6.70	0.74	0.44	0.148	2.49	0.08	1.46	0.05	3.36	0.23	15.42	2.17
SC4-11-B-19	76.90	42.20	7.87	3.49	0.06	0.38	0.134	2.08	0.06	1.10	0.04	2.57	0.06	8.68	0.12
SC4-11-B-20	91.41	49.85	7.87	15.24	0.29	0.46	0.214	1.84	0.03	4.16	0.05	2.62	0.21	13.79	0.36

[a] Flow rate not recorded.

nd = not detected; na = not analyzed.

Table 8-3. Core GH-CC-SC4-11-C.

Sample ID	Time (days)	Flow rate (g/day)	pH	Cd (ppb)	±	Cr (ppb)	±	Cu (ppb)	±	Ni (ppb)	±	Pb (ppb)	±	Zn (ppb)	±
SC4-11-C-1	0.47	a	7.96	0.52	0.01	1.00	0.51	13.71	0.26	4.96	0.12	2.13	0.02	22.43	0.31
SC4-11-C-2	1.42	41.64	7.66	1.15	0.01	0.30	0.24	2.09	0.10	1.97	0.06	1.96	0.00	10.96	0.15
SC4-11-C-3	2.35	42.49	7.84	2.50	0.00	0.34	0.13	2.07	0.06	1.65	0.03	2.21	0.02	13.31	0.13
SC4-11-C-4	3.34	43.00	7.85	4.55	0.02	0.32	0.11	2.02	0.07	1.49	0.05	2.06	0.01	12.71	0.13
SC4-11-C-5	4.41	43.67	7.85	na	na	na	na	na	na	na	na	na	na	na	na
SC4-11-C-6	5.42	43.84	7.86	14.59	0.20	0.45	0.07	1.38	0.07	1.17	0.03	3.97	0.03	21.49	0.16
SC4-11-C-7	6.39	44.19	7.84	16.04	0.06	0.29	0.11	1.54	0.05	1.67	0.06	4.09	0.04	21.71	0.13
SC4-11-C-8	7.37	44.33	7.86	15.70	0.07	0.27	0.07	1.54	0.08	na	na	3.63	0.04	20.65	0.23
SC4-11-C-9	11.36	45.42	7.91	23.54	0.11	0.28	0.05	2.05	0.12	2.30	0.03	6.34	0.05	29.54	0.33
SC4-11-C-10	14.19	46.02	7.83	22.85	0.24	0.39	0.04	2.43	0.15	2.33	0.08	4.73	0.06	31.06	0.37
SC4-11-C-11	18.43	47.27	7.80	19.52	0.17	0.29	0.06	2.80	0.19	2.21	0.02	6.30	0.07	28.26	0.36
SC4-11-C-12	21.23	47.04	7.74	19.52	0.10	0.26	0.10	2.97	0.06	na	na	4.18	0.03	25.56	0.09
SC4-11-C-13	25.72	48.10	7.81	23.94	3.95	nd	0.28	5.95	0.22	2.07	0.11	3.94	0.41	na	na
SC4-11-C-14	33.86	50.50	7.86	13.77	0.26	0.41	0.05	3.73	0.14	2.08	0.03	4.41	0.04	21.81	0.11
SC4-11-C-15	39.91	54.43	7.85	10.33	1.13	0.43	0.04	2.37	0.06	na	na	2.97	0.23	13.58	2.22
SC4-11-C-16	47.75	39.49	7.89	na	na	0.51	0.09	4.10	0.19	na	na	4.26	0.54	na	na
SC4-11-C-17	54.75	45.85	7.87	10.53	0.21	0.40	0.11	3.54	0.11	2.57	0.09	4.59	0.15	29.81	0.57
SC4-11-C-18	62.91	46.58	7.83	3.61	0.07	0.57	0.15	3.69	0.10	1.76	0.04	5.19	0.04	24.20	0.26
SC4-11-C-19	76.90	51.01	7.88	1.59	0.28	0.38	0.13	2.17	0.05	1.13	0.10	3.37	0.40	12.89	3.12

Table 8-4. Blank.

Sample ID	Time (days)	Flow rate (g/day)	pH	Cd (ppb)	±	Cr (ppb)	±	Cu (ppb)	±	Ni (ppb)	±	Pb (ppb)	±	Zn (ppb)	±
B-1	0.47	a	8.01	0.62	0.020	0.4	0.510	2.6	0.048	3.7	0.207	0.30	0.010	20.1	1.15
B-2	1.42	40.14	8.04	0.20	0.003	0.3	0.244	1.6	0.026	0.9	0.020	0.12	0.002	6.1	0.15
B-3	2.35	41.16	8.02	0.19	0.003	0.5	0.130	1.1	0.047	0.7	0.023	0.09	0.002	4.5	0.06
B-4	3.34	41.55	8	0.12	0.002	0.2	0.113	0.9	0.054	0.7	0.015	0.08	0.002	4.4	0.10
B-5	4.41	42.10	8.02	0.14	0.003	0.3	0.173	0.9	0.020	0.7	0.026	0.07	0.002	3.8	0.06
B-6	5.42	a	7.97	0.13	0.005	0.3	0.069	0.6	0.044	0.7	0.039	0.05	0.001	2.9	0.07
B-7	6.39	42.87	7.96	0.10	0.004	nd	0.114	0.5	0.025	0.5	0.031	0.04	0.001	2.7	0.04
B-8	7.37	42.96	8.1	0.12	0.004	0.2	0.074	0.5	0.029	0.7	0.023	0.06	0.001	3.3	0.04
B-9	11.36	44.27	7.96	0.10	0.005	0.3	0.053	0.4	0.037	0.9	0.032	0.04	0.001	2.4	0.04
B-10	14.19	44.61	8	0.13	0.002	0.3	0.045	0.5	0.030	0.9	0.028	0.04	0.001	2.7	0.02
B-11	18.43	45.35	7.94	0.11	0.002	0.2	0.057	0.5	0.015	0.9	0.017	0.03	0.001	2.4	0.03
B-12	21.23	45.53	8	0.20	0.007	0.9	0.096	0.8	0.035	1.3	0.033	0.04	0.001	3.0	0.04
B-13	25.72	46.33	7.9	0.10	0.014	nd	0.276	0.5	0.022	1.0	0.075	nd	na	2.5	0.39
B-14	33.86	47.11	7.92	na	0.000	0.1	0.050	0.4	0.030	0.9	0.152	nd	na	2.1	0.37
B-15	39.91	49.35	7.92	na	0.000	0.1	0.045	0.4	0.029	na	0.000	nd	na	na	0.00
B-16	47.75	39.18	7.87	0.11	0.017	nd	0.087	0.4	0.017	na	0.000	na	0.000	na	0.00
B-17	54.75	41.97	7.89	0.11	0.017	0.2	0.112	0.4	0.030	1.0	0.108	0.03	0.002	3.1	0.45
B-18	62.91	43.29	8.06	0.10	0.014	0.2	0.148	0.4	0.016	1.0	0.092	nd	na	na	0.00
B-19	76.90	46.33	8	0.11	0.016	0.2	0.134	0.4	0.025	1.1	0.064	nd	na	3.5	0.65
B-20	91.41	49.13	7.92	0.09	0.002	0.2	0.214	0.6	0.015	0.9	0.009	0.01	0.000	3.5	0.11

[a] Flow rate not recorded.

nd = not detected; na = not analyzed.

Table 9. Bulk sediment chemistry from Seaplane Lagoon cores GH-CC-C1, GH-CC-C2, GH-CC-C3, GH-CC-SC2, GH-CC-SC3, and GH-CC-SC4; reported as the average (± uncertainty) of 2–4 replicate analyses multiplied by 1.47 to correct for solution viscosity. If no uncertainty is reported, then replicate analyses were not made. Mercury analyses were made by cold vapor extraction of a separate fraction of the sediment sample and did not require a viscosity correction.

Table 9-1. Core GH-CC-C1.

Sample ID	Depth (cm)	Ag (ppm)	±	Al (ppm)	±	As (ppm)	Ba (ppm)	±	Ca (ppm)	±	Cd (ppm)	±	Co (ppm)	±	Cr (ppm)	±	Cu (ppm)	±
GH-CC-C1-1	75.0	<3		34657	4445	<36	163	15	9461	345	1.4	0.2	21.5	1.8	159	9	39.6	3.9
GH-CC-C1-2	55.0	44.6	8.5	31975	3840	<36	127	26	21925	630	1222.0	51.9	18.9	0.8	1726	93	232.0	8.1
GH-CC-C1-3	40.0	3.9	2.6	41841	5212	<36	106	29	8680	255	71.9	3.8	26.9	1.2	470	26	164.5	7.3
GH-CC-C1-4	30.0	<3		44646	5048	<36	160	23	8949	334	29.3	1.0	34.0	2.1	424	25	177.1	5.5
GH-CC-C1-5	20.0	<3		46458	4773	<36	167	19	8811	198	29.8	1.7	28.1	2.0	346	4	150.4	3.8
GH-CC-C1-6	13.5	<3		48344	4849	<36	135	30	8930	192	20.4	0.9	26.9	1.2	300	11	137.2	3.3
GH-CC-C1-7	10.5	<3		47775	4131	<36	120	30	8857	201	15.1	0.5	24.9	1.6	271	11	118.4	6.9
GH-CC-C1-8	7.5	<3		48511	6381	<36	156	37	10038	333	13.7	1.0	24.8	1.4	262	12	116.0	6.0
GH-CC-C1-9	4.5	<3		48245	4623	<36	131	36	9402	288	11.3	1.7	26.6	1.5	259	16	115.8	6.6
GH-CC-C1-10	1.5	<3		47045	6121	<36	106	27	9213	347	15.4	1.4	26.3	2.0	264	9	123.1	10.2

Sample ID	Depth (cm)	Fe (ppm)	±	Hg (ppm)	±	Li (ppm)	±	Mg (ppm)	±	Mn (ppm)	±	Ni (ppm)	±	Pb (ppm)	±	S (ppm)	±
GH-CC-C1-1	75.0	46131	4095	0.5	0.03	26.4	2.6	9673	2943	952	51	128.7	6.6	57	24	3944	81
GH-CC-C1-2	55.0	48393	3590	1.8	0.10	30.4	3.0	12284	3482	400	18	113.1	5.2	1396	135	4774	475
GH-CC-C1-3	40.0	51589	4088	1.6	0.09	37.9	3.3	13234	3776	398	20	153.9	9.2	645	69	4546	59
GH-CC-C1-4	30.0	54134	4305	2.4	0.13	41.0	4.2	13216	3774	427	23	153.0	4.6	475	53	4739	479
GH-CC-C1-5	20.0	55136	2990	1.6	0.09	41.6	1.8	13187	4235	479	6	145.4	4.7	347	55	4785	46
GH-CC-C1-6	13.5	57634	3507	1.2	0.07	44.4	0.9	13856	3870	508	19	145.1	3.4	241	27	5004	397
GH-CC-C1-7	10.5	56564	2514	1.1	0.06	43.3	1.2	13726	3757	508	17	144.2	2.6	195	24	4899	189
GH-CC-C1-8	7.5	55796	4057	1.1	0.06	40.9	0.2	14220	4693	505	25	140.2	9.6	185	37	4702	
GH-CC-C1-9	4.5	54732	2973	1.2	0.07	41.7	1.5	13871	3956	478	29	133.0	0.6	188	21	4590	
GH-CC-C1-10	1.5	52559	4461	1.3	0.07	36.4	0.9	13560	4550	430	23	130.8	10.3	206	45	4463	

Sample ID	Depth (cm)	Se (ppm)	±	Sn (ppm)	±	Sr (ppm)	±	Th (ppm)	±	Ti (ppm)	±	V (ppm)	±	Zn (ppm)	±
GH-CC-C1-1	75.0	105	40	228	72	96.1	3.9	45.2	6.4	2179	313	130.0	6.2	108	14
GH-CC-C1-2	55.0	112	62	245	45	155.3	5.6	40.8	6.0	2255	332	140.4	6.3	574	61
GH-CC-C1-3	40.0	140	96	216	50	86.8	3.5	54.4	8.7	2608	389	173.9	8.9	373	42
GH-CC-C1-4	30.0	132	68	211	71	87.5	3.8	58.4	7.7	2626	362	181.6	10.9	399	43
GH-CC-C1-5	20.0	116	67	250	62	89.2	1.3	58.1	14.9	2753	297	171.9	2.7	344	48
GH-CC-C1-6	13.5	136	57	242	79	85.3	3.0	59.3	8.5	2835	388	175.8	7.9	313	33
GH-CC-C1-7	10.5	101	72	240	78	83.2	2.7	53.7	3.8	2775	312	171.9	7.3	282	27
GH-CC-C1-8	7.5	131	47	205	59	89.4	4.3	57.2	11.9	2857	479	166.5	6.1	280	44
GH-CC-C1-9	4.5	134	51	215	76	88.2	4.9	60.1	10.2	2820	400	166.1	9.7	285	31
GH-CC-C1-10	1.5	286	511	202	63	84.3	8.3	56.9	13.9	2820	276	157.8	5.6	295	51

Table 9-2. Core GH-CC-C2.

Sample ID	Depth (cm)	Ag (ppm)	±	Al (ppm)	±	As (ppm)	Ba (ppm)	±	Ca (ppm)	±	Cd (ppm)	±	Co (ppm)	±	Cr (ppm)	±	Cu (ppm)	±
GH-CC-C2-1	1.5	<3		44086	6031	<36	108	27	9280	966	14.7	1.3	26.7	1.8	265	24	126	13
GH-CC-C2-2	4.5	<3		43771	6473	<36	138	28	9688	1315	13.4	2.0	27.2	2.6	264	32	131	14
GH-CC-C2-3	7.5	-<3		43772	6185	<36	108	35	8677	1033	18.3	2.1	28.0	2.6	281	30	137	11
GH-CC-C2-4	10.5	5.9	3.3	44984	6170	<36	112	21	9168	1057	58.1	7.1	28.1	2.1	373	37	150	13
GH-CC-C2-5	13.5	<3		46145	6547	<36	44	57	9120	1103	16.4	1.9	27.4	2.6	278	29	132	12
GH-CC-C2-6	20.0	<3		48379	6929	<36	90	31	9150	1124	19.8	2.5	28.0	2.7	309	33	146	13
GH-CC-C2-7	30.0	3.7	3.0	44990	6096	<36	117	10	9177	1039	39.6	4.1	43.7	3.9	455	44	167	13
GH-CC-C2-8	40.0	9.2	4.5	35960	4862	<36	96	12	9439	1018	72.9	9.7	156.9	17.2	544	51	227	19
GH-CC-C2-9	55.0	17.8	4.3	33388	4301	<36	94	8	12167	1280	274.3	33.9	19.8	1.4	774	73	197	14
GH-CC-C2-10	75.0	<3		31154	3710	<36	100	17	12290	773	1.1	0.4	14.4	0.7	100	6	19	3

Sample ID	Depth (cm)	Fe (ppm)	±	Hg (ppm)	±	Li (ppm)	±	Mg (ppm)	±	Mn (ppm)	±	Ni (ppm)	±	Pb (ppm)	±	S (ppm)	Se (ppm)	±
GH-CC-C2-1	1.5	51388	4599	1.3	0.07	38.2	2.1	14689	3980	434	41	136	12	234	49	11809	95	42
GH-CC-C2-2	4.5	51725	5988	1.2	0.07	38.7	5.1	14710	4001	442	56	130	18	231	49	13014	112	52
GH-CC-C2-3	7.5	52575	5435	1.3	0.07	39.0	1.3	14528	3962	441	49	135	15	269	64	13450	79	42
GH-CC-C2-4	10.5	53888	5140	1.4	0.08	44.3	5.9	15485	4079	458	47	140	15	451	89	14193	80	50
GH-CC-C2-5	13.5	53297	5437	1.2	0.07	42.7	3.4	15139	4039	460	52	141	16	266	52	14322	92	42
GH-CC-C2-6	20.0	55273	5547	1.3	0.07	48.3	11.4	16160	4304	484	53	150	17	313	67	14933	98	37
GH-CC-C2-7	30.0	51980	4955	1.8	0.10	43.0	4.7	15775	4214	414	41	154	15	514	96	14513	79	55
GH-CC-C2-8	40.0	49204	4875	1.8	0.10	34.9	3.6	14807	3958	350	35	173	20	1169	231	13482	88	52
GH-CC-C2-9	55.0	46153	4218	1.9	0.11	28.4	0.5	13524	3467	406	38	114	12	895	162	16272	116	46
GH-CC-C2-10	75.0	23337	1613	0.3	0.02	18.0	1.8	6550	1798	341	24	73	5	55	13	6571	90	79

Sample ID	Depth (cm)	Sn (ppm)	±	Sr (ppm)	±	Th (ppm)	±	Ti (ppm)	±	V (ppm)	±	Zn (ppm)	±
GH-CC-C2-1	1.5	188	50	86.3	4.7	55	17	2694	439	159	14	318	55
GH-CC-C2-2	4.5	185	61	91.9	6.1	58	16	2720	434	158	19	322	61
GH-CC-C2-3	7.5	184	65	83.1	4.6	63	13	2732	445	160	16	336	61
GH-CC-C2-4	10.5	181	60	85.7	5.2	68	19	2790	443	168	16	361	62
GH-CC-C2-5	13.5	180	69	67.8	6.0	62	11	2783	433	166	18	322	57
GH-CC-C2-6	20.0	181	55	82.9	5.5	62	19	2882	404	177	20	351	62
GH-CC-C2-7	30.0	184	64	81.9	4.7	61	14	2755	346	180	17	395	68
GH-CC-C2-8	40.0	186	50	87.7	4.8	59	10	2456	323	160	15	518	92
GH-CC-C2-9	55.0	199	52	104.9	6.2	51	13	2257	264	145	14	492	82
GH-CC-C2-10	75.0	184	61	132.0	3.9	29	12	1677	117	83	5	85	14

Table 9-3. Core GH-CC-C3.

Sample ID	Depth (cm)	Ag (ppm)	±	Al (ppm)	±	As (ppm)	Ba (ppm)	±	Ca (ppm)	±	Cd (ppm)	±	Co (ppm)	±	Cr (ppm)	±
GH-CC-C3-1	1.5	<3		46260	5613	<36	30	18	9579	584	7.7	0.6	26.0	0.7	238	14
GH-CC-C3-2	4.5	<3		47903	6175	<36	38	26	10722	760	9.7	1.0	24.9	1.2	252	16
GH-CC-C3-3	7.5	<3		50566	6076	<36	88	25	9324	634	10.8	0.6	25.7	1.7	264	16
GH-CC-C3-4	10.5	<3		49165	6719	<36	59	17	9396	830	10.7	1.2	24.4	2.5	262	20
GH-CC-C3-5	13.5	<3		51323	7138	<36	37	18	9259	672	16.1	2.0	27.6	3.0	282	15
GH-CC-C3-6	20.0	<3		46931	5789	<36	44	17	9723	620	18.2	1.5	25.6	2.1	276	15
GH-CC-C3-7	30.0	<3		54123	15518	<36	84	79	9836	1489	28.4	5.1	36.7	7.2	475	89
GH-CC-C3-8	40.0	6.3	2.5	40888	5348	<36	44	18	9333	542	67.8	4.7	102.9	5.7	511	24
GH-CC-C3-9	55.0	18.5	4.4	39818	5448	<36	52	20	10299	556	214.2	16.2	27.9	1.7	792	34
GH-CC-C3-10	75.0	21.9	4.4	31053	4113	<36	18	11	9999	659	391.3	33.3	18.3	1.6	869	43
GH-CC-C3-11	95.0	<3		41747	5100	<36	8	9	10521	660	0.9	0.6	24.0	1.3	184	9

Sample ID	Depth (cm)	Cu (ppm)	±	Fe (ppm)	±	Hg (ppm)	±	Li (ppm)	±	Mg (ppm)	±	Mn (ppm)	±	Ni (ppm)	±	Pb (ppm)	±
GH-CC-C3-1	1.5	115.3	6.3	51693	3129	1.2	0.07	38.9	0.6	15023	4014	434	28	132	9	182	29
GH-CC-C3-2	4.5	124.2	8.8	55027	3934	1.1	0.06	40.8	1.6	15891	4337	461	35	136	11	201	39
GH-CC-C3-3	7.5	121.2	13.8	56944	3597	1.1	0.06	46.4	4.2	16580	4408	528	36	146	10	209	38
GH-CC-C3-4	10.5	116.5	11.8	55934	4637	1.0	0.06	46.9	8.2	16375	4604	518	44	148	15	196	40
GH-CC-C3-5	13.5	132.3	9.5	57584	4209	1.1	0.06	45.6	4.4	16963	5046	523	34	153	13	233	46
GH-CC-C3-6	20.0	127.1	7.0	53039	3299	1.2	0.07	40.1	1.7	15654	4220	466	30	138	9	276	48
GH-CC-C3-7	30.0	221.2	48.4	58198	11643			49.9	17.6	18221	4279	478	86	176	31	600	124
GH-CC-C3-8	40.0	170.3	7.9	49382	3128	1.7	0.10	36.5	5.2	15141	3524	364	18	177	10	739	102
GH-CC-C3-9	55.0	204.9	10.9	47523	2893	2.3	0.13	35.3	3.5	14354	3519	379	19	136	9	1371	220
GH-CC-C3-10	75.0	214.3	10.6	49072	2742	1.7	0.10	28.9	4.4	13887	3204	503	30	119	7	1005	137
GH-CC-C3-11	95.0	40.0	4.3	52210	2944	0.6	0.03	27.1	4.3	12642	2792	490	23	155	9	73	11

Sample ID	Depth (cm)	S (ppm)	Se (ppm)	±	Sn (ppm)	±	Sr (ppm)	±	Th (ppm)	±	Ti (ppm)	±	V (ppm)	±	Zn (ppm)	±
GH-CC-C3-1	1.5	9464	93	51	175	64	76.3	5.6	60	11	2490	157	158	10	285	42
GH-CC-C3-2	4.5	12333	100	21	180	59	86.3	6.1	56	13	2608	202	165	11	311	50
GH-CC-C3-3	7.5	14310	105	73	178	64	80.6	3.2	63	14	2753	348	175	10	321	49
GH-CC-C3-4	10.5	14103	73	32	176	66	77.8	4.9	56	12	2653	212	172	13	297	51
GH-CC-C3-5	13.5	14476	66	95	176	49	81.7	4.4	69	13	2718	265	178	9	329	54
GH-CC-C3-6	20.0	14963	90	45	176	65	85.5	3.6	55	15	2559	184	166	9	325	50
GH-CC-C3-7	30.0	27965	97	30	185	90	90.5	19.9	54	23	2942	902	206	34	531	123
GH-CC-C3-8	40.0	15762	76	36	172	54	82.1	4.5	58	13	2420	183	167	7	426	56
GH-CC-C3-9	55.0	16887	65	52	157	46	85.0	2.7	57	15	2439	206	155	6	486	69
GH-CC-C3-10	75.0	14707	72	47	187	57	66.9	5.1	52	17	2147	186	144	8	428	61
GH-CC-C3-11	95.0	10948	122	86	168	64	54.1	5.8	57	17	2297	135	149	6	125	17

Table 9-4. Core GH-CC-SC2.

Sample ID	Depth (cm)	Ag (ppm)	Al (ppm)	±	As (ppm)	Ba (ppm)	±	Ca (ppm)	±	Cd (ppm)	±	Co (ppm)	±	Cr (ppm)	±
GH-CC-SC2-1	1.5	<3	41695	4934	<36	102	49	11014	908	11.0	2.0	22.2	2.9	230	24
GH-CC-SC2-2	4.5	<3	45278	4168	<36	159	23	9841	206	12.7	0.4	24.6	0.1	248	7
GH-CC-SC2-3	7.5	<3	46325	3936	<36	196	23	8512	334	18.8	0.2	24.7	0.8	284	14
GH-CC-SC2-4	10.5	<3	49016	3434	<36	148	43	8822	405	28.1	1.8	29.3	0.5	355	21
GH-CC-SC2-5	13.5	<3	48353	3882	<36	111	37	8733	531	32.7	2.9	31.0	2.8	385	32
GH-CC-SC2-6	16.5	<3	45134	3247	<36	209	8	8508	408	30.4	0.8	28.1	0.5	386	20
GH-CC-SC2-7	19.5	<3	45476	4811	<36	144	39	20918	560	33.1	1.9	26.9	1.7	392	20
GH-CC-SC2-8	22.5	<3	44165	4045	<36	164	39	7773	213	38.9	0.9	30.2	1.1	425	18
GH-CC-SC2-9	25.5	<3	45794	4279	<36	177	16	8037	220	53.4	1.1	50.6	2.4	494	27

Sample ID	Depth (cm)	Cu (ppm)	±	Fe (ppm)	±	Hg (ppm)	±	Li (ppm)	±	Mg (ppm)	Mn (ppm)	±	Ni (ppm)	±	Pb (ppm)	±	S (ppm)
GH-CC-SC2-1	1.5	98.0	7.2	41343	4728	1.1	0.06	28.4	5.7	7353	382	36	107.8	11.8	183	21	9954
GH-CC-SC2-2	4.5	107.6	1.6	48682	1621	1.2	0.07	35.4	4.1	9177	447	8	125.1	1.9	200	21	13395
GH-CC-SC2-3	7.5	129.2	3.4	51752	1707	1.3	0.07	38.9	2.2	9837	456	17	136.0	1.3	240	43	15756
GH-CC-SC2-4	10.5	156.5	8.3	53706	2584	1.6	0.09	43.3	3.8	10303	467	24	147.8	9.4	365	27	16587
GH-CC-SC2-5	13.5	164.1	10.5	53371	3942	1.8	0.10	42.3	6.3	10326	459	33	146.6	10.8	415	28	16624
GH-CC-SC2-6	16.5	162.8	5.4	50425	1380	1.8	0.10	39.2	1.0	9887	424	16	139.1	2.4	387	46	15769
GH-CC-SC2-7	19.5	174.4	5.6	48963	3225	1.9	0.11	40.2	5.8	9438	402	19	138.1	8.1	414	44	14233
GH-CC-SC2-8	22.5	167.6	3.8	46914	1643	2.0	0.12	37.0	1.6	9434	386	12	137.4	3.2	453	36	13934
GH-CC-SC2-9	25.5	163.3	5.1	47983	2750	1.8	0.10	37.9	2.6	9792	384	17	146.0	4.0	568	42	13242

Sample ID	Depth (cm)	Se (ppm)	±	Sn (ppm)	±	Sr (ppm)	±	Th (ppm)	±	Ti (ppm)	±	V (ppm)	±	Zn (ppm)	±
GH-CC-SC2-1	1.5	97	54	237	113	106.8	7.4	42.1	1.3	2299	245	126.4	12.5	240	22
GH-CC-SC2-2	4.5	111	48	219	77	95.7	2.3	43.9	10.5	2601	296	148.3	4.1	268	31
GH-CC-SC2-3	7.5	163	99	180	61	90.4	2.3	47.9	8.6	2720	393	158.6	8.0	298	28
GH-CC-SC2-4	10.5	157	90	236	98	95.8	5.1	62.4	7.3	2842	327	169.1	10.8	357	29
GH-CC-SC2-5	13.5	142	114	241	125	89.5	4.7	58.8	1.8	2842	318	170.4	14.6	395	25
GH-CC-SC2-6	16.5	114	83	217	92	90.8	3.7	49.9	7.0	2722	353	165.2	8.8	369	36
GH-CC-SC2-7	19.5	145	63	223	98	143.8	6.3	53.4	12.0	2689	415	165.8	7.9	373	41
GH-CC-SC2-8	22.5	121	77	214	78	88.1	2.7	46.5	1.4	2687	386	162.6	7.3	373	39
GH-CC-SC2-9	25.5	127	77	215	86	87.0	4.4	47.9	1.8	2723	380	170.0	8.8	389	39

Table 9-5. Core GH-CC-SC3.

Sample ID	Depth (cm)	Ag (ppm)	±	Al (ppm)	±	As (ppm)	±	Ba (ppm)	±	Ca (ppm)	±	Cd (ppm)	±	Co (ppm)	±	Cr (ppm)	±
GH-CC-SC3-1	1.5	<3		41559	4266	<36		88	31	9276	216	16.6	0.9	22.6	0.2	248	8
GH-CC-SC3-2	4.5	<3		42782	3767	<36		105	37	10285	428	15.5	1.2	21.4	1.8	240	12
GH-CC-SC3-3	7.5	<3		42935	4477	<36		187	30	13237	289	12.7	0.2	22.7	0.5	242	8
GH-CC-SC3-6	16.5	<3		41114	3377	<36		99	29	10123	387	46.2	0.8	42.8	1.7	419	16
GH-CC-SC3-7	19.5	5.9	1.5	44527	5055	<36		54	46	9109	555	83.8	5.2	69.1	4.7	550	51
GH-CC-SC3-8	22.5	3.6	1.0	45771	6644	<36		158	30	9332	1095	81.2	12.1	33.2	2.6	481	68
GH-CC-SC3-9	25.5	19.5	1.1	33548	3133	<36		129	14	10034	335	346.7	14.3	26.1	1.7	876	57
GH-CC-SC3-10	28.5	24.5	2.5	38217	4292	<36		140	12	9966	45	284.8	8.2	19.7	0.2	865	33
GH-CC-SC3-11	31.5	21.6	2.7	37383	4041	<36		159	16	11217	573	358.2	23.7	22.2	1.9	1151	96
GH-CC-SC3-12	34.5	19.7	2.8	34611	5085	<36		198	14	14118	1110	315.7	32.7	19.0	1.7	830	74
GH-CC-SC3-13	37.5	15.8	3.0	35405	4935	39.3	37.0	101	27	10393	660	269.1	23.2	20.0	1.6	691	57

Sample ID	Depth (cm)	Cu (ppm)	±	Fe (ppm)	±	Hg (ppm)	±	Li (ppm)	±	Mg (ppm)	±	Mn (ppm)	±	Ni (ppm)	±	Pb (ppm)	±
GH-CC-SC3-1	1.5	105.7	4.1	43743	1424	1.0	0.06	30.3	2.4	9417	2909	384	7	112.4	2.8	210	26
GH-CC-SC3-2	4.5	107.4	0.6	43839	1606	1.0	0.05	33.4	4.6	10113	2879	392	16	111.9	4.4	210	6
GH-CC-SC3-3	7.5	106.6	2.7	46845	1610	0.9	0.05	36.1	2.5	10944	3321	425	11	117.4	1.2	199	15
GH-CC-SC3-6	16.5	149.4	5.0	45091	877	1.8	0.10	34.6	0.8	11128	3365	371	10	146.9	1.0	516	47
GH-CC-SC3-7	19.5	199.0	14.1	49439	4574	1.9	0.11	40.5	8.5	12260	3331	382	32	186.3	10.1	898	70
GH-CC-SC3-8	22.5	162.2	17.0	56249	8423	1.5	0.08	42.5	8.6	13372	3450	436	60	162.6	23.0	676	103
GH-CC-SC3-9	25.5	216.4	9.4	47721	2873	1.8	0.10	37.4	8.4	12413	3575	440	24	147.2	7.4	955	63
GH-CC-SC3-10	28.5	206.9	4.1	49248	2493	2.2	0.13	38.9	8.5	12513	4032	429	12	118.9	5.5	1121	129
GH-CC-SC3-11	31.5	236.4	10.3	52792	4420	1.9	0.11	35.4	2.4	12442	3537	399	28	150.4	9.8	1127	111
GH-CC-SC3-12	34.5	241.2	18.2	48793	5956	2.4	0.13	33.0	4.8	11146	3613	364	34	136.7	16.0	1226	188
GH-CC-SC3-13	37.5	224.5	13.0	49317	5337	2.6	0.15	33.9	5.5	11374	3354	385	30	124.8	11.6	784	108

Sample ID	Depth (ppm)	S (ppm)	±	Se (ppm)	±	Sn (ppm)	±	Sr (ppm)	±	Th (ppm)	±	Ti (ppm)	±	V (ppm)	±	Zn (ppm)	±
GH-CC-SC3-1	1.5	10719		110	44	204	88	88.4	1.8	44.9	9.8	2447	351	131.0	4.3	257	30
GH-CC-SC3-2	4.5	12280		102	86	215	98	101.0	2.3	42.5	7.7	2344	348	133.4	7.5	251	23
GH-CC-SC3-3	7.5	13405		113	49	216	87	109.6	2.2	44.3	9.8	2501	403	141.0	5.1	256	29
GH-CC-SC3-6	16.5	13737		104	47	220	81	90.3	2.9	50.5	7.1	2562	358	156.2	6.3	354	41
GH-CC-SC3-7	19.5	14066		117	52	248	84	76.4	4.4	52.7	12.2	2759	372	177.9	15.5	445	40
GH-CC-SC3-8	22.5	16358		152	133	260	100	91.1	9.9	64.2	7.2	2846	407	173.1	23.5	377	40
GH-CC-SC3-9	25.5	13659		124	70	248	61	93.3	5.5	49.0	9.6	2937	352	146.3	10.2	386	38
GH-CC-SC3-10	28.5	17871		126	51	237	50	87.2	2.2	48.2	13.9	2601	417	149.4	4.5	525	70
GH-CC-SC3-11	31.5	20902		101	67	258	81	95.5	6.6	52.1	8.5	2524	348	200.3	16.8	631	62
GH-CC-SC3-12	34.5	18926	938	145	80	233	46	104.7	6.8	48.6	11.9	2472	347	150.2	12.9	481	72
GH-CC-SC3-13	37.5	18923	167	157	97	268	61	95.0	5.8	55.6	13.5	2462	377	152.9	11.7	475	58

Table 9-6. Core GH-CC-SC4.

Sample ID	Depth (cm)	Ag (ppm)	±	Al (ppm)	±	As (ppm)	Ba (ppm)	±	Ca (ppm)	±	Cd (ppm)	±	Co (ppm)	±	Cr (ppm)	±
GH-CC-SC4-1	1.5	<3		44303	6128	<36	89	22	11184	1061	14.7	1.8	23.5	2.1	243	23
GH-CC-SC4-2	4.5	<3		46904	6463	<36	75	23	9750	1119	17.1	2.4	24.8	1.7	275	27
GH-CC-SC4-3	7.5	<3		47132	6117	<36	74	47	9739	1103	18.7	1.5	25.3	1.1	278	28
GH-CC-SC4-4	10.5	<3		48311	6115	<36	115	50	10178	1212	15.4	2.3	26.3	1.4	279	29
GH-CC-SC4-5	13.5	<3		48904	4864	<36	110	23	10259	896	21.0	1.9	25.6	1.5	280	21
GH-CC-SC4-6	16.5	4.5	2.1	48528	4836	<36	64	26	10574	878	38.5	3.2	26.6	1.5	327	24
GH-CC-SC4-7	19.5	<3		47785	4641	<36	174	14	9194	780	37.6	3.4	27.8	2.2	351	26
GH-CC-SC4-8	22.5	4.4	2.6	46820	4552	<36	90	19	9743	719	55.7	4.6	32.1	2.3	422	27
GH-CC-SC4-9	25.5	5.8	2.7	46857	4325	<36	82	17	8923	635	65.7	5.4	36.3	1.7	456	26
GH-CC-SC4-10	28.5	3.7	1.7	48223	4900	<36	168	17	9630	304	77.6	3.3	46.6	1.3	493	15
GH-CC-SC4-11	31.5	6.1	3.2	44703	7021	<36	89	29	14820	1280	135.6	14.3	27.0	1.8	584	38
GH-CC-SC4-12	34.5	15.8	4.7	46200	6211	<36	53	20	10632	744	191.7	17.9	30.7	1.9	766	45

Sample ID	Depth (cm)	Cu (ppm)	±	Fe (ppm)	±	Hg (ppm)	±	Li (ppm)	±	Mg (ppm)	±	Mn (ppm)	±	Ni (ppm)	±	Pb (ppm)	±
GH-CC-SC4-1	1.5	107.7	7.8	44009	3936	1.0	0.06	31.6	2.2	11860	3406	429	40	120	11	214	40
GH-CC-SC4-2	4.5	122.6	15.0	49103	4730	1.2	0.07	40.5	3.6	13601	3683	443	46	130	15	242	49
GH-CC-SC4-3	7.5	130.8	10.4	50650	4559	1.2	0.07	41.4	4.6	14027	3567	474	48	132	12	249	45
GH-CC-SC4-4	10.5	133.2	8.3	52627	5140	1.2	0.07	41.6	1.9	14656	3633	504	54	138	17	242	42
GH-CC-SC4-5	13.5	128.3	11.1	51097	3726	1.2	0.07	39.1	3.4	15925	3139	503	38	137	12	251	33
GH-CC-SC4-6	16.5	128.6	12.9	51112	3631	1.3	0.07	39.8	1.9	15798	3226	543	40	139	10	338	47
GH-CC-SC4-7	19.5	147.8	11.6	50759	3558	1.5	0.08	42.7	4.2	15875	3159	528	40	140	12	393	55
GH-CC-SC4-8	22.5	172.4	11.1	49628	3134	1.8	0.10	42.0	3.7	15619	3232	541	35	145	10	593	79
GH-CC-SC4-9	25.5	166.3	10.5	49696	2848	1.8	0.10	38.8	0.5	15668	3110	526	30	148	10	562	69
GH-CC-SC4-10	28.5	185.8	12.9	53770	1758	1.8	0.10	39.5	0.3	15383	3840	518	21	173	4	831	97
GH-CC-SC4-11	31.5	201.8	13.2	54212	4831	1.5	0.08	36.7	0.9	14949	4738	435	35	155	13	946	192
GH-CC-SC4-12	34.5	209.8	13.8	53495	3871	2.6	0.15	37.4	2.2	15163	4342	422	30	155	11	1269	225

Sample ID	Depth (cm)	S (ppm)	Se (ppm)	±	Sn (ppm)	±	Sr (ppm)	±	Th (ppm)	±	Ti (ppm)	±	V (ppm)	±	Zn (ppm)	±
GH-CC-SC4-1	1.5	10059	125	43	183	73	105.7	6.6	48	15	2312	193	138	12	287	52
GH-CC-SC4-2	4.5	11987	99	34	185	58	93.1	6.1	56	16	2589	295	154	16	322	57
GH-CC-SC4-3	7.5	12830	89	55	180	62	89.0	4.6	59	16	2663	396	158	16	318	53
GH-CC-SC4-4	10.5	13282	115	45	189	67	89.0	4.7	68	19	2758	422	164	16	326	54
GH-CC-SC4-5	13.5	13242	95	46	156	50	86.5	3.8	54	12	2878	337	161	12	331	40
GH-CC-SC4-6	16.5	14672	98	28	155	50	83.7	3.2	59	11	2829	320	161	11	346	43
GH-CC-SC4-7	19.5	15200	74	51	159	54	90.1	4.2	48	7	2891	324	165	12	374	45
GH-CC-SC4-8	22.5	14859	92	24	163	48	87.8	3.4	61	15	2834	304	166	11	426	52
GH-CC-SC4-9	25.5	15279	94	39	155	47	84.0	2.8	53	9	2910	359	171	10	432	47
GH-CC-SC4-10	28.5	16573	152	105	215	85	91.9	1.5	63	9	2714	254	185	6	463	55
GH-CC-SC4-11	31.5	16702	115	45	200	48	101.0	7.1	58	12	2487	312	165	11	496	90
GH-CC-SC4-12	34.5	17145	109	65	185	59	87.6	4.5	58	18	2625	229	168	10	515	84

Table 10. Trace-metal speciation from XAFS, where R(Å) is the distance between atom pairs, N is the coordination number, σ^2(Å^2) and ΔE_0 (eV) are fitting parameters.

Table 10-1. Cd XAFS.

Core	Sediments					Precipitates				
		R (Å)	N[a]	σ^2 (Å^2)	ΔE_0 (eV)		R (Å)	N[a]	σ^2 (Å^2)	ΔE_0 (eV)
GH-CC-C1-2 55 cm	Cd-S	2.50	4.1	0.0050	−1.6	$Cd_{1.0}S$	2.51	4.7	0.0064	−1.5
GH-CC-SC4-12 34.5 cm	Cd-S	2.50	3.9	0.0038	−1.4	$Cd_{0.75}S$	2.51	4.2	0.0051	−2.1
GH-CC-SC9-12 30 cm	Cd-S	2.50	4.4	0.0046	−1.6	$Cd_{0.50}S$	2.51	4.5	0.0053	−1.4
GH-CC-SC4-11 Leached 31.5 cm	Cd-S[b]	2.49	2.7	0.0054	−1.5	$Cd_{0.25}S$	2.51	4.6	0.0056	−2.7
	Cd-O[b]	2.27	3.3	0.0194						

[a]Scale factor (S_0^2) = 1.4.

[b]$R_o/R_s = 0.33$.

Table 10-2. Cr XAFS.

Core		Oxide Component			
		R (Å)	N	σ^2 (Å^2)	ΔE_0 (eV)
GH-CC-SC4-12 34.5 cm	Cr-O	1.97	5.7	0.00313	−7.0
	Cr-Fe	3.43	3.7	0.0100	
	Cr-Fe	4.79	3.4	0.0039	
GH-CC-SC9-1 2.5 cm	Cr-O	2.01	5.3	0.0041	−1.5
	Cr-Fe	—	—	—	
GH-CC-SC9-12 30.0 cm	Cr-O	1.97	5.7	0.0050	−7.2
	Cr-Fe	—	—	—	

Table 10-3. Pb XAFS.

Core		Oxide component			
		R (Å)	N	σ^2 (Å^2)	ΔE_0 (eV)
GH-CC-SC4-12	Pb-O	2.39	3.6	0.0202	–10.3
34.5 cm	Pb-O	2.65	2.9	0.0174	
GH-CC-SC9-12	Pb-O	2.39	2.1	0.0213	–5.6
30.0 cm	Pb-O	2.63	3.5	0.0147	

Table 10-4. Zn XAFS.

Core		Sulfide component				Oxide component				
		R (Å)	N	σ^2 (Å^2)		R (Å)	N	σ^2 (Å^2)	ΔE_0 (eV)	R_o/R_s[a]
GH-CC-C3-9	Zn-S	2.31	4.1	0.0056	Zn-O	2.02	1.1	0.0064	–8.7	0.16
55.0 cm	Zn-Zn	3.82	3.2	0.0144	Zn-Fe		b			
	Zn-S	4.41	12.3	0.0210	Zn-Si		b			
GH-CC-SC4-1	Zn-S	2.31	4.0	0.0072	Zn-O	2.00	1.3	0.0075	–7.7	0.19
2.5 cm	Zn-Zn	3.82	1.5	0.0058	Zn-Fe	3.13	0.6	0.0030		
	Zn- S	4.42	7.3	0.0177	Zn-Si	3.47	1.0	0.0030		
GH-CC-SC4-12	Zn-S	2.32	4.0	0.0072	Zn-O	1.96	1.2	0.0038	–7.9	0.27
34.5 cm	Zn-Zn	3.82	1.1	0.0034	Zn-Fe	3.16	0.6	0.0049		
	Zn- S	4.43	6.2	0.0118	Zn-Si	3.48	1.1	0.0045		
GH-CC-SC4-11	Zn-S	2.33	0.8	0.0116	Zn-O	2.03	5.2	0.0096	–7.6	3.10
Leached	Zn-Zn	3.82	0.3	0.0036	Zn-Fe[c]	3.13	1.2	0.0052		
31.5 cm	Zn- S	4.44	10.1	0.0228	Zn-Fe[c]	3.32	0.9	0.0093		

[a] Ratio of fitted first-shell peak heights of the oxide (R_o) and sulfide (R_s) components of the spectrum.

[b] Backscattering from these shells is present, but too weak to be reliably fit.

[c] This component can be fit with either Fe or Zn atoms, or a mixture of the two.

5. Discussion of Results

The increase in trace-element concentrations with depth indicate that the Seaplane Lagoon sediments have been contaminated with cadmium, chromium, copper, lead, mercury, and zinc (Figs. 10 and 11, pp. 30–33). Clearly, sediments deeper than 20 to 25 cm are more contaminated than shallower sediments. Nickel appears to be an exception when compared with the other trace elements. Nickel concentrations decrease slightly from the surface to the deeper sediments.

In this section, we discuss the mobility of trace elements from the sediment to the porewater for the sediments as they exist today and for dredged sediments. We are concerned about the trace-element reactions between the porewaters and the sediments, because these reactions are related to the hazard of these sediments. Simply stated, the trace elements are more bioavailable if they are dissolved in the waters than if they are associated with the sediments.

Although the sediments are a long-term source for trace elements in porewaters, the absolute concentrations are limited by sorption, dissolution, and precipitation reactions with the clays, carbonates, and sulfides. The importance of these reactions in limiting the trace-element concentrations in the porewaters can be seen by comparing the porewater concentrations with the sediment concentrations (Fig. 7, pp. 25–27; Figs. 10 and 11, pp. 30–33). Trace-element concentrations in the sediments (100s of ppm) are several orders of magnitude greater than trace-element concentrations in the porewaters (10s of ppb).

5.1 *In Situ Geochemical Reactions of Seaplane Lagoon Sediments*

Trace elements are transferred from sediments to porewaters in the suboxic region of the sediments to 10-cm depth and potentially by diffusion from the deeper sediments. Because we cannot measure trace-element porewater concentrations directly with the microelectrode, we show trace-element mobility in the top 5 cm with the range of iron, manganese, and sulfur measured in porewaters (1) with the microelectrode across the oxic-suboxic-anoxic boundaries (Figs. 2–4, pp. 20–22), and(2) with the trace-metal leaching rates (Figs. 8 and 9, pp. 28–29).

Iron, manganese, sulfur, and associated trace metals are transferred from the sediments to the porewaters as the sediments cycle from oxidizing to reducing environments and vise versa. Important oxidation-reduction reactions from surface to deeper sediments are organic carbon oxidation by dissolved oxygen, then by nitrite, then by manganese (IV) solids, then by iron (III) solids, and then by dissolved sulfate. As the oxidation of organic carbon produces dissolved CO_2, Mn(II), Fe(II), and S(–II), manganese and iron form carbonate and/or sulfide minerals decreasing the porewater concentrations. As sediments are oxidized, cadmium and zinc will be dissolved from sulfide phases, and a significant portion of zinc and some cadmium will be removed from solution by sorbing to an oxide phase such as a clay or an iron-hydroxide. When oxidized sediments are reduced, cadmium, iron, and zinc concentrations will increase as the iron-hydroxides and iron-rich clays dissolve, and then decrease as CdS and ZnS precipitate. Copper, mercury, and nickel may behave similarly, but we do not know with which minerals these trace elements are associated because their concentrations were too low to determine speciation by XAS. Transfer of chromium and lead from the sediments to porewaters within the suboxic zone is minimal. Both chromium and lead are associated with oxide (possibly carbonate for lead). The dissolution of these phases is much slower than the dissolution of CdS and ZnS.

Below the suboxic region, trace elements may also diffuse from more concentrated porewaters in the deeper sediments to the less concentrated shallower sediments (Fig. 7, pp. 25–27), although we have not calculated the porewater diffusion rate. This process would be enhanced as porewaters move to shallow depths as older and deeper sediments compact under the burden of new sediments. The higher porewater concentrations at depth cannot be explained with the available thermodynamic data. It is likely that the trace elements complex with dissolved organics increasing the total solubility. The concentration of these organics need only be a few ppb, therefore we would not expect to see the difference between total organic carbon and total inorganic carbon dissolved in the porewaters (Fig. 7, pp. 25–27).

5.2 Impact of Dredging on Trace-Element Mobility

There are two major concerns regarding sediment remediation by dredging. One concern is that sediments will be oxidized, and the hazardous metals will dissolve into the waters making them more bioavailable. Another concern is that after dredging, the contaminated sediments must still be disposed. If the Alameda sediments are dredged, our results show there is greatest concern for cadmium, then zinc, then copper, nickel, and lead, and the least concern for chromium (Figs. 8 and 9, pp. 28–29).

Cadmium and zinc are reactive when the reduced sediments are exposed with seawater, because they are present as sulfides, which are not stable in the presence of dissolved oxygen. After cadmium and zinc dissolve, they partially sorb to secondary oxide minerals. Eventually the leaching rates are controlled by these sorption reactions, which significantly lower the net amount of cadmium and zinc in the water. Cadmium is more of a concern than zinc because cadmium does not efficiently sorb to the secondary oxides. After 90 days, about 40% of the cadmium in the initial sediment was lost to the seawater compared with a loss of only 12% for zinc. This is also reflected in the residual sediments, which contain about 30% Cd-O component compared with about 70% Zn-O component.

Chromium- and lead-leaching rates are low and constant because they are present as stable or metastable oxides or carbonates in both reduced and oxidized sediments. Less than 2% of the lead and less than 0.2% of the chromium was leached into seawater after 90 days.

It is not possible to say much about the reactivity of copper and nickel, because we were not able to determine their speciation in the solid phases. We can only say that their net leaching rates are less than zinc and greater than chromium.

6. References

Baes, C.F.J., and R.E. Mesmer (1976), *The Hydrolysis of Cations*, Wiley-Interscience.

Bethke, C.M. (1994), *The Geochemist's Workbench. A users guide to Rxn, Act2, TAct, React, and Gtplot*, 2nd ed., University of Illinois.

Bilinski, H., and P. Schindler (1982), "Solubility and equilibrium constants of lead in carbonate solutions," *Geochim. Cosmochim. Acta* **46**, 921–928.

Bourcier, W.L., and H.L. Barnes (1987), "Ore solution chemistry—VII. Stabilities of chloride and bisulfide complexes of zinc to 350°C," *Economic Geology* **82**, 1839–1863.

Boyle, J.W., and E.A. Wu (1997), "Low blank preconcentration technique for the determination of lead, copper, and cadmium in small-volume seawater by isotope dilution ICPMS," *Anal. Chem.* **69**, 2464–2470.

Brendal, P.J., and G.W. Luther III (1995), "Development of a gold amalgam voltammetric microelectrode for the determination of dissolved Fe, Mn, O_2 and S(–II) in porewaters of marine and freshwater sediments," *Env. Sci. Tech.* **29**, 751–761.

Cox, J.D., D.D. Wagman, and V.A. Medvedev (1989), "CODATA key values for thermodynmics," *Hemisphere*.

Dellien, I., F.M. Hall, and L.G. Helper (1976), "Chromium, molybdenum, tungsten: Thermodynamic properties, chemical equilibria, and standard potentials," *Chem. Rev.* **76**, 283–310.

Helgeson, H.C., J.M. Delany, H.W. Nesbitt, and D.K. Bird (1978), "Summary and critique of the thermodynamic properties of rock-forming minerals." *Amer. J. Sci.* **278-A**, 1–229.

Johnson, J.W., E.H. Oelkers, and H.C. Helgeson (1992), "SUPCRT92: A softwater package for calculating the standard molal thermodynamic properties of minerals, gases, aqueous species, and reactions from 1 to 5000 bar and 0 to 1000°C," *Comput. Geosci.* **18**, 899–947.

Knauss, K.G., and T.J. Wolery (1986), "Dependence of albite dissolution kinetics on pH and time at 25°C and 70°C," *Geochim. Cosmochim. Acta* **50**, 2481–2497.

Pokrovskii, V.A., and H.C. Helgeson (1995), "Thermodynamic properties of aqueous species and the solubilities of minerals at high pressures and temperatures: The system Al_2O_3–H_2O–NaCl," *Amer. J. Sci.* **295**, 1255–1342.

Rehr, J.J., R.C. Albers, and S.I. Zabinsky (1992), "High-order multiple scattering calculations of x-ray absorption fine structure," *Phys. Rev. Lett.* **69**, 3397–3400.

Rehr, J.J. (1993), "Recent developments in multiple-scattering calculations of XAFS and XANES," *J. Appl. Phys.*, suppl. 32-2, 8–12.

Robie, R.A., B S. Hemingway, and J.S. Fisher (1979), "Thermodynamic properties of minerals and related substances at 298.15 K and 1 bar (105 Pascals) pressure and at higher temperatures," *U.S. Geol. Survey Bull.* **1452**, 1–456.

Schindler, P., M. Reinert., and H. Gamsjäger (1969), "Löslichkeitskostanten und free buildungsenthalpien von $ZnCO_3$ and $Zn_5(OH)_6(CO_3)^2$ bei 25°C." *Hel. Chim. Acta* **52**, 2327–2332.

Smith, R.M., and A.E. Martell (1989), *Critical Stability Constants*, Plenum Press, New York.

Stipp, S.L.S., G.A. Parks, D.K. Nordstrom, and J.O. Leckie (1993), "Solubility-product constant and thermodynamic properties for synthetic otavite, $CdCO_3$(s), and aqueous association constants for the Cd(II)–CO_2–H_2O system," *Geochim. Cosmochim. Acta* **57**, 2699–2714.

Vaughan, D.J., and J.R. Craig (1978), *Mineral chemistry of metal sulfides*, Cambridge, MA, Cambridge Univ. Press.

Wagman, D.D., W.H. Evans, V.B. Parker, R.H. Schumm, I. Halow, S.M. Bailey, K.L. Churney, and R.L. Nuttall (1982), "The NBS tables of chemical themodynamic properties," *J. Phys. Chem. Ref. Data* 11(Suppl. 2).

Wolery, T.J. (1978), *Some aspects of hydrothermal processes at mid-ocean ridges—A theoretical study. I. Basalt-sea water reaction and chemical cycling between the ocean crust and the oceans. II. Calculation of chemical equilibrium between aqueous solutions and minerals,* Northwestern University, Evanston, IL.

Zachara, J.M., J.A. Kittrick, L.S. Dake, and J.B. Harsh (1989), "Solubility and surface spectroscopy of zinc precipitates on calcite," *Geochim. Cosmochim. Acta* **53**, 9–20.